The role of raptor during brain development and in adult forebrain neurons

Inauguraldissertation

zur

Erlangen der Würde eines Doktors der Philosophie

vorgelegt der

Philosophisch-Naturwissenschaftlichen Fakultät

der Universität Basel

von

Regula Maria Lustenberger

aus Romoos (LU)

Biozentrum der Universität Basel

Basel, August 2012

Genehmigt von der Philosophisch-Naturwissenschaftlichen Fakultät auf Antrag von

Prof. Dr. Markus A. Rüegg

Prof. Dr. Kaspar E. Vogt

Basel, den 26. Juni 2012

Prof. Dr. Martin Spiess

Dekan der Philosophisch-Naturwissenschaftlichen Fakultät

Namensnennung-Keine kommerzielle Nutzung-Keine Bearbeitung 2.5 Schweiz

Sie dürfen:

das Werk vervielfältigen, verbreiten und öffentlich zugänglich machen

Zu den folgenden Bedingungen:

Namensnennung. Sie müssen den Namen des Autors/Rechteinhabers in der von ihm festgelegten Weise nennen (wodurch aber nicht der Eindruck entstehen darf, Sie oder die Nutzung des Werkes durch Sie würden entlohnt).

Keine kommerzielle Nutzung. Dieses Werk darf nicht für kommerzielle Zwecke verwendet werden.

Keine Bearbeitung. Dieses Werk darf nicht bearbeitet oder in anderer Weise verändert werden.

- Im Falle einer Verbreitung müssen Sie anderen die Lizenzbedingungen, unter welche dieses Werk fällt, mitteilen. Am Einfachsten ist es, einen Link auf diese Seite einzubinden.
- Jede der vorgenannten Bedingungen kann aufgehoben werden, sofern Sie die Einwilligung des Rechteinhabers dazu erhalten.
- Diese Lizenz lässt die Urheberpersönlichkeitsrechte unberührt.

Die gesetzlichen Schranken des Urheberrechts bleiben hiervon unberührt.

Die Commons Deed ist eine Zusammenfassung des Lizenzvertrags in allgemeinverständlicher Sprache:

http://creativecommons.org/licenses/by-nc-nd/2.5/ch/legalcode.de

Haftungsausschluss:
Die Commons Deed ist kein Lizenzvertrag. Sie ist lediglich ein Referenztext, der den zugrundeliegenden Lizenzvertrag übersichtlich und in allgemeinverständlicher Sprache wiedergibt. Die Deed selbst entfaltet keine juristische Wirkung und erscheint im eigentlichen Lizenzvertrag nicht. Creative Commons ist keine Rechtsanwaltsgesellschaft und leistet keine Rechtsberatung. Die Weitergabe und Verlinkung des Commons Deeds führt zu keinem Mandatsverhältnis.

Quelle: http://creativecommons.org/licenses/by-nc-nd/2.5/ch/ Datum: 3.4.2009

“Nerve paths are something fixed, ended, immutable. Everything may die; nothing may be regenerated.”

Santiago Ramón y Cajal

This citation from the founder of the “neuron theory” and probably one of the most important and popular scientist ever since in the field of neuroscience is escorting me since my Master studies. At that time, I worked on neuronal progenitor cells and their capacity to proliferate after spinal cord injury. As it is well described today, the mammalian nervous system is not a completely post-mitotic tissue but rather harbors certain pools of cells that are able to divide and to functionally integrate into pre-existing networks. Thus, the conclusion I draw after my Master studies was the following: as brilliant Mr. Cajal was, at least in his statement about the regenerative capacity of the nervous system he eventually was wrong.
Now, after several additional years in neuroscience, working on a PhD project focusing on synaptic plasticity in the adult mouse brain, there is another statement of Santiago Ramón y Cajal that I have to reconsider: e.g. with focus on individual synapses or spines, the attributes “fixed, ended, immutable” do not fit any more into the current understanding of synaptic rearrangement, spine motility or very generally spoken to the theory of synaptic plasticity and learning and memory.

With these notions, by no means I intend to subtract the remarkable and valuable contribution of Santiago Ramón y Cajal to modern neuroscience. Rather, they shall serve as an illustration of how convertible knowledge is. The driving force of science to constantly gain new insights into any kind of mechanism is ultimately followed by the consequence that pre-existing knowledge is dropped or modified. Due to this fact, as a scientist one constantly proceeds on a tightrope walk, trading well accepted knowledge off against the basic principle of science – that is constant questioning and discovering. Therefore, what the citation of Santiago Ramón y Cajal – or in other words studying the nervous system during my Master’s and PhD – taught me is that in general nothing may be fixed or ended or immutable…

TABLE OF CONTENT

1 SUMMARY

mTOR is a serine/threonine protein kinase that appears in two functionally distinct multi-protein complexes. mTOR together with the scaffold protein raptor forms mTOR complex1 (mTORC1) that is inhibited in its function by rapamycin. In contrast, mTORC2 is dependent on the interaction with rictor and is considered to be rapamycin insensitive. mTORC1 controls a wide range of cellular processes, including protein synthesis, ribosome biogenesis, cell growth, gene transcription, autophagy and metabolism. In the developing CNS, mTORC1 was shown to be involved in axonal outgrowth and navigation, dendritic arborization as well as spine and filopodia formation. In the adult brain, the dysfunction of mTORC1 signaling has been linked to several neurodegenerative disorders like Parkinson's, Alzheimer's, or Huntington's disease and to some mental disorders, such as schizophrenia or autism spectrum disorders. However, it is not known whether altered mTORC1 signaling is cause or consequence of those pathologies. In addition, mTORC1 has also been suggested to be involved in synaptic plasticity and the process of learning and memory. To study the role of mTORC1 during development as well as in the adult stage of the brain, we deleted the mTORC1-defining component raptor by crossing floxed *rptor* mice with mice expressing the Cre-recombinase under the control of the Nestin promoter (RAbKO mice) or under the control of the α-CamKII promoter (*R*cKO mice), respectively.

Analysis of the RAbKO mice revealed that several aspects of brain development are critically controlled by mTORC1. RAbKO mice showed a pronounced microcephaly which is evenly expressed in all brain structures and gets apparent at E17.5. The observed change in brain size is likely due to reduced cell size and cell number. The latter is potentially the result of two mechanisms that are altered in RAbKO mice. First, raptor-depletion results in an increased incidence of apoptosis at late embryonic stages. Secondly, RAbKO mice show reduced proliferation at E17.5 and prolonged cell cycle length earlier during development. Furthermore, RAbKO mice show deficits in glial differentiation, probably mediated by altered STAT3 signaling that is observed in those mice. Moreover, ablation of mTORC1 activity during brain development affects cortical and hippocampal layering.

Due to the immediate postnatal lethality of RAbKO mice, there was need for the generation of a second knockout-mouse strain based on α-CamKII-Cre mediated recombination to further analyze the postnatal role of mTORC1 in the brain (*R*cKO mice). The data that were obtained from this mouse model indicate that mTORC1 is involved in cell size maintenance in adult neurons but does not affect apoptosis in the adult brain. Further, *R*cKO mice display a distinct deficit in learning and memory in the Morris water maze. Under long inter-training-interval conditions where consolidation takes place within

a time window that relies on *de novo* protein synthesis, the learning and memory performance of *R*cKO mice is reduced. This deficit can be overcome by an acquisition phase with short inter-training-intervals. Additionally, *R*cKO mice do exhibit impairments in fear extinction learning whereas the learning as well as context- and cue-memory is not affected in the fear conditioning paradigm in *R*cKO mice compared to control. These behavioral phenotypes are resembled by impaired E-LTP and L-LTP maintenance in *R*cKO mice. In addition to these plasticity-related aspects, also basal synaptic function of CA1 hippocampal neurons is altered in *R*cKO mice.

In summary, the data obtained from the two mouse models provide evidence that mTORC1 signaling controls several aspects of brain development and adult brain function. While during embryogenesis mainly cellular processes such as proliferation, differentiation and growth are affected by raptor deficiency, in the adult brain – besides the cell size control – primarily synaptic and plasticity-related functions depend on mTORC1 signaling. Further examination of mTORC1-related functions such as autophagy and mitochondrial regulation in *R*cKO mice potentially will provide new insights into mechanism of brain aging and neurodegenerative diseases, both of which are processes that are discussed to be dependent on mTORC1 signaling.

2 LIST OF ABBREVIATIONS

TOR	target of rapamycin
mTORC1/mTORC2	mammalian TOR complex 1/2
RAbKO	raptor brain knockout
*R*cKO	*rptor* conditional knockout
α-CamKII	Calcium/calmodulin-dependent protein kinase type II subunit alpha
CNS	central nervous system
E17.5	embryonic day 17.5
STAT3	signal transducer and activator of transcription 3
LTP	long-term potentiation
LTD	long-term depression
E-LTP	early-LTP
L-LTP	late-LTP
CA1/2/3	cornu ammonis region 1/2/3
DG	gyrus dentatus
PIKK	phosphatidylinositol kinase-related kinase
HEAT	Hantignton, EF3, A subunit of PP2A, TOR1
FRB	FKBP12-rapamycin-binding
FAT	FRAP, ATM, and TRRAP
FATC	FAT C-terminus
Raptor	regulatory associated protein of mTOR
GβL	G-protein β-subunit-like protein
mLST8	mammalian lethal with sec13 protein 8
PRAS40	proline-rich Akt substrate 40 kDa
deptor	DEP domain containing mTOR-interactin protein
rictor	rapamycin-insensitive companion of mTOR
mSin1	mammalian stress-activated MAP kinase-interacting protein 1
protor	protein observed with rictor
Akt/PKB	protein kinase B
IRS	insulin receptor substrate
PI3K	phosphoinositide-3-kinase
PIP_3	phosphatidylinositol-3,4,5-triphosphate
TSC1/2	tuberous sclerosis complex 1/2
Rheb	Ras homolog enriched in brain

MAPK	Mitogen-activated protein kinases
GAP	GTPase-activating protein
AMP	adenosine monophosphate
AMPK	5’AMP-activated protein kinase
ATP	adenosine triphosphate
LKB1	liver kinase b 1
HIF1α	hypoxia inducible factor 1α
REDD1	regulated in development and DNA damage response 1
p53	protein 53
PTEN	phosphatase and tensin homolog deleted on chromosome 10
BAD	Bcl-2-associated death promoter
RSK1	ribosomal S6 kinase 1
IKKβ	inhibitor of nuclear factor-κB
S6	ribosomal protein S6
S6K	S6 kinase
4E-BPs	eIF4E-binding proteins
UTR	untranslated region
UBF	upstream binding factor
SREBP	sterol regulatory element-binding protein
PPARγ	peroxisome proliferator-activated receptor-γ
ULK1	unc-51-like kinase 1
ATG13	autophagy-related protein 13
TFEB	transcription factor EB
mRNA	messenger ribonucleic acid
eIF4A/B/C/D/E	eukaryotic translation initiation factor 4A/B/C/D/E
5’TOP mRNA	5’ oligo-pyrimidine tract containing mRNA
5’UTR	5’ untranslated region
SREBPs	sterol regulatory element-binding proteins
PPARγ	peroxisome proliferator-activated receptor-γ
DAP1	death-associated protein 1
WIPI2	WD repeat domain phosphoinositide-interacting protein 2
PGC1α	PPARγ coactivator 1α
PKC	protein kinase C
SGK1	serum-and glucocorticoid-induced protein kinase 1
MEFs	mouse embryo fibroblasts
AD	Alzheimer’s disease

FMRP	fragile X mental retardation protein
Arc	activity-regulated cytoskeleton-associated protein
PSD95	post-synaptic density protein 95
APP	amyloid precursor protein
Aβ	amyloid beta
PIKE	PI3K enhancer
Ras	rat sarcoma
AMPA-R	α-amino-3-hydroxy-5-methyl-4-isoxazolepropionic acid receptor
NMDA-R	N-methyl-D-aspartate receptor
mGluRs	metabotropic glutamate receptors
VDCCs	voltage-dependent calcium channels
RyR	ryanodine receptor
HFS	high frequency stimulation
PKA	protein kinase A
PKMζ	protein kinase Mζ
ERK	extracellular-signal related kinase
CamKK	CamK kinase
CPEs	cytoplasmic polyadenylation elements
CPSF	cleavage and polyadenylation-specificity factor
RISC	RNA-induced silencing complex
CREB	cAMP-responding element binding protein
Elk-1	E twenty-six (ETS)-like transcription factor 1
BDNF	brain-derived neurotrophic factor
BrdU	Bromodeoxyuridine
Sox2	sex determining region Y box 2
Tbr2	T-box brain protein 2
PH3	phosphorylated histone 3
VZ	ventricular zone
SVZ	subventricular zone
IZ	intermediate zone
NeuN	neuronal nuclei
Map2	microtubule-associated protein 2
GFAP	glial fibrillary acidic protein
BLBP	brain lipid binding protein
Hsp90	heat-shock protein 90
EGF	epidermal growth factor

3 INTRODUCTION

The history of TOR (target of rapamycin) started in the 1960's with a Canadian expedition to Easter Island (in the native language named Rapa Nui) that aimed to collect plant and soil samples for subsequent analysis. One of such a soil sample contained the bacterium *Streptomyces hygroscopicus* that was found to produce a secondary metabolite, rapamycin, which displayed potent antifungal activity (Sehgal et al., 1975). After this first characterization of rapamycin as an antifungal agent and the finding of additional qualities such as immunosuppressive and cytostatic, the molecular targets of rapamycin were discovered in a yeast genetic screen by the group of M.N. Hall in Basel in 1991. These targets were named TOR1 and TOR2 (Heitman et al., 1991). Today, several years of investigation later, the field of knowledge about the target of rapamycin has grown exponentially. TOR is a large serine/threonine protein kinase that is conserved from yeast to human and is found in two distinct multi-protein complexes named TORC1 and TORC2 (Loewith et al., 2002).

In contrast to yeast, only one TOR ortholog has been identified in higher eukaryotes. The mammalian TOR (mTOR) forms two distinct protein complexes termed mTORC1 and mTORC2, respectively. mTORC1 and mTORC2 signaling are involved in a variety of cellular processes such as protein synthesis, autophagy, cell cycle progression, growth, metabolism, cytoskeletal organization and cell survival. As a consequence of this wide range of action, mTOR has been linked to cancer, metabolic disease such as obesity, fatty liver disease, insulin resistance and diabetes as well as several neurodegenerative diseases such as Parkinson's, Alzheimer's, or Huntington's disease and to some mental disorders, such as schizophrenia or autism spectrum disorders (Laplante and Sabatini, 2012). Proper basic neuronal function was recently intensively discussed to be dependent on balanced mTORC1 signaling. However, little is known about the mechanisms underlying altered mTORC1 signaling that was observed in a broad range of neuropathologies and brain disorders.

Given the fact that mTOR plays a central role in growing and dividing cells and additionally in post-mitotic adult tissues, it is still a challenge to therapeutically target and modulate this pathway specifically in respect to the above mentioned pathologies. Therefore, a better understanding of the mTOR signaling pathway in different organs and cell types in a healthy state as well as under disease conditions is crucial for future potential therapeutic targeting. The data presented here are the first that describe the genetically based depletion of mTORC1 signaling specifically in the developing brain and in adult excitatory neurons, respectively. In this study, we provide evidence for a crucial role of mTORC1 signaling during brain development and in adult forebrain neurons and describe the detrimental effects of the lack of mTORC1 activity during embryogenesis and the diminished synaptic efficiency accompanied by reduced cognitive abilities resulting from an inactivation of mTORC1 in the adult forebrain.

3.1 The mTORC1 pathway

3.1.1 Domain structure of mTOR and assembly of mTORC1 and mTORC2

The mammalian target of rapamycin (mTOR) is an atypical serine/threonine kinase of the phosphatidylinositol kinase-related kinase (PIKK) family. mTOR is a high molecular weight protein of approximately 290 kDa and contains 2549 amino acids (Figure 1). The C-terminal half of the protein is framed by two domains that are found in all PIKK family members, namely the FATC domain and the FAT domain. Between those two parts, the kinase domain and the FRB (FKBP12-rapamycin-binding) domain - the latter providing the docking-site for the binding of the FKBP12-rapamycin complex - are mapped. The N-terminus contains 20 tandem HEAT (Hantignton, EF3, A subunit of PP2A, TOR1) repeats (Fingar and Blenis, 2004). Such tandem HEAT repeats are found in many proteins and are associated with protein-protein interactions (Andrade and Bork, 1995). This HEAT repeat-rich N-terminal part of mTOR is the region which is described to be important for the mTOR-raptor interaction. Raptor (regulatory associated protein of mTOR) was found by Kim *et al*. to form a stoichiometric complex with mTOR and thereby to positively regulate mTOR activity (Kim et al., 2002). Similarly, mLST8 (mammalian lethal with sec13 protein 8, identified as GβL), discovered originally by the group of Michael N. Hall (Loewith et al., 2002), was identified to be an additional binding partner of mTOR. Upon interaction of mLST8 with the mTOR kinase domain, the mTOR kinase activity is stimulated and the raptor-mTOR interaction gets stabilized (Kim et al., 2003). mTOR, raptor and mLST8 form a rapamycin-sensitive complex that is termed mTORC1. After the initial identification of the above mentioned components of mTORC1, several additional proteins were described to interact with mTOR and the formation of two distinct multi-protein complexes was proposed. Currently, the following proteins are included in mTORC1: mTOR, raptor, PRAS40, deptor and

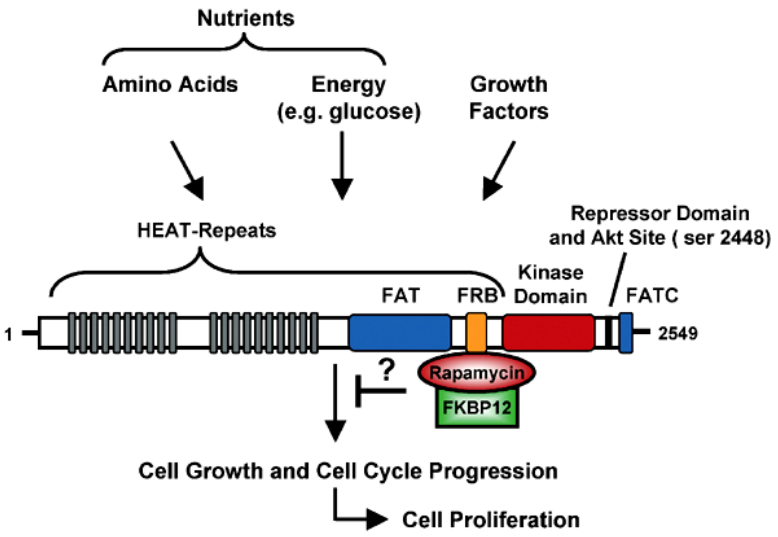

Figure 1. Domain structure of TOR. The NH2-terminal half of TOR is composed of tandem HEAT repeats. The COOH-terminal half of the protein contains the central FAT domain, followed by the FRB, the kinase, and the FATC domains. mTOR is regulated by nutrients (amino acids and energy) and by growth factors to modulate rates of cell growth and cell cycle progression, which coordinately control cell proliferation. rapamycin, in complex with FKBP12, directly binds to the FRB domain to inhibit mTOR-dependent downstream signaling. (adapted from: Diane C Fingar and John Blenis *Oncogene* (2004) 23)

mLST8. The mTORC2 is defined as the assembly of: mTOR, rictor, mSin1, protor, deptor and mLST8 (Laplante and Sabatini, 2012). The most striking difference between these two multi-protein complexes is their sensitivity to rapamycin. mTORC1 can be inhibited by short-term application of rapamycin, but only prolonged exposure is able to inhibit mTORC2 signaling in some cell types and an acute treatment does not affect the latter (Sarbassov et al., 2006). Thus, the general knowledge about mTORC2 is relatively limited. It still remains to be clarified what kind of inputs converge onto mTORC2. So far, only PI3K (phosphoinositide-3-kinase) and ribosomes were discussed to be upstream components of the mTORC2 pathway, but the signaling steps beyond PI3K are distinct from those upstream of mTORC1 and still unknown (Cybulski and Hall, 2009; Zinzalla et al., 2011). The downstream effectors of mTORC2 were identified just recently. The first direct substrate of mTORC2, Akt/PKB (protein kinase B), was found in 2005 by the group of David M. Sabatini (Sarbassov et al., 2005). They demonstrated that mTORC2 specifically phosphorylates Akt/PKB at the residue Ser473. Akt/PKB belongs to the AGC subfamily of kinases that are implicated in the control of several important cellular processes as well as diseases such as cancer and diabetes (Pearce et al., 2010). In the course of further investigation, other AGC kinases such as different PKCs (protein kinase C) and SGK1 (serum-and glucocorticoid-induced protein kinase 1) were identified as direct substrates of mTORC2 (Facchinetti et al., 2008; Garcia-Martinez and Alessi, 2008; Sarbassov et al., 2004). Whereas the activity of SGK1 and several members of the PKC family are dependent on mTORC2, the phosphorylation of Akt/PKB by mTORC2 seems to be of minor importance for Akt/PKB activity (Laplante and Sabatini, 2012). Besides these AGC kinases also Rho GTPases belong to the targets of mTORC2 (Jacinto et al., 2004). Based on the characterized functions of those downstream targets of mTORC2 it is generally thought that mTORC2 signaling is involved in the regulation of cell survival, metabolism and cytoskeletal organization.

In contrast to the marginal knowledge about mTORC2, the characterization of mTORC1 has remarkably expanded over the past fifteen years. This is mainly due to the advantage of rapamycin as a specific mTORC1 inhibitor. Rapamycin forms a complex with FKBP12 (12 kDa FK506-binding protein), which subsequently interacts with mTORC1 and inhibits its activity (Brown et al., 1994; Sabatini et al., 1994). In the next two chapters, the up- and downstream components of the mTORC1 pathway will be discussed in more detail.

3.1.2 Upstream control of mTORC1

The mTORC1 pathway is a very complex and diverse signaling network that consists of several input-branches that converge onto mTORC1 (Figure 2). The most commonly discussed intracellular and extracellular signals that are integrated by mTORC1 are the following: growth factors, energy status, amino acids, and stress. Additionally, other signaling pathways such as the Ras-ERK and TNFα can trigger the activation of mTORC1 (Laplante and Sabatini, 2012). In the next five sections, each of these upstream components of mTORC1 will briefly be described. The regulatory mechanisms that act specifically in the brain are described in the subsequent chapters 3.2-3.3.

Growth factors The general characteristic of mTORC1 as a controller of cell growth makes the link to upstream signaling molecules such as growth factors, mitogens and hormones conclusive. Insulin, as a prime example for this kind of upstream regulators, binds to its receptor and activates the PI3K-Akt/PKB pathway via IRS (insulin receptor substrate). Akt/PKB is recruited to the plasma membrane where it gets fully activated by PIP_3 and subsequently directly phosphorylates TSC2 and

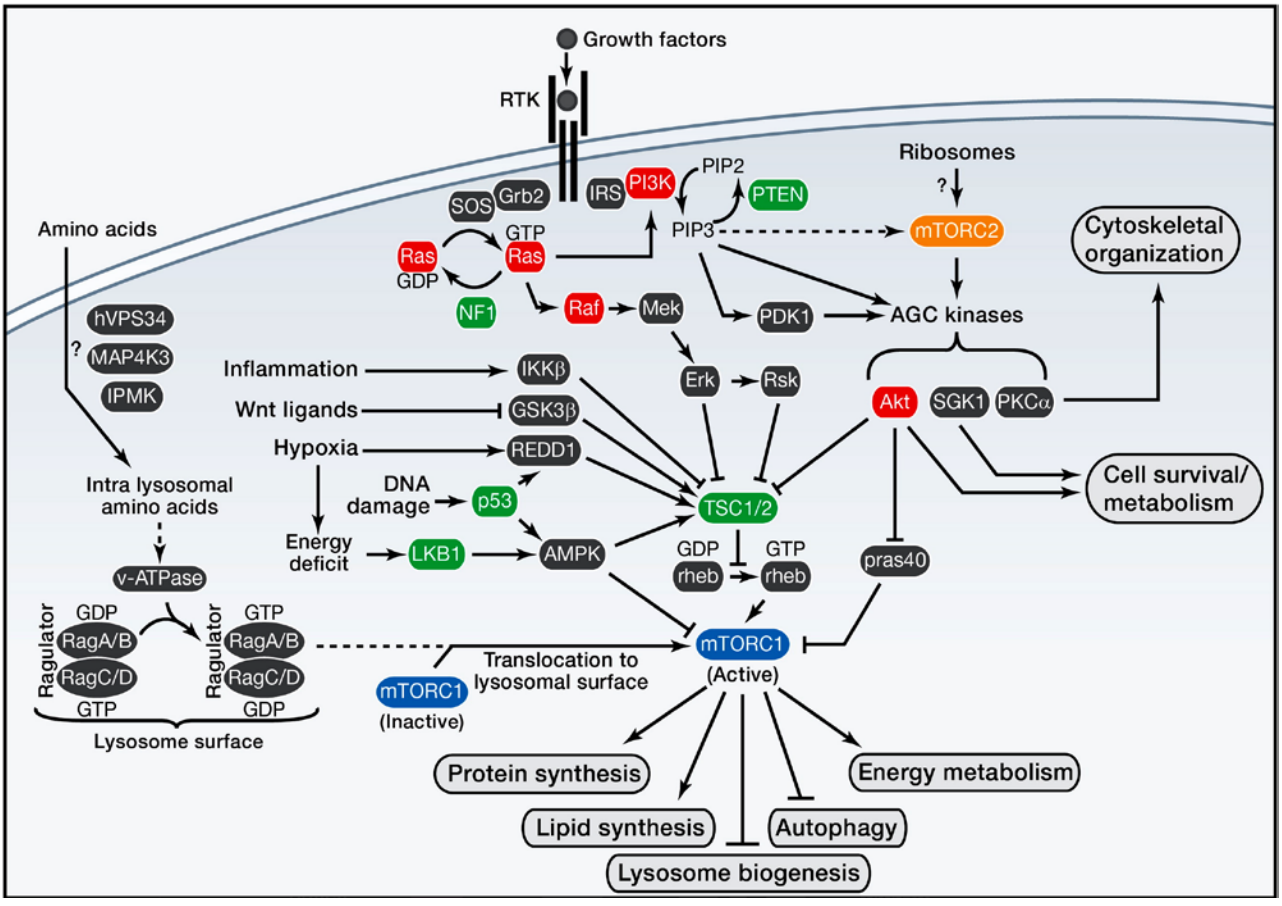

Figure 2. The mTOR signaling pathway. Critical inputs regulating mTORC1 include growth factors, amino acids, stress, energy status, and oxygen. When active, mTORC1 promotes protein synthesis, lipogenesis, and energy metabolism and inhibits autophagy and lysosome biogenesis. (adapted from: Mathieu Laplante and David M. Sabatini *Cell* (2012) 149)

thereby causes an inactivation of the TSC1/2 complex that otherwise acts as a negative regulator of mTORC1 (Manning and Cantley, 2003). A second signaling branch emanating from mitogen-activated Ras/MAPK/ERK/RSK1 pathway converges on TSC2 (Roux et al., 2004). The phosphorylation events on TSC2 by the kinases of both branches result in an inhibition of the TSC1/2 complex and thus up-regulate the mTORC1 activity. However, the link between TSC1/2 and mTORC1 is not direct but the signaling proceeds via the small GTPase Rheb (Ras homolog enriched in brain) towards which TSC2 exhibits a selective GAP (GTPase-activating protein) activity (Garami et al., 2003). The GTPase-activating protein domain of TSC2 stimulates the intrinsic GTPase activity of Rheb, thereby enhancing the conversion of Rheb to its GDP-bound, inactive state. Only in its GTP-bound form, Rheb is a potent activator of mTORC1. Thus, active TSC1/2 negatively regulates mTORC1 by converting Rheb to its inactive state towards mTOR (Inoki et al., 2003a).

Energy status The coordination between cell growth and cellular energy levels is critical for the survival of any cell. In consideration of the fact that the best-known role of mTOR is growth control, it is not surprising that the energy status of a cell affects mTORC1 activity and its function on protein synthesis. However, there was a debate on how mTOR senses the cellular energy state – in a direct or indirect way. To date, there is evidence that AMPK (5'AMP-activated protein kinase) couples the information of limited amounts of ATP to the mTORC1 pathway (Kimura et al., 2003). AMPK is a master regulator of cellular energy metabolism. Activation of AMPK restores cellular energy levels by stimulating catabolic pathways, such as glucose uptake and/or glycolysis and fatty acid oxidation, as well as by inhibiting energy-consuming anabolic processes such as protein synthesis. A low cellular energy state is characterized by a shift in the intracellular AMP/ATP ratio that is sensed by AMPK (Hardie et al., 1998). Thus, when cellular energy levels are low, AMPK is activated and subsequently phosphorylates TSC2 at its activating residues Ser1345 and Thr1227 (Inoki et al., 2003b) and raptor at the residues Ser792 and Ser722 (Gwinn et al., 2008). Both phosphorylation events lead to the inhibition of mTORC1. In addition to the activation of AMPK through AMP/ATP levels, AMPK was found to be a substrate of the tumor suppressor LKB1 (liver kinase b 1), a protein that is associated with the autosomal dominant inherited cancer disorder Peutz-Jeghers syndrome (Woods et al., 2003). Under normal conditions, LKB1 is constitutively active and phosphorylates AMPK in order to prime it to further activation by AMP (Shaw et al., 2005).

Amino acids In yeast, it was well described that TOR signaling is sensitive to nutrients such as amino acids (Crespo and Hall, 2002). In case of mammals, Hara *et al*. were the first to provide evidence for the sensitivity of mTORC1 to amino-acid deprivation (Hara et al., 1998). The mechanism responsible for amino acid sensing of the mTORC1 was disclosed just recently. Rag GTPases were identified by Kim *et al*. and Sancak *et al*. as activators of mTORC1 in response to amino acids signals. The four known mammalian Rag proteins (RagA, RagB, RagC, RagD) form the heterodimers RagA/B

and RagC/D. Effectual amino acids availability induces the formation of GTP-bound RagA/B complex which subsequently interacts with raptor. As a result of the Rag-raptor interaction, mTORC1 dislocates to the lysosome. In this cellular compartment, the main activator of mTORC1, namely Rheb, was found to preferentially be localized. Thus, amino acids might control the activity of the mTORC1 pathway by regulating the movement of mTOR to the same intracellular compartment that contains the mTORC1 activator Rheb (Kim et al., 2008; Sancak et al., 2008).

Stress Several cellular conditions can cause “stress-situations” that act as inhibitory on mTORC1. Among those, low energy levels, hypoxia and DNA damage are the best characterized. Down-regulation of mTORC1 activity in response to low energy levels is mediated by AMPK and TSC2 as described above. In the case of hypoxia, besides AMPK-mediated TSC2 activation, also HIF (hypoxia inducible factor) regulates mTORC1 inhibition via TSC2. Under low oxygen conditions HIF induces the expression of DNA damage response 1 (REDD1) that subsequently activates TSC2 (Brugarolas et al., 2004). Furthermore, also genotoxic stresses such as radiation-induced DNA damage or oncogene activation interfere with the mTORC1 pathway via TSC2 by yet other initial components, namely p53 and PTEN. Feng *et al*. showed that p53 activation inhibits mTORC1 activity via AMPK and TSC2 (Feng et al., 2005). Additionally, p53 transcriptionally controls PTEN (phosphatase and tensin homolog deleted on chromosome 10) via a DNA-binding site directly upstream of the *pten* locus (Stambolic et al., 2001). PTEN is an upstream regulator of mTOR that acts as an inhibitor of PI3K and therefore negatively affects mTORC1 signaling (Vivanco and Sawyers, 2002).

Ras-ERK and TNFα signaling The Ras-ERK pathway is well described to control gene transcription and protein translation. Just recently, it has been shown that the Ras-ERK pathway also feeds into mTORC1 signaling by at least two mechanisms. First, ERK (extracellular-signal related kinase) can directly phosphorylate TSC2 and thereby reduce its inhibitory function on mTORC1. Secondly, the downstream target of ERK, RSK (ribosomal S6 kinase), exhibits phosphorylation-activity towards TSC2 and raptor, resulting in increased mTORC1 kinase activity (Ma and Blenis, 2009). Besides TSC2, also TSC1 is a described target for upstream mTORC1 regulation. The major effector of the TNFα signaling pathway, IKKβ (inhibitor of nuclear factor-κB), has recently been shown to phosphorylate TSC1, resulting in activation of mTORC1 (Lee et al., 2007).

3.1.3 Downstream targets of mTORC1

The diversity of upstream regulatory mechanisms that merge onto mTORC1 – as discussed in the previous chapter – is reflected in the variety of cellular processes that are controlled by mTORC1 signaling. The best characterized function of mTORC1 is growth control. Ultimately, controlling growth means nothing else than regulating protein synthesis, lipid synthesis and proliferation. However, these processes need to be in balance with the energy levels that are disposable for a given cell at a given time. Therefore, in a low-energy state the cell switches from the “synthesis-program” to a “recycling-program”. The latter provides a backup source of metabolites in order to keep up with the basic functions for cell survival. mTORC1 plays a central role within these processes by regulating protein synthesis through S6K and 4E-BPs, lipid synthesis through SREBP and PPARγ, autophagy through ULK1 and ATG13, and lysosome biogenesis through TFEB (Figure 3). Moreover, mTORC1 contributes to cell survival via S6K-mediated inhibition of the pro-apoptotic protein BAD (Bcl-2 associated death promoter). Most of these downstream effectors and the molecular consequences of their regulation by mTORC1 will be described in the subsequent sections.

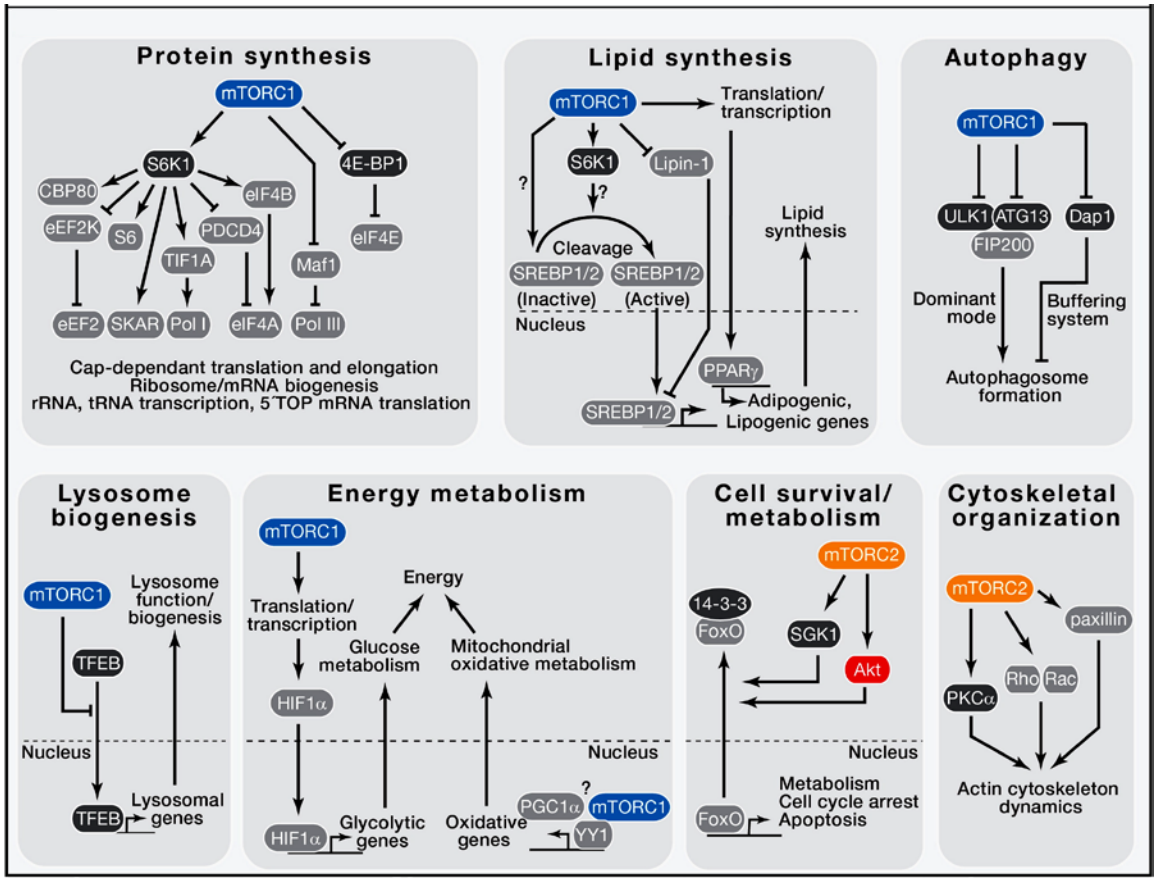

Figure 3. Downstream signaling of mTORC1 and mTORC2. (adapted from: Mathieu Laplante and David M. Sabatini *Cell* (2012) 149)

Protein synthesis The best described downstream targets of mTORC1 – S6K and 4E-BPs – are control-components of the mRNA translation machinery. The initial step of protein synthesis (once the mRNA is produced) is the recruitment of a ribosome to the 5' end of the mRNA (Hershey, 1991). The 5' end of most mRNAs is characterized by a so-called cap, a structure that is specifically recognized by the eukaryotic translation initiation factor 4E (eIF4E) (Altmann et al., 1989). The binding of eIF4E to the cap is the first event in the assembly of the ribosome initiation complex at the 5' end of a given mRNA (Gingras et al., 1999). As the name already suggests, the mTORC1 downstream targets 4E-BPs (eIF4E-binding proteins) interfere with this critical step of translation initiation. 4E-BPs compete for the binding site on eIF4E with other proteins that belong to the ribosome initiation complex and consequently 4E-BP-bound eIF4E locks translation initiation (Mader et al., 1995). The phosphorylation of 4E-BPs by mTORC1 prevents the binding of 4E-BPs to eIF4E and therefore allows the formation of the ribosome initiation complex at the mRNA and the subsequent accomplishment of the protein synthesis procedure (Heesom and Denton, 1999). Processes involved in translation initiation are schematically summarized in Figure 4.

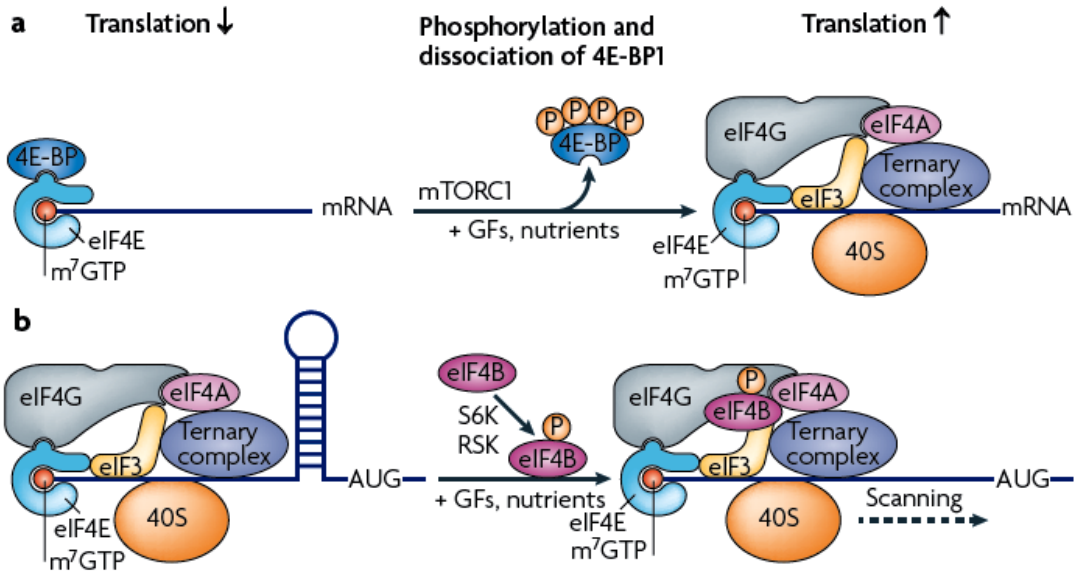

Figure 4. Regulation of cap-dependent translation innitiation. **a** The recruitment of the 40S ribosomal subunit to the 5' end of mRNA is a crucial and rate-limiting step during cap-dependent translation. A number of translation initiation factors, including the 5' cap-binding protein eukaryotic translation initiation factor 4E (eIF4E), have essential roles in this process. Phosphorylated 4E-binding proteins (4E-BPs) bind tightly to eIF4E, thereby preventing its interaction with eIF4G and thus inhibiting translation. mTORC1-mediated phosphorylation of 4E-BPs releases the 4E-BP from eIF4E, resulting in the recruitment of eIF4G to the 5' cap, and thereby allowing translation initiation to proceed. **b** Another well-studied initiation factor that is targeted by signal transduction pathways is eIF4B. Following 40S ribosomal protein S6 kinase (S6K)- or ribosomal S6 kinase (RSK)-mediated phosphorylation, eIF4B is recruited to the translation pre-initiation complex and enhances the RNA helicase activity of eIF4A. This is particularly important for translating mRNAs that contain long and structured 5' untranslated region sequences, because the unwinding of these RNA structures is required for efficient 40S ribosomal subunit scanning towards the initiation codon. (adapted from: Xiaoju M. Ma and John Blenis *Nature Reviews Molecular Cell Biology* (2009) 10)

Besides the 4E-BPs also S6K is involved in protein synthesis by promoting increased mRNA translation. S6K is an intensively studied effector of mTORC1 but in contrast to 4E-BPs, which contribute to overall cap-dependent translation, it was thought that S6K is triggering only a specific subset of mRNA that is characterized by an oligo-pyrimidine tract at the 5' end (Jefferies et al., 1994). This subclass of mRNA is called 5'TOP mRNA and encodes primarily ribosomal proteins and certain other components of the translation machinery. For a long time it was hypothesized that S6K triggers protein synthesis of these mRNAs mainly via phosphorylation of its substrate S6 (ribosomal protein S6) (Thomas, 2002). Several recent studies, however, are inconsistent with this hypothesis as e.g. genetic inactivation of S6K1 has no effect on TOP mRNA translation, rapamycin only partially blocks translational activation of these mRNAs and no deficiency in TOP translation could be observed in a phospho-mutant of S6 (Ma and Blenis, 2009). Therefore, it is suggested, that mTOR regulates TOP mRNA translation independently of mTORC1 and S6K. A more established mechanism by which S6K controls mRNA translation is via phosphorylation of eIF4B (eukaryotic translation initiation factor 4B) and thereby stimulating the helicase activity of eIF4A (Raught et al., 2004). This helicase activity is particularly required for the linearization of long hairpin structures that are often found in the 5' UTR (untranslated region) of a specific subset of mRNAs that code for proteins involved in cell growth and proliferation as reviewed by Nissim Hay and Nahum Sonenberg (Hay and Sonenberg, 2004). By unwinding these stable hairpin structures, eIF4A provides the structural prerequisites for the ribosome to bind and scan these mRNAs (Figure 4b). Additionally, mTORC1 mediated S6K activation promotes ribosome biogenesis via phosphorylation of the transcription factor UBF (upstream binding factor) that subsequently induces 45S ribosomal gene transcription (Hannan et al., 2003). Therefore, mTORC1 contributes dually to overall mRNA translation by phosphorylating both 4E-BPs and S6K that synergistically promote protein synthesis.

Lipid synthesis While the link between mTORC1 to cell growth and underlying protein synthesis has been accepted for many years, the regulation of lipid biosynthesis by mTORC1 just more recently attracted notice. The known ability of mTORC1 to sense the energy status of a cell and the observation that mTORC1 is highly activated in adipose tissue of obese mice led to the hypothesis that mTORC1 may play a role in lipogenesis and adipogenesis (Um et al., 2004). As soon as the balance of energy intake versus energy expenditure is shifted towards more intake than consumption, the spared carbohydrates will be converted to adipose tissue by lipogenesis (Kersten, 2001). Key regulators of *de novo* lipogenesis are the transcription factors SREBPs (sterol regulatory element-binding proteins). SREBPs control lipid homeostasis by controlling gene expression of various genes that are involved in the synthesis of cholesterol, fatty acid, triglyceride and phospholipids (Foretz et al., 1999; Kersten, 2001). SREBPs are activated by the IRS-Akt/PKB pathway in an mTORC1-dependent manner (Porstmann et al., 2008) and fatty acid metabolism was shown to be rapamycin sensitive (Brown et al., 2007).

The term adipogenesis refers to the differentiation of pre-adipocytes into mature fat cells. This process is controlled by a highly specific geneprogram that finally results in the activation of PPARγ (peroxisome proliferator-activated receptor-γ) as described by Evan D. Rosen and Ormond A. MacDougald (Rosen and MacDougald, 2006). mTORC1 is hypothesized to be involved in this process by regulating the expression and activation of PPARγ (Kim and Chen, 2004). Especially the phosphorylation of 4E-BPs by mTORC1 was shown to be a critical step in the translational regulation of PPARγ and other proteins involved in adipogenesis (El-Chaar et al., 2004).

Autophagy In contrast to protein and lipid synthesis, both of which are process occurring under high energy availability, autophagy is initiated during conditions of insufficient nutrient and energy supply. Once autophagy is activated, cellular components are embedded into autophagosomes, which then are further fused with lysosomes where the enclosed cellular components are degraded. This process ultimately provides a nutrient source to maintain vital cellular activities. The first evidence for a contribution of mTORC1 in the regulation of autophagy comes from studies in yeast, where Noda *et al.* showed that treatment of yeast cells with rapamycin induced autophagy even in cells growing in nutrient-rich medium (Noda and Ohsumi, 1998). The mechanism by which mTORC1 negatively controls autophagy is mainly through phosphorylation of ATG13 (autophagy-related gene 13) and ULK1 (unc-51-like kinase 1). These phosphorylation events are regulated in a nutrient-dependent manner and result in the suppression of the ULK1/ATG13/FIP200 protein-complex, a complex required for the initiation of autophagy (Ganley et al., 2009; Hosokawa et al., 2009). Additionally, other autophagy-related proteins, such as DAP1 (death-associated protein 1) and WIPI2 (WD repeat domain phosphoinositide-interacting protein 2) were reported to be targets of mTORC1 (Hsu et al., 2011; Koren et al., 2010). Thus, low mTORC1 activity inhibits growth and induces autophagy. Therefore, mTORC1 has a key role not only in nutrient response, but also in cellular energy homeostasis.

Energy metabolism An important component of the mTORC1 up- and downstream signaling is HIF1α. Under hypoxic conditions, HIF acts upstream of mTOR and activates TSC2, thereby inhibiting mTORC1 (see 3.1.2). On the other hand, mTORC1 was shown to promote the transcription and translation of HIF1α and thereby to activate several metabolic genes (Duvel et al., 2010). Therefore, mTORC1 activates specific energetic and anabolic cellular processes. Furthermore, mTORC1 is correlated with mitochondrial metabolism (Schieke et al., 2006). The ability of mTORC1 to modulate the oxygen consumption and oxidative capacity appears to be independent of S6K and 4E-BPs. Thus, yet another downstream target of mTORC1, namely PGC1α (PPARγ coactivator 1α), is supposed to link mTORC1 signaling to the control of mitochondrial biogenesis and oxidative function (Cunningham et al., 2007). PGC1α acts as a co-activator of the transcription factor PPARγ. Thereby, PGC1α triggers the expression of genes that encode mitochondrial respiratory chain proteins and 5-

aminolevulinate synthase, as well as mitochondrial transcription factor A, a regulator of mitochondrial DNA transcription and replication (Wu and Boss, 2007).

3.1.4 Feedback inhibition within mTORC1 signaling

An important feature of the mTORC1 pathway regulation is the negative feedback loop that S6K exhibits on IRS – in terms of both transcriptional suppression and phosphorylation-dependent activity, respectively (Harrington et al., 2004). The initial observation of such a potential feedback loop was made in MEFs (mouse embryo fibroblasts) lacking either TSC1 or TSC2. In such cells, the stimulation with different growth factors, in particular insulin, failed to induce an activation of the PI3K-Akt/PKB pathway (Harrington et al., 2004; Zhang et al., 2003). The underlying mechanism is mainly based on the phosphorylation of IRS1 at Ser302 by S6K. Phosphorylation of this site prevents IRS1 to interact with the insulin receptor and thus the insulin-PI3K-Akt/PKB pathway is attenuated. As a consequence of long-term mTORC1 activation, also the transcription level of IRS1 was found to be reduced (Shah et al., 2004). Upon application of rapamycin or upon other approaches that lead to inactivation of mTORC1 signaling the feedback inhibition is absent (Bentzinger et al., 2008; Chen et al., 2010). This in turn can result in an increased PI3K-Akt/PKB activity that has to be taken into consideration whenever manipulating the mTORC1 signaling pathway. This negative feedback inhibition has important implications in several diseases such as diabetes and tumor syndromes (Manning, 2004; Um et al., 2004).

3.2 mTORC1 in the developmental and adult brain

During the last decades the interest of neurobiologists in the mTORC1 signaling pathway has grown extensively. A main reason why mTORC1 became more and more attractive in the field of neuroscience is based on the hypothesis that abnormal mTORC1 signaling during brain development is the cause of many brain malformations and pathologies. Additionally, new methodological possibilities for *in vivo* genetic modifications of specific subsets of neurons or glia cells in parallel with an increased basic knowledge about a bunch of neurodegenerative diseases and psychiatric disorders further pushed the intention to investigate the role of mTORC1 in the brain. The following chapters will give an overview of what is known about mTORC1 in brain development and brain pathologies.

3.2.1 mTORC1 in neuronal development

The major feature of mTORC1 is the control of growth and proliferation. During development, these processes are of particular importance. However, the role of mTORC1 in neuronal development goes beyond the simple control of cell size and number. Initial experiments in cell culture systems revealed that mTORC1 is involved in axonal outgrowth and pathfinding, dendritic arborization as well as control of spine number and morphology. For example, treatment of cultured neurons with rapamycin alters the responsiveness of growth cones mediated by Semaphorine3A and Netrin most likely in a protein synthesis-dependent manner (Campbell and Holt, 2001; Piper et al., 2006). Since directional axonal growth is a crucial early step during brain development, this and similar other observations propose that mTORC1 signaling is important already at very early steps during brain development. Furthermore, mTORC1 was shown to promote the growth and branching of dendrites (Jaworski et al., 2005). Jaworski *et al*. showed that the complexity of the dendritic tree was reduced in the presence of rapamycin and the opposite phenotype was observed in neuron cultures lacking the mTORC1 negative regulator PTEN. The synergistic signaling between PI3K-Akt/PKB-mTORC1 and the Ras pathway was shown for dendritic tree expansion (Kumar et al., 2005). Additionally, Kumar *et al*. and others (Tavazoie et al., 2005) reviewed that also the very small morphological units of a neuron, namely the spines, are controlled by mTORC1 in terms of number and shape. Finally, not only morphological features but also the regulation of differentiation into glial/neuronal cells is dependent on mTORC1 activity as shown by several groups. However, whether the glial or neuronal linage is induced by mTORC1 signaling is still not conclusive (Han et al., 2008; Uhlmann et al., 2002). Unfortunately, most of the studies on the involvement of mTORC1 in neuronal development were carried out in cell culture systems due to the early embryonic lethality of several knockout mouse models such as *mTOR* $^{-/-}$, *rptor* $^{-/-}$ or *mLST8*$^{-/-}$ (Gangloff et al., 2004; Guertin et al., 2006). Thus, for future directions the use of cell type specific knockout mouse models eventually will provide more

detailed insight into the function of mTORC1 in the developing nervous system. A first step towards a better understanding of mTORC1 signaling during brain development was done in our study where we deleted the mTORC1-defining protein raptor in all neuronal cells by the use of the Cre-LoxP system (see chapter 4.2).

3.2.2 mTORC1 in brain physiology and pathologies

As shown for other tissues, the balanced activity of mTORC1 is also crucial for the maintenance of physiological functions in the brain. However, other than most of the organs in the body, the brain is composed of a big number of diverse specialized structures that all contain a selective pool of excitatory and inhibitory neurons and therefore is even more susceptible to failures in pivotal signaling cascades. In recent years, the mTOR pathway was linked to cancer and to the pathogenesis of a variety of diseases such as Alzheimer's disease, Parkinson's disease, Huntington's disease, Tuberous sclerosis complex, neurofibromatosis, Fragile X syndrome and epilepsy. Furthermore, also mental disorders such as schizophrenia, depression and autism spectrum disorders have been related to unbalanced mTORC1 activity (Chong et al., 2010). In the subsequent paragraphs, most of these diseases will be discussed with regard to mTORC1 dysfunction. The main findings on the contribution of mTORC1 signaling to these different diseases are summarized in Table 1.

Alzheimer's disease (AD) Alzheimer's disease is characterized by brain atrophy, the formation of senile plaques – mainly consisting of amyloid beta (Aβ) – and the accumulation of neurofibrillary tangles made of Tau aggregates. The main physiological function of the protein Tau is to promote the assembly and stabilization of the microtubule structure in neurons. Tau is a protein with multiple phosphorylation sites. Phosphorylation is essential for its function and Tau protein is susceptible to hyperphosphorylation, which commutes it into an inactive state in which it preferentially forms aggregates, which is a hallmark of Alzheimer's disease. Several kinases and phosphatases have been identified to regulate the phosphorylation of Tau (Pei and Hugon, 2008). The role of mTORC1 in Alzheimer's disease is controversially discussed. Currently, two hypotheses are debated: 1) It is suggested that mTORC1 activity is reduced in AD. This hypothesis is supported by the findings of Ma *et al*. where they published an impaired mTORC1 activity in a mouse model of Alzheimer's disease. This study reports a compromised LTP in their mouse model of Alzheimer's disease that could be prevented by pharmacological and genetic upregulation of mTOR signaling (Ma et al., 2010). Furthermore, inhibition of mTORC1 activity was observed in cultured neurons that were exposed to the major component of the senile plaques, Aβ (Lafay-Chebassier et al., 2005). Accordingly, a decrease in the level of protein synthesis has been described in the brain of AD patients (Langstrom et al., 1989). 2) On the other hand, several groups reported an increase in mTORC1 activity and other pathway components in samples of AD patients (An et al., 2003; Griffin et al., 2005; Lafay-Chebassier

et al., 2005). In line with these observations, the expression and phosphorylation level of Tau was observed to nicely correlate with the activity of mTORC1 (Pei et al., 2008). Studies in *Drosophila* further indicate that Tau-induced neurodegeneration is triggered by mTORC1 and can be suppressed by rapamycin (Khurana et al., 2006). Therefore, upon these studies it is hypothesized that mTORC1 activity is increased in Alzheimer's disease and subsequently results in elevated translation levels of toxic proteins. Further studies are necessary to more specifically disclose the role of mTORC1 for Alzheimer's disease – in both, the development and progression of the disease – in order to eventually approach the mTORC1 pathway as a therapeutic target for AD.

Parkinson's disease Besides Alzheimer's Disease, Parkinson's disease is the second most common degenerative disorder of the central nervous system. The disease is progressive and results from loss of dopaminergic neurons in the substantia nigra pars compacta (Parkinson, 2002). The link between mTORC1 and Parkinson's disease arises from the stress response protein REDD1 (also known in this context as RTP801). As described in chapter 3.1.2, REDD1 is a negative regulator of mTORC1 signaling, acting upstream of TSC1/2 but downstream of Akt/PKB (Corradetti et al., 2005). REDD1 is highly induced in cellular models as well as in mouse models of Parkinson's disease and was also found to be elevated in dopaminergic neurons of patients (Chong et al., 2010). Furthermore, the expression of a major pro-survival factor in dopaminergic neurons, Engrailed 1, was shown to be induced by mTORC1 (Di Nardo et al., 2007). Together, these data suggest that due to a cellular stress response the mTORC1 signaling is inhibited through REDD1 and results in down-regulation of specific pro-survival factors in dopaminergic neurons of individuals suffering from Parkinson's disease. Interestingly, however, it is not conclusive why treatment with rapamycin in a mouse model of Parkinson's disease was shown to protect against neuronal death (Malagelada et al., 2010). The authors of this study hypothesize that the observed neuroprotective effect of rapamycin arises from its selective suppression of some (e.g. blocking of protein synthesis, in particular of REDD1) but not all actions of mTOR. Further investigations have to be done to more clearly determine the role of mTORC1 in the genesis and progression of Parkinson's disease.

Huntington's disease The autosomal dominant neurodegenerative Huntington's disease is caused by a mutation in the gene encoding the protein huntingtin. This mutation causes an abnormal translation of the mRNA encoding huntingtin resulting in huntingtin proteins with long polyglutamine tracts that form intraneuronal aggregates which are detrimental for neurons (Rubinsztein, 2002). The current understanding of how mTORC1 is involved in the progression of Huntington's disease is via its inhibitory control of autophagy. The clearance of the polyglutamine aggregates by induction of autophagy is a potential therapeutic strategy in Huntington's disease. In line with this, rapamycin treatment attenuates the progression of the disease and protects against neurotoxicity (Berger et al., 2006).

Tuberous sclerosis complex Also TSC is an autosomal dominant genetic disease caused by either mutation of the gene encoding TSC1 or TSC2. As TSC1/2 functions as a negative regulator of mTORC1, a mutation in either gene results in an exaggerated activation of the mTORC1 pathway and therefore excessive protein synthesis. Patients frequently display intellectual disabilities, autistic characteristics, epileptic seizures and show the formation of tubers consisting of giant neurons and astrocytes (Tomasoni and Mondino, 2011). Mice that carry heterozygous mutations in the genes encoding TSC1 or TSC2, respectively, show impaired learning and memory, impaired social behavior and abnormalities in contextual fear conditioning (Goorden et al., 2007). Furthermore, also oxidative stress is observed in TSC and contributes to neuronal dysfunction. Therefore, it is not surprising that treatment of TSC with rapamycin is promising and showed improvement of distinct characteristics in different animal models (Ehninger et al., 2008).

Fragile X syndrome Like in TSC, also in Fragile X syndrome the origin of the disease is found in a genetic mutation that leads to exaggerated protein synthesis. The disease is based on a massive trinucleotide repeat expansion within the gene encoding the fragile X mental retardation protein (FMRP) located on the X chromosome. These trinucleotide repeat accumulations result in transcriptional silencing and loss of the FMRP (Kremer et al., 1991). FMRP is a RNA-binding protein that binds several mRNAs of neuron-specific proteins (including its own), such as Arc, αCamKII, PSD95, APP, PIKE and thereby regulates transcription of those in dendrites and spines in response to neuronal activity (Berry-Kravis et al., 2011; Weiler et al., 1997). In the absence of FMRP the synthesis of many proteins is dysregulated and results in altered LTP and LTD. Additionally, also learning and memory impairments in different paradigms were reported in the mouse model of Fragile X syndrome (Berry-Kravis et al., 2011). It has been proposed that the up-regulation of mTORC1 activity observed in mouse models of Fragile X syndrome is the consequence of the increased expression of PIKE (PI3K enhancer), that activates PI3K and subsequently Akt/PKB, mTOR, S6K and 4E-BP (Sharma et al., 2010).

Schizophrenia Deregulated gene expression is a characteristic of schizophrenic patients. Especially the reduced expression and activity of the PI3K-Akt/PKB-mTOR signaling components was observed (Kalkman, 2006). Mutations in the gene encoding Akt/PKB are associated with the genetic form of schizophrenia and reduced Akt/PKB phosphorylation as well as diminished kinase activity have been found in post-mortem brains of schizophrenic patiens (Santini and Klann, 2011). In line with this correlation, several therapeutic strategies for schizophrenia treatment results in an increased activity of the PI3K- and mTORC1 pathway as reviewed by Kalkman. However, whether the mTORC1 is directly involved in schizophrenia has not been clearly shown to date. Recently, an alternative hypothesis was discussed which suggests that dysregulation of mTORC2 causes reduced Akt/PKB activity (Siuta et al., 2010). However, data that are supportive of this hypothesis are still lacking.

Summarizing this extensive body of work on mTORC1 signaling in brain diseases and disorders, it can generally be concluded that adjusted mTORC1 activity is crucial for proper neuronal function. An imbalance towards either an increased or decreased mTORC1 activity may be detrimental for normal function of the brain, cell survival and cognition. However, to date it is not at all clear whether the observed changes in mTORC1 activity and its pathway components in either animal models, cell culture systems or in human tissue samples are cause or consequence of the according diseases and disorders. In this regard, it is of high importance to unravel the role of mTORC1 signaling in the development and progression of those diseases. Especially the analysis of different cell types, individual stages of a disease and the physiological consequences of altered mTORC1 activity will be crucial for prospective pharmacological therapies.

Disorder	mTORC1 signaling	Readout	Brain regions examined	Impact of rapamycin on behavior
Fragile X syndrome	↑	p-mTOR, p-4E-BP, p-S6K1, mTOR/Raptor, eIF4E/eIF4G interactions	Hippocampus, cortex	Not examined
Tuberous sclerosis complex	↑	p-S6	Hippocampus	Rescue of deficits in spatial memory (Morris water maze) and context discrimination
PTEN mutation (autism)	↑	p-S6	Hippocampus	Rescue of impaired social behaviors, seizures, and macrocephaly
Depression	↓	Ketamine-induced p-mTOR, p-S6K1, and p-4E-BP	Prefrontal cortex	Blockade of antidepressant effects of ketamine (forced swim and novelty suppressed feeding tests)
Schizophrenia Parkinson's disease	↑ ↓ in PD ↑ in l-DOPA-induced dyskinesia	p-S6 p-S6K1, p-S6, p-4E-BP, and p-eIF4E	Hippocampus Striatum	Not examined Reduction of l-DOPA-induced dyskinesia
Huntington's disease	↓	p-S6K, p-S6, and p-4E-BP	Striatum and cortex	Improvement of performance in rotarod, grip, and wire tests; reduction of tremor
Alzheimer's disease	↑ ↓	p-mTOR, p-S6K1, p-4E-BP, and p-eIF4E	Cortex, hippocampus, cerebellum	Rescue of spatial memory (Morris water maze)
Cannabis (THC)	↑	p-S6K1, p-S6, p-eIF4E, p-eIF4G, p-4E-BP	Hippocampus	Blockade of amnesic-like effects of THC (novel object recognition and context discrimination tests)
Cocaine	↑	p-S6K, p-S6	Ventral tegmental area (VTA), nucleus accumbens	Reduction of cocaine-induced locomotor sensitization and cue-induced seeking behavior

Table 1. Summary of altered mTORC1 signaling in brain disorders. (adapted from: Emanuela Santini and Eric Klann *Frontiers in behavioral neuroscience* (2011) 5)

3.3 mTORC1 in synaptic plasticity and learning and memory

The human brain consists of around 100 billion neurons and each neuron possesses around 1000 – 10'000 synapses which allows one cell to connect and to communicate with up to 30'000 other cells. Just by considering these three numeric facts one can anticipate the complexity of the total network that finally forms the brain. The basic principle of how information is processed and stored within this gigantic number of interconnected cells is the plastic modulation of neuronal circuits – and further down in the scale to the level of individual synapses – to a given environmental stimulus. Since the time of Santiago Ramón y Cajal it was hypothesized that the mechanism of informational storage in the brain is based on activity dependent changes in synaptic efficiency. This concept was later refined by Donald O. Hebb in 1949 when he published his paper "*The Organization of Behavior: A Neuropsychological Theory*". The Hebbian theory states that an increase in synaptic efficacy arises from a repeated and persistent stimulation from the presynaptic cell on the postsynaptic neuron (Brown, 2006). While at the time of Hebb's publication this concept was only a theory, the first "Hebbian synapse" was described in 1973 by Terje Lomo and Timothy V.P. Bliss who electrically stimulated the perforant path of rabbit brains and reported a sustained increase of the efficiency of synaptic transmission to the granule cells of the hippocampus (Bliss and Lomo, 1973). Today, this phenomenon is called long-term potentiation (LTP) and is generally thought to be the cellular mechanism underlying synaptic plasticity and learning and memory.

3.3.1 Mechanisms of synaptic plasticity

When talking about synaptic plasticity, one basically has to separate two distinct forms: 1) *functional plasticity* that refers to the change in synaptic strength and efficiency, and 2) *structural plasticity* that involves changes in synapse number, dendritic branching and synaptic connectivity (Wiegert and Bading, 2011). Both forms depend on protein synthesis and gene expression and eventually together add up to what is generally called learning and memory. Within the scope of this manuscript, only functional plasticity will be discussed.

The molecular mechanisms that underlie synaptic plasticity were discovered and still are mainly studied in the hippocampus due to its well described function for learning and memory in humans and the suitable anatomical architecture for electrophysiological approaches. In terms of LTP, two temporally and functionally different forms have been described. E-LTP (early-LTP) lasts for 1-2 hours and is independent of transcription and translation but rather relies on the autonomous kinase activation of several postsynaptic proteins (Roberson et al., 1996). In contrast, L-LTP (late-LTP) lasts several hours and requires new protein synthesis and at later stages also transcription (Reymann and Frey, 2007). Using the example of a "classical" LTP at the CA3-CA1 synapse in the murine

hippocampus, the following section will describe the main steps that are involved in the induction and progression of E-LTP and L-LTP.

Upon neurotransmitter release (typically glutamate) and binding of the transmitter to corresponding postsynaptic receptors (typically AMPA-R) the postsynaptic membrane is depolarized (mainly by Na^+ influx through AMPA-Rs), which subsequently results in the release of the Mg^{2+} block of the NMDA-Rs. The removal of the Mg^{2+} block is a critical step in the induction of LTP and results in a substantial influx of Ca^{2+} through NMDA-Rs into the spine. This event causes a further depolarization of the membrane and activates multiple signaling cascades and triggers subsequent steps (Herron et al., 1986; Reymann et al., 1989). Along with the NMDA-R activation, additional receptors (depending on the induction protocol) such as mGluRs (metabotropic glutamate receptors), VDCCs (voltage-dependent calcium channels) or RyRs (ryanodine receptors, located in the endoplasmatic reticulum) may contribute to the Ca^{2+} influx into the postsynaptic cell (Reymann and Frey, 2007). As a result of the increase in Ca^{2+} in the postsynaptic compartment, different mechanisms are induced (eventually depending on the type of receptors that were involved in the Ca^{2+} influx) that account for distinct types of LTP (E-LTP or L-LTP). These different mechanisms can be roughly classified as follows: post-translational modification, dendritic protein synthesis and nuclear gene regulation.

Post-translational modification Upon weak stimulation, such as 1 HFS (high frequency stimulation), the potentiation of the postsynaptic response is temporally restricted to 1-2 h and typically independent of local protein synthesis. This type of synaptic plasticity is called E-LTP and mainly involves immediate (within 1 min) activation of CamKII by Ca^{2+} and its subsequent autophosphorylation that keeps the kinase in a constitutively activated state up to 1 h post initial activation (Fukunaga et al., 1993). Autophosphorylation of CamKII leads to its association with the PSD where it phosphorylates the GluR1 subunit of the AMPA-Rs (Lisman et al., 2002). It is suggested that the phosphorylation of GluR1 increases the AMPA-R mediated current across the membrane due to an increased conductance of the channel and additionally also by modulation of the receptor trafficking within the synaptic membrane (Soderling and Derkach, 2000). This mechanism is further enhanced by the contribution of other kinases such as PKA and PKC. PKA is activated by cyclic-AMP (cAMP) and inhibits the process of protein phosphatase-mediated dephosphorylation of GluR1 and CamKII and secondly, PKA can directly phosphorylate GluR1 which apparently results in an increased AMPA-R current (Roberson and Sweatt, 1996; Soderling and Derkach, 2000). The involvement of PKC is linked to synaptic mGluR (metabotropic glutamate receptor) activation that leads to the production of diacylglycerol. It was reported that as a consequence of diacylglycerol-mediated activation of PKC, the latter can phosphorylate NMDA-Rs, resulting in an increased Ca^{2+} influx into the postsynapse (Fitzjohn et al., 1996). However, a more important role is assigned to PKC for the control of protein synthesis-dependent mechanisms during L-LTP. A schematic illustration of the mechanisms involved in E-LTP is depicted in Figure 5.

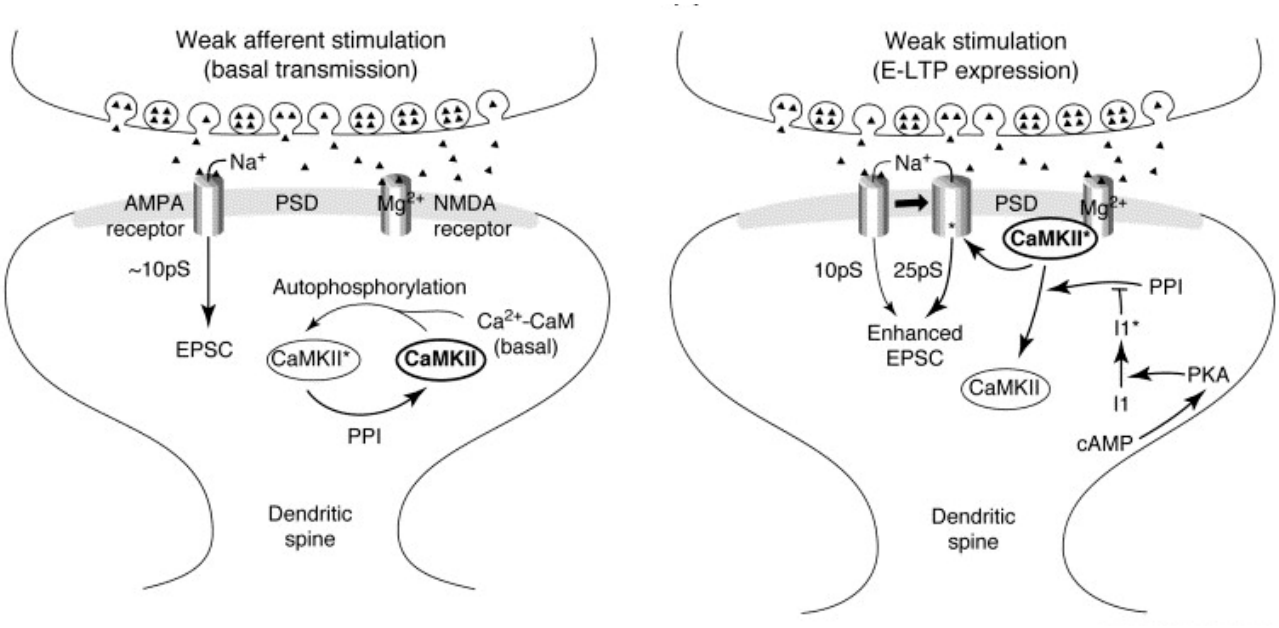

Figure 5. Postsynaptic protein phosphorylation mechanisms during LTP in the CA1 region of hippocampus. *Left*: Basal synaptic transmission via glutamate (triangles) is mediated largely by low-conductance state (~10pS) AMPA receptors that give rise to an EPSC. NMDA receptors are inactive because of voltage-dependent block of their channels by Mg^{2+}. Little of the Ca^{2+}/calmodulin-dependent protein kinase II (CaMKII) is in the activated, phosphorylated state (*), owing to low basal concentrations of Ca^{2+}–calmodulin (Ca^{2+}–CaM) and high activity of protein phosphatase 1 (PP1). *Right*: Early-phase LTP (E-LTP) expression is due, in part, to CaMKII-mediated phosphorylation of the AMPA receptor GluR1 subunit (*), which converts it largely to higher conductance states (~25 pS). The CaMKII is maintained in its autophosphorylated, constitutively active form, owing to protein kinase A-mediated phosphorylation of inhibitor 1 (I1), which blocks the ability of PP1 to dephosphorylate CaMKII and perhaps GluR1. (adapted from: T.R. Soderling and V.A. Derkach *Trends Neuroscience* (2000) 23)

Dendritic protein synthesis As it is the case for all long-lasting cell biological phenomena, the late-phase of LTP requires new protein synthesis. The hypothesis of the dependence of the later phase of LTP on protein synthesis is consistent with the early findings that 1) multiple inhibitors of protein synthesis, with varying modes of action, can affect L-LTP maintenance and 2) that polyribosomes move into activated spines after L-LTP induction (Abraham and Williams, 2008). A L-LTP is typically induced by several HFS pulses that are applied in an inter-stimulus-interval of 1 to 5 min. The signaling components that are thought to link the initial activity in the dendritic spine upon such an intensive stimulation regime to a sustained enhancement of the synaptic efficiency include kinases such as CamKII, PKC, ERK and mTOR (Raymond, 2007). As discussed above, the activation of CamKII is triggered by Ca^{2+} and is required for the induction of an E-LTP and L-LTP. A similar crucial function for the induction of LTP is attributed to PKC (Malinow et al., 1989). Unlike CamKII and PKC, the catalytic fragment of the atypical isoform PKCζ, namely PKMζ, is constitutively active and does not require Ca^{2+} or diacylglycerol for its activation. PKCζ is transcribed independently of PKCζ and its mRNA is transported specifically to dendrites where it is preferentially translated upon LTP induction and subsequently the PKMζ protein contributes to the maintenance of the late, protein

synthesis-dependent phase of LTP by mediating an increased number of AMPA-Rs at the synapse (Ling et al., 2006; Yao et al., 2008). The function of ERK and mTOR is to control local protein synthesis upon L-LTP induction. It was shown recently that besides PKC also the NMDA-R-dependent activation of CamKI by CamKK can trigger the activation of ERK that subsequently regulates mRNA translation via phosphorylation of S6K as well as eIF4E and 4E-BP1 (Schmitt et al., 2005). Similarly, mTORC1 is known to be activated upon neuronal activity via various pathways (see chapter 3.3.2) and mTORC1 triggers both cap-dependent protein synthesis and translation of 5'TOP mRNA by regulating 4E-BPs, S6K and potentially other substrates (Swiech et al., 2008). Proteins encoded by mRNAs containing 5′TOPs have been observed in dendrites (Asaki et al., 2003). However, whether mTORC1-mediated S6K activation is critical for the translation of this specific subset of dendritic mRNA is still controversially discussed (Stolovich et al., 2002). Irrespective of the ongoing discussion on 5'TOP mRNA translation, it is generally thought that ERK and mTORC1 activation results in increased translation initiation of specific mRNAs that code for proteins that are required for the maintenance of L-LTP, such as CamKII or AMPA-R subunits. However, several observations indicate that the global amount of protein synthesis is reduced upon increased neuronal activity. Thus, it is hypothesized that global protein synthesis eventually is differently regulated during LTP than the translation of a specific mRNA pool that encodes for plasticity related proteins (Sutton and Schuman, 2005). In line with this hypothesis, the translational regulation of a subset of mRNAs (including CamKII mRNA) is known to be mediated by cytoplasmic polyadenylation of the 3' end upon neuronal activity. These mRNAs contain short sequences known as cytoplasmic polyadenylation elements (CPEs; UUUUAU or similar) and an AAUAAA sequence (Figure 6). The CPEs are recognized by the CPE-binding protein (CPEB) that functions as a translational repressor when bound to Maskin – an eIF4E binding protein – and as a polyadenylation stimulator and translational activator when phosphorylated. CPEB is phosphorylated by the protein kinase Aurora (also known as Eg2), which induces CPEB to interact with cleavage and polyadenylation-specificity factor (CPSF) on the AAUAAA sequence

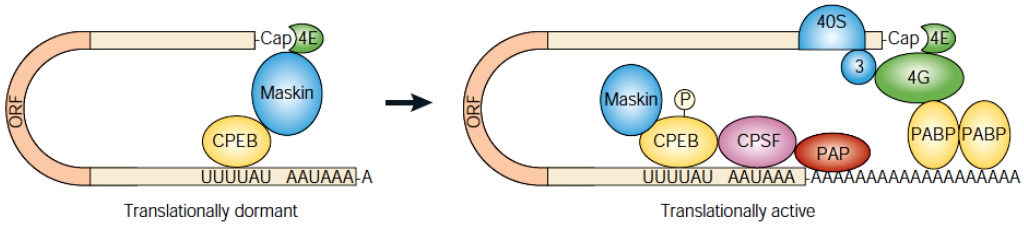

Figure 6. Messenger RNAs containing a cytoplasmic polyadenylation element (CPE) are translationally dormant (masked) and reside in a complex containing the CPE-binding protein (CPEB), maskin and eIF4E. Newly phosphorylated CPEB (by the kinase Eg2) recruits the cleavage and polyadenylation specificity factor (CPSF) and poly(A) polymerase (PAP), which elongates the poly(A) tail. At a time coincident with this elongation, maskin dissociates from eIF4E. One possible cause of this maskin–eIF4E dissociation is the formation of a stable poly(A)-binding protein (PABP)–eIF4G complex, which outcompetes maskin for binding to eIF4E and thereby assembles the 48S complex. (adapted from: R. Mendez and J.D. Richter *Nature Reviews Molecular Cell Biology* (2001) 2)

(Huang et al., 2002; Mendez et al., 2000). Upon CPSF recruitment, the poly(A) tail of the mRNA is lengthened by the poly(A) polymerase. Polyadenylation subsequently causes Maskin to dissociate from eIF4E, permitting the binding of eIF4E to eIF4G, and the subsequent recruitment of ribosomes in order to increase translation (Mendez and Richter, 2001). The inhibition or knockout of CPEB results in impaired synaptic plasticity and deficits in learning and memory (Zearfoss et al., 2008). Similarly, also FMRP – as introduced in chapter 3.2.2 – is an RNA-binding protein that has a well-described function in the transport and translational control of certain mRNAs. FMRP is highly expressed in the brain and preferentially found in the dendritic compartment of neurons where it is associated with ribosomes. In a phosphorylated state, FMRP represses the translation of its target mRNAs (such as PSD95) via the RNA-induced silencing complex (RISC). Upon neuronal activity, FMRP is dephosphorylated by protein phosphatase-2A that leads to a release of RISC from the target mRNAs and enables translation (Mercaldo et al., 2009). Besides these putative mechanisms of selective mRNA-translation control, it was reported that upon L-LTP induction the number of polyribosomes is increased in activated spines (Bourne et al., 2007). Therefore, the current theory of plasticity-related protein synthesis suggests that only about 10 % of the abundant mRNA is capable of undergoing an activity-induced transition from a rather translationally inactive to a preferentially active state. However, there is still not much known about which exact mRNAs belong to the privileged ones that are translated, or what the exact mechanisms are that are involved in the specific mRNA processing, and finally what the initial trigger for the specific mRNA translation is. An overview of the main mechanisms that are known to date to be involved in protein synthesis-dependent L-LTP is depicted in Figure 7.

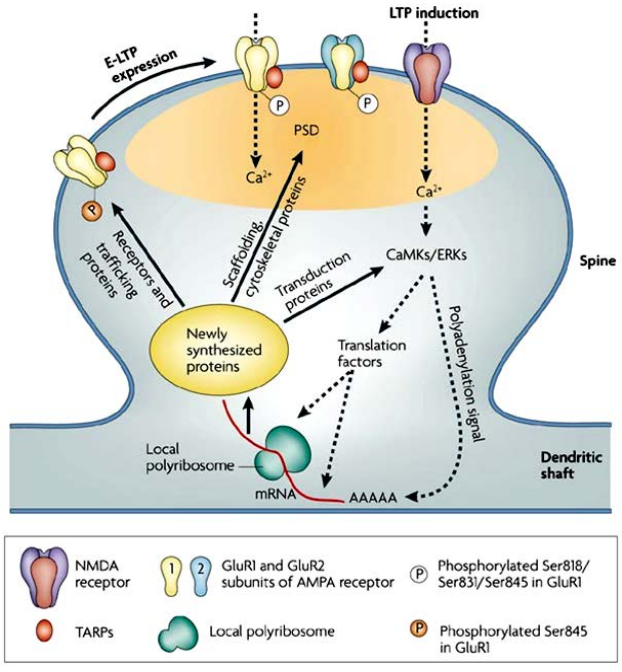

Figure 7. Stimulation of synaptic NMDARs (for example, long-term potentiation (LTP) induction) promotes Ca^{2+} influx that activates calcium/calmodulin-dependent protein kinases (CaMKs) and extracellular signal-related kinases (ERKs) in dendritic spines. These kinases phosphorylate and activate translation factors (for example, eIF4E, 4E-BP1 and CPEB) that are required for the stabilization of local mRNAs through their polyadenylation, and to initiate translation of mRNAs that have been selectively transported into the dendrites and/or spines. This local protein synthesis provides a feedforward mechanism to increase receptor numbers, receptor trafficking, levels of scaffolding and cytoskeleton proteins that promote surface expression, and lateral diffusion and stabilization of AMPARs at potentiated synapses. E-LTP, early phase LTP; PSD, postsynaptic density; TARPs, transmembrane AMPAR regulatory proteins (adapted from: Victor A. Derkach et al *Nature Reviews Neuroscience* (2007) 8)

Gene regulation In contrast to the described mechanisms above, gene transcription is spatially separated from the initial site of activity. Therefore, to trigger gene transcription in the soma, changes in Ca^{2+} concentration at the level of the synapse are in most cases not sufficient but generally rather require additional involvement of VDCCs (Raymond, 2007). The main transcription factors that regulate LTP-specific gene transcription are CREB (cAMP-responding element binding protein) and Elk-1 (E twenty-six (ETS)-like transcription factor 1) and the main immediate early genes involved in L-LTP are *cfos*, *cjun*, *zif268*, *arc* and *homer*. Upon initial elevation of the Ca^{2+} concentration in the spine, several signaling pathways can be triggered which result in CREB or Elk-1 activation: Ca^{2+}/cAMP/PKA/CREB; Ca^{2+}/CamKII/CREB; Ca^{2+}/Ras/ERK/CREB; Ca^{2+}/cAMP/ERK/Elk-1 (Davis et al., 2003). Subsequently, CREB and ElK-1 induce the transcription of the above mentioned immediately early genes that further induce activation of late response genes that encode for proteins such as receptors and structural cell components (Walton et al., 1999).

3.3.2 The role of mTORC1 in synaptic plasticity

In neurons, mTORC1 activity can be triggered by various stimuli, including neurotrophic factors (e.g. BDNF, brain-derived neurotrophic factor), cytokines (e.g. leptin), Ca^{2+} and neurotransmitter activation via G protein-coupled receptors or ionotropic receptors (Swiech et al., 2008). With regard to synaptic plasticity, especially the response of mTORC1 to ionotropic receptor activation, elevated Ca^{2+} levels and BDNF are of interest. Different signaling cascades that converge onto mTORC1 upon neuronal activity are depicted in Figure 8. mTORC1 is considered to be a regulator of local protein synthesis during L-LTP. This assumption is based on several observations. 1) Rapamycin application prevents CA1 L-LTP maintenance in rat hippocampal slices (Tang et al., 2002). 2) Tang *et al*. also showed that mTOR, the translation initiation component eIF4E and the mTORC1 substrate 4E-BP co-localize with post-synaptic markers. These observations strongly suggest that mTOR inhibition with rapamycin targets the postsynaptic translation machinery. 3) It was show that L-LTP is sensitive to application of rapamycin only during the induction paradigm, whereas inhibition of mTORC1 after the establishment of L-LTP was ineffective. 4) Phosphorylation of S6K by mTORC1 has been shown to be induced in an NMDA-R- and PI3K-dependent manner throughout the dendrites but not in the cell bodies of CA1 neurons in hippocampal slices after L-LTP induction. Thus, it is generally hypothesized that the NMDA-R/PI3K-dependent dendritic activation of the mTORC1 pathway is necessary for the induction of protein synthesis-dependent synaptic plasticity (Cammalleri et al., 2003). Several mRNAs of plasticity-related proteins are reported to be translated in response to mTORC1 activity, such as NR1, αCamKII, PSD95, Arc or PKMζ (Garelick and Kennedy, 2011). Furthermore, the relevance of mTORC1 signaling for synaptic plasticity was additionally confirmed in several learning and memory tasks. For instance, rapamycin injections into the amygdala impaired the memory performance in the

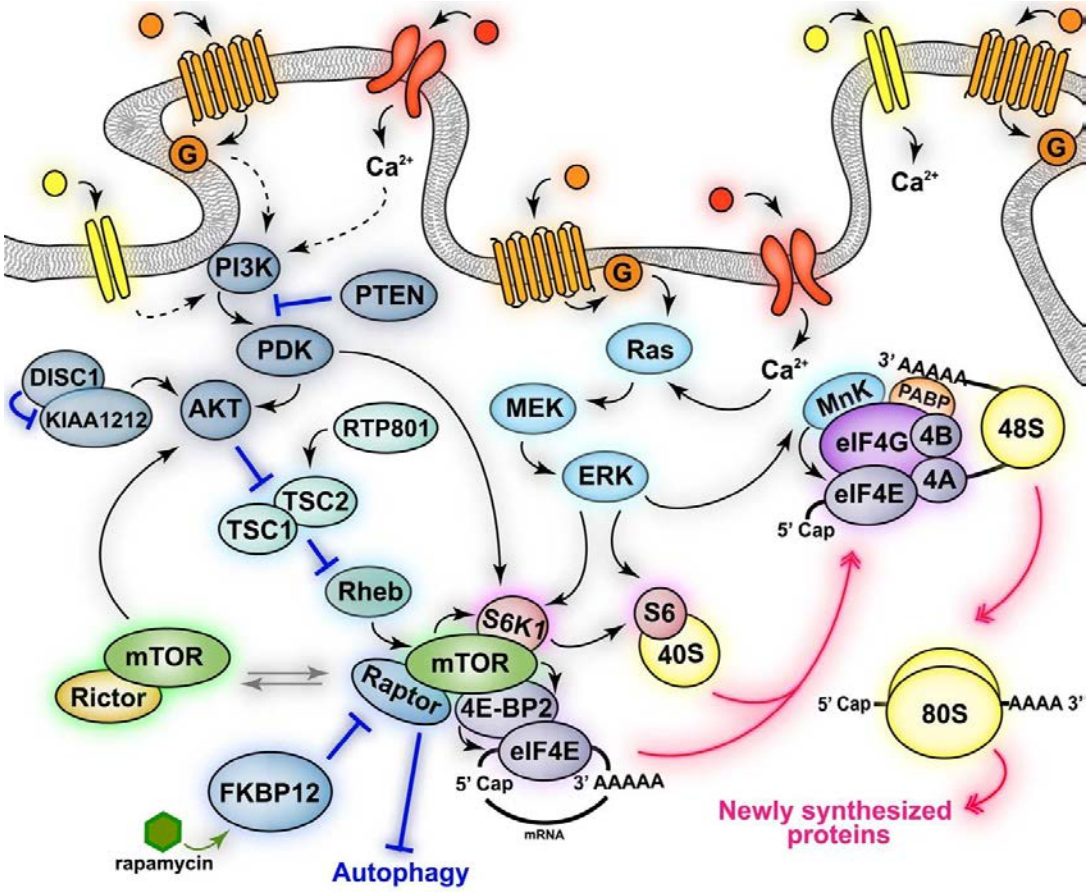

Figure 8. Schematic model of neuronal mTOR signaling pathways. Activation of neuronal receptors and channels (mGluRs, NMDARs, TrkB, D1Rs, and D2Rs) leads to activation of mTORC1 and mTORC2. mTORC1 activation increases some neuronal processes (protein synthesis) while inhibiting others (autophagy). mTORC1 regulates the activity of downstream effectors involved in translation (S6K1, 4E-BP2), some of which are also directly phosphorylated via convergent activation of the MAPK signaling pathway (S6K1, MnK, S6). mTORC1-dependent phosphorylation of 4E-BP2 results in the association of eIF4E with eIF4G and the formation of the active eIF4F (eIF4E–eIF4A–eIF4G) complex. eIF4F recruits eIF4B and MnK and promotes the binding of mRNAs to the 43S pre-initiation complex to form the 48S initiation complex. The eIF4F complex and the poly(A) tail act synergistically together with MnK-dependent phosphorylation of eIF4E to stimulate cap-dependent translation initiation. Black solid arrows indicate direct phosphorylation/activation, pink double arrows represent molecular association/dissociation and blue lines indicate inhibition. (adapted from: Emanuela Santini and Eric Klann *Frontiers in Behavioral Neuroscience* (2011))

cued fear conditioning paradigm. Similarly, rapamycin disrupted memory consolidation in hippocampus-dependent spatial tasks, auditory cortex-dependent memory paradigms and prefrontal cortex-dependent trace fear memory tests (Garelick and Kennedy, 2011). Upon these first descriptions of mTORC1 contribution in L-LTP progression – all of which were mainly based on rapamycin application – several studies aimed to analyze different knockout mouse models in which up- or downstream components of the mTORC1 signaling pathway were depleted. A summary of the findings from such knockout mouse models is depicted in Table 2. Striking with regard to these

genetic studies is the variety of phenotypes that were reported at both the level of behavior and the level of electrophysiology. One explanation for this diversity in phenotypes could be that different genetic approaches were used, such as global knockout, cell type-specific knockout, virus-induced knockout, or heterozygous knockout. Second, the complexity of the mTORC1 signaling pathway, and in particular the negative feedback loop onto IRS, has to be taken into account when the results of a particular knockout animal model are discussed. Depending on whether a particular protein of interest lies up- or downstream of mTORC1 and depending on how expansively the potentially altered feedback inhibition influences the components and activity of the total signaling network, the knockout phenotypes of two closely related proteins can eventually vary quite extensively. Therefore, in future it will be important to carefully analyze the role of mTORC1 at the level of individual cell types and in the bigger context of mTORC1 as an integrator of various signals ranging from neuronal activity, growth factors, survival cues or stress. An attempt towards this goal was carried out by the studies on which is reported in this manuscript.

gene	mouse model	mTORC1 activity	behavior phenotype	LTP / LTD phenotype	electrophysiological properties	comments	reference
PTEN	αCamKII-Cre mediated cKO	↑	MWM: decreased memory	LTP: decreased LTD: decreased	PPF: no change input-output: no change mEPSC: no change	rescue of LTP / LTD phenotype with PDK cKO; no rescue of MWM deficits	(Sperow et al., 2012)
PDK1	αCamKII-Cre mediated cKO	↓	not analyzed	LTP: no change LTD: no change	not analyzed	normal hippocampal architecure	(Sperow et al., 2012)
TSC1	GFAP-Cre mediated cKO	↑	FC: decreased memory MWM: decreased acquisition	LTP: decreased	mEPSC: no change	elevated extracellular glutamate levels	(Zeng et al., 2007)
TSC1	AAV-Cre virus mediated KO	↑	not analyzed	LTD: mGluR-LTD disrupted NMDA-dependent LTD unchanged	mEPSC: no change evoked excitatory currents: increased	increased soma size	(Bateup et al., 2011)
TSC2	$TSC2^{+/-}$ (Eker rat)	↑	not analyzed	LTP: decreased LTD: decreased	PPF: increased input-output: no change	LTP phenotype independent of GABAergic system	(von der Brelie et al., 2006)
FKBP12	αCamKII-Cre mediated cKO	↑	FC: enhanced context LTM MWM: increased preservation	LTP: increased LTD: not analyzed	PPF: no change input-output: no change E-LTP: no change	increased raptor-mTOR interaction	(Hoeffer et al., 2008)
mTOR	$mTOR^{-/+}$ mice + low dose of rapamycin	↓	FC: decreased memory	LTP: decreased	PPF: no change input-output: no change	impaired reconsolidation	(Stoica et al., 2011)
S6K1	$S6K1^{-/-}$	↓	FC: decreased memory MWM: modest spatial learning deficit	L-LTP: no change E-LTP: decreased	PPF: no change input-output: no change	S6K2 knockout have no deficit in E-LTP	(Antion et al., 2008)
4E-BP2	$4E\text{-}BP2^{-/-}$	↑	MWM: impaired learning and memory	E-LTP: increased L-LTP: decreased	PPF: no change input-output: no change	rescue of E-LTP phenotype by rapamycin application	(Banko et al., 2005)

Table 2. mTORC1 related mouse models. The targeted genes and the phenotypes in different behavior- and electrophysiological paradigms are indicated. Abbreviations: MWM, Morris water maze; FC, fear conditioning; E-LTP, early long-term potentiation; L-LTP, late long-term potentiation; LTD, long-term depression; PPF, paired-pulse facilitation; mEPSC, miniature excitatory postsynaptic current.

3.4 The aim of the study

The goal of this study was to analyze the specific contribution of mTORC1 in 1) brain development and 2) adult neuronal functions such as synaptic efficiency, synaptic plasticity and learning and memory. Due to the fact that null mutants of *mTOR*, *rptor* and *mLST8* are early embryonically lethal, a detailed analysis of mTORC1 in the brain was precluded so far. In regard to brain development, most of the knowledge about mTORC1 signaling that was obtained to date is based on rapamycin application in primary neuron cultures. Similarly, also the role of mTORC1 in adult synaptic plasticity was preferentially studied by treatment of hippocampal slices with rapamycin. The major drawback of pharmacological inhibition lies in the fact that both the compound specificity and the effect specificity are not guaranteed.

To circumvent premature death of whole body knockout mice and certain unpredictable side effects or non-cellautonomous effects by the use of pharmacological inhibiton, two conditional knockout mouse models were generated on the basis of the Cre-LoxP system. As a consequence of the existence of two functionally different multi-protein complexes – mTORC1 and mTORC2 – that both include mTOR as the catalytic component of the respective complex, the genetic targeting of mTOR would not result in a specific mTORC1 deficiency. Thus, we generated mice with floxed *rptor* alleles in our lab. Raptor is the regulatory associated protein of mTOR necessary for mTORC1 function.

For the analysis of the role of mTORC1 during brain development, Cre-mediated knockout of *rptor* was achieved by crossing floxed mice with mice expressing the Cre recombinase under the Nestin promoter that gets activated as early as E10.5 in neuronal tissue. The characterization of these mice was primarily performed by Dimitri Cloëtta and Venus Thomanetz.

In order to study the involvement of mTORC1 in postnatal excitatory neuronal function, the same floxed mice were used in combination with an α-CamKII-Cre mouse line. The α-CamKII promoter starts to be active about P18 and reaches full activity by P29. Therefore, the embryonic development and postnatal maturation should not be compromised in these mice. Such a conditional knockout mouse model serves as an ideal tool to study basic neuronal functions, synaptic plasticity and learning and memory.

4 RESULTS

4.1 Paper 1 (in preparation)

Raptor controls mTORC1, synaptic efficiency, plasticity and learning and memory in the adult murine brain

Regula M. Lustenberger[1], David P. Wolfer[2,3], Kaspar E. Vogt[1], and Markus A. Rüegg[1]

[1]Biozentrum, University of Basel, CH-4056 Basel, Switzerland
[2]Institute of Anatomy, University of Zurich, CH-8057 Zurich, Switzerland
[3]Institute of Human Movement Sciences and Sport, ETH Zurich, CH-8057 Zurich, Switzerland

Key words: synaptic plasticity, Morris water maze, fear extinction, E-LTP, L-LTP, cell size

Send correspondence to:
Markus A. Rüegg, Ph.D.
Biozentrum, University of Basel
Klingelbergstrasse 70
CH-4056 Basel, Switzerland
Phone: +41 61 267 22 23
Fax: +41 61 267 22 08
email: markus-a.ruegg@unibas.ch

ABSTRACT

The mammalian target of rapamycin complex 1 (mTORC1) regulates many processes, including cell growth, survival and proliferation. In the central nervous system, deregulation of mTORC1 has further been implicated in neurodegenerative diseases, autism spectrum disorders and plasticity. Here we investigated the role of the mTORC1-defining component raptor in adult forebrain neurons by postnatal, tissue-specific deletion of the *rptor* gene (*R*cKO mice). Biochemical analysis showed successful inhibition of the mTORC1 downstream substrates S6 and 4E-BP1 and hyperactivation of the IRS-Akt/PKB-TSC axis due to relief of S6K-mediated feedback inhibition. Electrophysiological recordings revealed reduced synaptic efficiency and impairment in both early and late forms of LTP. Behaviorally, *R*cKO mice showed learning and memory deficits in the Morris water maze and impaired fear extinction. Interestingly, the deficits in the water maze paradigm could be occluded by short training-intervals during the acquisition phase. Furthermore, the targeted brain-regions showed a reduction in size. In summary, our data show that in the adult brain mTORC1 activity is crucial to maintain neuron function and synaptic plasticity. These results thus indicate that prolonged treatment with mTORC1 inhibitors might be detrimental for brain function.

INTRODUCTION

In the adult brain, information processing takes place within neuronal networks down in the scale to the level of individual synapses. One of the most studied forms of information processing, synaptic modification and its underlying molecular features is hippocampus-dependent learning and memory. Synaptic strength can bidirectionally be modified upon a previously received input depending on the temporal pattern and intensity of the received stimulus. This ability of synapses to undergo long-lasting changes on the functional, structural as well as biochemical level in response to certain activation is termed synaptic plasticity. It is reflected in the electrophysiological concept of long-term potentiation or depression (LTP or LTD), respectively. Temporal forms of LTP are characterized by an early phase of LTP (E-LTP) lasting 1-2 hours, which is transcription and translation independent, and a late phase of LTP (L-LTP) lasting several hours, which is dependent on new protein synthesis and transcription (Bartsch et al., 1998; Frey et al., 1988; Frey and Morris, 1997; Kelleher et al., 2004). The ability of isolated CA1-dendrites to undergo L-LTP provides evidence that local mRNA translation plays a critical role in protein synthesis-dependent forms of plasticity (Kang and Schuman, 1996; Tsokas et al., 2005). Multiple components of the translational machinery were shown to be localized within dendrites or even spines, which corroborates the importance of *de novo* protein synthesis within these structures (Steward and Schuman, 2003). Several protein kinases have been implicated in the initiation or maintenance of translation-dependent LTP. Among these, CamKII, mitogen-activated protein kinase (MAPK), extracellular signal-related protein kinase (ERK), protein kinase C (PKC) and the mammalian target of rapamycin (mTOR) have been associated to plasticity-related processes (Kelleher et al., 2004; Klann et al., 1991, 1993; Malinow et al., 1989; Tsokas et al., 2007).

mTOR is a serine/threonine protein kinase that associates with two biochemically and functionally distinct multiprotein complexes. mTOR together with the scaffold protein raptor forms the mTOR complex1 (mTORC1) that is inhibited by the immunosuppressant rapamycin. mTORC2, with rictor as the complex-defining protein, is largely rapamycin insensitive (Kim et al., 2002; Sarbassov et al., 2004). The mTORC1 signaling pathway is activated by various growth factors and the insulin receptor substrate (IRS) that activates PI3K, which in turn phosphorylates Akt/PKB. Activated Akt/PKB causes the phosphorylation of TSC2 and subsequent activation of Rheb (Ras enriched in brain). Rheb, in turn, activates mTORC1 that controls a wide range of cellular processes, including protein synthesis, ribosome biogenesis, cell growth, gene transcription, autophagy and metabolism (Wang and Proud, 2011). In the CNS, mTORC1 has been shown to be involved in axonal outgrowth and navigation, dendritic arborization as well as spine and filopodia formation (Campbell and Holt, 2001; Jaworski et al., 2005; Kumar et al., 2005; Piper et al., 2006; Tavazoie et al., 2005). Recently, several neurodegenerative disorders like Parkinson's-, Alzheimer's- and Huntington's disease and mental disorders, such as schizophrenia or autism have been linked to mTORC1 dysfunction (Santini and

Klann, 2011; Swiech et al., 2008). However, whether altered mTORC1 signaling is cause or consequence of these pathologies remains to be elucidated.

Besides this wide range of diseases, the role of mTORC1 in synaptic plasticity and learning and memory has been discussed. The induction of LTP was shown to activate mTORC1 that subsequently phosphorylates its downstream targets ribosomal S6 kinase (S6K) and the translation regulator 4E-BP. These phosphorylation events are suggested to positively regulate 5'TOP mRNA and cap-dependent translation (Gelinas et al., 2007; Tsokas et al., 2007). Thus, mTORC1 is a prominent candidate to trigger protein synthesis-dependent processes locally at the synapse. Yet, there is still debate about the role of the mTORC1-S6K axis in 5'TOP mRNA translation during LTP. Rapamycin only partially blocks TOP mRNA translation and mice lacking S6K do not show a defect in TOP mRNA translation (Shima et al., 1998; Stolovich et al., 2002). Further, neither S6K1 nor S6K2 knockout mice show deficits in L-LTP progression (Antion et al., 2008). On the other hand, increased activity of the mTOR pathway was shown to substantially affect synaptic plasticity. Both, the ablation of upstream negative regulators of mTORC1, such as PTEN, TSC and FKBP12 (Hoeffer et al., 2008; Sperow et al., 2012; von der Brelie et al., 2006) and the knockout of the mTORC1 downstream target 4E-BP (Banko et al., 2005), alter L-LTP. Thus, the question arises, whether mTORC1 signaling only affects synaptic plasticity when hyperactivated but does not prevent LTP when inactivated. No direct genetic targeting of mTORC1 has so far been applied to clarify this open question. Furthermore, data from long-term inactivation of mTORC1 in the postnatal brain are currently lacking.

RESULTS

Reduced brain size in mice lacking mTORC1 signaling in forebrain neurons

To analyze the *in vivo* neuronal function of mTORC1 in the adult brain and more specifically its role in processes involved in synaptic plasticity and learning and memory we generated mice lacking the mTORC1-defining protein raptor in forebrain excitatory neurons. We therefore crossed *rptor*$^{fl/fl}$ (Bentzinger et al., 2008) mice with mice expressing Cre-recombinase under the control of the α-CaMKII-promoter (Tsien et al., 1996), hereafter called *R*cKO mice (Fig. 1A). The successful recombination of the floxed *rptor*-alleles was shown by PCR and revealed the removal of exon 6 in the cortex (CX), the CA1 and CA3 area of the hippocampus as well as the dentate gyrus (DG). No recombination was detected in the cerebellum and in non-CNS parts of the body, such as the tail, indicative of the specificity of the recombination process (Fig. 1B). On the protein level, raptor was reduced in lysates of the CA1-region as well as in the CX of *R*cKO mice. The phosphorylation of mTOR at serine 2448, a site reflecting mTORC1 activity, as well as phosphorylation of the well-known mTORC1 downstream targets S6(Ser235/236) and 4E-BP1(Ser37/46) were found to be reduced in *R*cKO brains compared to controls (Fig 1C; Supplementary Table S1). In addition, immunohistochemical staining of pS6 revealed a significant reduction in the CA1 region of *R*cKO mice as well as a partially reduced signal in the CA3 region and the DG (Fig. 1Fd). Besides the reduction of raptor and the phosphorylation levels of mTORC1 downstream targets, we additionally observed a significant reduction of mTOR protein (Fig. 1C; Supplementary Table S1). The mTORC1 signaling cascade has a well described feedback inhibition that is exhibited from S6K to IRS1. To address whether the reduced phosphorylation of S6 is also reflected in a lack of this feedback loop, we analyzed mTORC1 upstream targets. As shown in Figure 1D, the phosphorylation levels of IRS1(Ser636/639), Akt/PKB(Thr308), Akt/PKB(Ser473) and TSC2(Ser1432) were increased in *R*cKO lysates. Since Akt/PKB(Ser473) is also phsophorlyated by mTORC2 (Wullschleger et al., 2006), we tested the activity of mTORC2 by quantifying mTOR-phosphorylation at the complex2-specific residue Ser2481, by quantifying the protein rictor and the phosphorylation of the mTORC2 downstream targets PKCα and PKCγ (Fig. 1E; Supplementary Table S1). No difference in these phosphorylation sites or in the amount of rictor between control and *R*cKO mice could be detected. These data indicate that deletion of *rptor* by α-CaMKII-driven recombination specifically inactivates mTORC1 signaling and does not affect mTORC2. This inactivation of mTORC1, in turn causes increased phosphorylation of the IRS-Akt/PKB-TSC axis due to the lack of the negative feedback-loop that S6K normally exhibits on IRS. In addition, we could not detect any change in mTORC2-signaling.

To address whether the absence of mTORC1 signaling in forebrain neurons affects the general appearance of *R*cKO mice, we tested for several brain-specific and general physiological parameters (Fig. 1F and 1G). The overall brain size of *R*cKO mice was reduced without altering the basic structural architecture of the brain. The hippocampus was formed correctly in *R*cKO brains but was

significantly reduced in its weight. Measurements of dendritic length and soma size of *R*cKO CA1 hippocampal neurons revealed a significant decrease in both parameters compared to control mice (Supplementary Figure S1). Additionally, a reduction in the weight of the cortical tissue fraction was observed. To exclude that the reduction in brain weight was the result of apoptosis, we also examined cleaved caspase3 and ubiquitinylation in tissue sections and protein lysates, respectively (Supplementary Figure S2). No signs of increased degradation or cell death were observed in *R*cKO brains. Furthermore, no change in the weight of the cerebellum was detected, indicative for a specific weight reduction only in those brain structures that also showed recombination of the floxed *rptor* alleles. This observation is in line with the well-described function of mTORC1 in cell size control (for review see: (Wullschleger et al., 2006)). Despite the smaller size, the spine density seemed not changed in raptor-deficient CA1 neurons as determined by Golgi staining, suggesting that postnatal synaptogenesis and formation of the overall neuronal networks were not altered in *R*cKO mice. The lifespan of *R*cKO mice and control littermates did not differ and no difference in the body weight could be detected (data not shown). Furthermore, no abnormalities in motor function could be detected (data not shown). Proper motor control is essential for several behavioral tasks. Taken together, our data show that mTORC1 is not active in excitatory neurons of the forebrain in *R*cKO mice, which led us to conclude that they are ideally suited to study the role of mTORC1 signaling electrophysiologically and behaviorally.

Raptor depletion causes task-specific impairment in learning and memory

Synaptic plasticity on a long-term scale is known to depend on local *de novo* protein synthesis and based on experiments using rapamycin, mTORC1 has been suggested to contribute to such synaptic translational events (Gafford et al., 2011; Stoica et al., 2011; Tsokas et al., 2005). To test this hypothesis more directly, we tested whether the lack of mTORC1 signaling in *R*cKO mice caused alterations in spatial and associative learning and memory in the Morris water maze (MWM) and fear conditioning (FC) paradigm, respectively.

First, the MWM experiment consisted of two training sessions per day over 14 days with a probe trial at day 10 as well as two probe trials after training (24 h and 14 days post training). During the acquisition phase, the *R*cKO mice performed clearly worse than littermate controls. While control mice showed a constant and significant reduction of the escape latency and the swim path, the learning-curve of *R*cKO mice differed significantly from that of control mice in both the swim path and escape latency (Fig. 2A). These data indicate that the knockout mice exhibit a pronounced spatial learning impairment. To assess memory performance, the mice were tested in 3 individual probe trials. The first probe trial on day 10 within the acquisition phase revealed a significant preference of both genotypes for the target zone, yet the time that the *R*cKO spent in the target zone was significantly lower compared to controls (Fig 2A). On probe trial 2 (24 hours after training), both genotypes showed

a significant preference for the area where the platform formerly was located without any difference between genotypes. In contrast, *R*cKO mice performed clearly worse than controls in the last probe trial (14 days after training). While the preference for the target zone remained high in coltrol mice, *R*cKO mice completely lost their formerly acquired preference for the target zone and performed significantly worse compared to control mice (Fig 2A). These data identify mTORC1 as an important component for the acquisition and maintenance of spatial long-term memory.

To test whether the remarkable deficits of *R*cKO mice in learning and memory were modifiable by an efficient within-day-training, we used a second configuration of the MWM. This consisted of a similar total number of trials arranged in 6 training sessions per day over a total of 4 days followed by two probe trials. This version of the MWM is characterized by an intensive acquisition phase with short time intervals between individual training sessions. The *R*cKO mice showed an initial learning deficit during the very first day (Fig. 2B). However, this deficit disappeared over the total acquisition phase and both control and mutant mice showed a significant reduction in escape latency and swim path over the total training phase. This indicates that the learning impairment in *R*cKO mice can be largely occluded by short training intervals. Subsequently, the memory performance was tested in two separate probe trials. Surprisingly, both genotypes displayed in probe trial 1 (24 h post training) and probe trial 2 (14 days post training) a clear preference for the target zone (Fig. 2B). These data indicate that both the learning and the long-term memory deficit of *R*cKO mice can be overcome in paradigms with a temporal arrangement of the training sessions that does not involve extensive overnight consolidation.

To determine whether mTORC1 would also be involved in other forms of learning and memory, we tested the mice with a conditioned fear paradigm. The mice were trained with 3 shocks paired with a tone and freezing upon conditioning was analyzed. Both genotypes showed very low and similar levels of freezing prior to the training and displayed an increased freezing in response to the training. The training effect was even higher in *R*cKO mice compared to controls (Fig 2C). Associative memory was tested 24 h and 14 days after the conditioning and we found no significant differences at both time points in either the cue or the context test between control and KO mice (Fig 2C). Control as well as *R*cKO mice demonstrated similar freezing levels at 24 h and 14-21 days post training, indicating that the formation of a context and cue associative long-term memory under these particular training conditions is mTORC1 independent. Following the testing of long-term memory in the cue and context test, we performed an extinction test. Extinction of fear refers to the reduction in the measured level of freezing to a cue previously paired with an aversive event when that cue is presented repeatedly in the absence of the aversive event. This process is thought to represent not an erasure of the original fear memory but instead an active form of learning (Davis, 2011). The performance of *R*cKO mice in the extinction test disclosed a clear deficit compared to control mice. Both control and mutant mice showed decreased freezing in response to the extinction training; however, the learning curve in raptor

deficient mice was significantly slower compared to controls (Fig 2D). This observation indicates that besides spatial learning and memory, the mTORC1 signaling pathway is also critically involved in the distinct process underlying extinction learning.

Loss of raptor affects aspects of basal synaptic activity

Based on the learning and memory deficits of the *R*cKO mice, we next investigated whether the lack of raptor also affected synaptic function and plasticity. To asses synptic propoerties, we first analyzed miniature excitatory postsynaptic currents (mEPSC) in CA1 neurons by patch-clamp recording. While no difference in the mean frequency was observed, the mean amplitude of the mEPSCs in *R*cKO mice was significantly smaller than in controls (Fig. 3A). In addition, the input-output relationship in field recordings from *R*cKO mice was shifted towards a smaller ratio of fEPSP slope and fibervolley (Fv) amplitude (Fig. 3C). Consistent with these observations, protein levels of GluR2 were reduced in lysates of the CA1 region from *R*cKO mice (Fig. 3D). Together, these results indicate that the efficiency of the postsynapse in raptor-deficient neurons is impaired.

To investigate whether mTORC1 was also involved in presynaptic short-term plasticity, we analyzed paired-pulse facilitation (PPF) in field recordings at the Schaffer collateral-CA1 synapse. No difference between control and *R*cKO mice could be observed in an inter-pulse-interval in the range from 20 - 200 ms (Fig. 3B). These data suggest that presynaptic properties are not affected in *R*cKO mice.

Impaired E-LTP and L-LTP in *R*cKO mice

To determine whether the observed deficits in learning and memory of *R*cKO mice in the MWM and the FC-extinction test was also reflected in altered LTP, we examined the expression of both L-LTP and E-LTP. Previous work based on the application of rapamycin suggested that protein synthesis dependent L-LTP requires mTORC1 signaling, whereas the translation-independent E-LTP did not (Cammalleri et al., 2003; Tang et al., 2002; Tsokas et al., 2005). However, genetic ablation of S6K1/S6K2, the main downstream targets of mTORC1, did not interfere with the maintenance of L-LTP but rather compromised E-LTP (Antion et al., 2008). Therefore, it is still controversial what role mTORC1 plays in different forms of LTP. To address this open question, we first measured L-LTP in hippocampal slices of *R*cKO and control mice by applying three trains of high frequency stimulation (HFS) to the Schaffer collaterals. In control mice, such stimulation induced an increase of the field excitatory postsynaptic potential (fEPSP) that lasted for the entire duration of recording of 4 hours. In contrast, the potentiation of the *R*cKO fEPSPs constantly decreased over time and reached baseline level after 3-4 hours (Fig. 4A). This observation indicates that the maintenance of the protein synthesis-dependent form of LTP induced by HFS requires mTORC1 signaling in the hippocampus. To test whether rapamycin would have a similar effect on L-LTP maintenance when added to control

slices and to test whether LTP progression of *R*cKO slices was further changed by rapamycin, we performed L-LTP recordings in the presence of 1 µM rapamycin. Such treatment did not further alter the course of the L-LTP in *R*cKO slices (Fig. 4B), whereas the maintenance of the potentiation in control slices was abolished (Fig. 4C). This is the first time that direct genetic interference with mTORC1 is shown to resemble the pharmacological inhibition of mTORC1 by the use of rapamycin regarding the L-LTP phenotype (summarized in Fig. 4D). Further, the L-LTP progression of *R*cKO and control slices in the presence of the ERK-inhibitor PD98059 were indistinguishable from each other (Supplementary Figure S3). Thus, potential compensatory mechanisms by increased ERK signanling (Chen et al., 2010) are unlikely in *R*cKO mice.

To address whether E-LTP was also affected by the raptor deficiency, we used a single HFS applied to the Schaffer collaterals to induce an early-LTP response in the CA1 neurons. Surprisingly, this *de novo* protein synthesis-independent form of plasticity was also altered in the *R*cKO mice. The decline of the fEPSP slope after HFS stimulation was more pronounced in knockout slices and significantly differed from control 1 h post LTP induction (Fig. 4E, F).

DISCUSSION

mTORC1 signaling is activated by diverse neuronal signals such as glutamate or BDNF and mTORC1 dysfunction has been linked to several neurodegenerative and mental disorders (Swiech et al., 2008). Therefore, this pathway is thought to critically regulate neuronal function and plasticity in the adult brain. However, data supporting this notion originate from retrospective observations in mice modeling neurodegenerative disorders or from interference with mTORC1 signaling using either rapamycin or genetic approaches that target up- or downstream targets of mTORC1. In most of those mouse models mTORC1 activity is increased. Furthermore, results from these genetic approaches are controversial, e.g. for LTP and memory performance in mice with conditional or constitutive deletion of the genes coding for TSC2, 4E-BP2 or FKBP12 mice (Banko et al., 2005; Hoeffer et al., 2008; von der Brelie et al., 2006). The only mouse model in which mTORC1 signaling was diminished are mice with a deletion of the genes encoding S6K1 and S6K2 (Antion et al., 2008). These mice, however, did not show a deficit in L-LTP but in E-LTP. The impairment of the early form is not consistent with studies using rapamycin where only forms of L-LTP were altered (Cammalleri et al., 2003; Tang et al., 2002). Finally, the data using pharmacological inhibitors of mTORC1 are controversial. There, the effect depends on the brain structure, the application scheme and the species (mice, rats, humans). In some studies, treatment with rapamycin had a very restrictive or even an enhancing effect on LTP or memory (Lang et al., 2009; Panja et al., 2009; Tsokas et al., 2007). Thus, despite the several studies published, the function of mTORC1 in adult neurons remained unclear as its role was so far not directly studied.

We therefore aimed to study the impact of a temporally and spatially restricted inhibition of mTORC1 signaling on a genetic based mouse model. Due to the fact, that mTOR can be found in at least two distinct multi-protein complexes, depletion of mTOR itself does not allow an analysis of the specific function of mTORC1. To overcome this problem, we choose the mTORC1-defining protein raptor as target for our genetic approach. We took advantage of the Cre-LoxP system and found that α-CamKII-Cre mediated depletion of exon 6 of the gene encoding raptor resulted in specific recombination of the targeted allele in the cortex, the hippocampus but not in the cerebellum or non-CNS parts of the body. Further, we could show that the presence of raptor is critical for mTORC1 signaling in the brain since ablation of raptor led to decreased phosphorylation of the two well-known downstream targets S6 and 4E-BP. In other tissues, it is described that S6K exhibits a negative feedback loop onto IRS to prevent exaggerated mTORC1 signaling (Bentzinger et al., 2008). We could clearly show that this feedback inhibition also exists in the brain. Especially the pronounced increase in Akt/PKB phosphorylation on both residues Thr308 and Ser473 indicates how sensitively mTORC1 regulates Akt/PKB in the CNS. Since we could not detect any significant change in mTORC2 signaling, the activation of Akt/PKB(Ser473) is very likely mTORC2 independent, as it has been also shown previously in our lab on muscle tissue (Bentzinger et al., 2008). Akt/PKB signaling is

involved in the control of apoptosis and ubiquitin-related aging (Low, 2011). Previous studies on enhanced Akt/PKB signaling in the brain reported an increased susceptibility to seizures and increased neuronal cell size (Tokuda et al., 2011). So far, we could not detect any detrimental effects of the remarkably increased Akt/PKB activity in *R*cKO brains. No signs of tumorgenesis, deregulated ubiquitinylation or apoptosis could be detected and neuron size was not increased but reduced in *R*cKO mice. Thus, we have evidence that constitutively activated Akt/PKB in combination with repressed mTORC1 signaling does not detrimentally affect cell survival in the adult brain. Further, we hypothesize that at least the increase in cell size induced by increased Akt/PKB-activity that has been reported by Tokuda *et al.* is likely dependent on mTORC1-activity. Despite the downstream and feedback loop targets of mTORC1 we surprisingly found, that the amount of mTOR protein was also reduced in KO tissue, indicative for the importance of raptor for the abundance of mTOR in the brain. The same observation was done in the study of Kim *et al*. where they showed that reduced levels of raptor negatively regulates mTOR abundance without affecting its mRNA levels (Kim et al., 2002). However, this was not observed in in other tissue-specific *rptor* knockout mice so far.

A key finding of our study is that mTORC1 has a distinctive role in learning and memory. We show that in learning tasks which rely on consolidation over a long time window (several hours), a process that strongly depends on new protein synthesis, mTORC1 is crucial for acquisition and retrieval of the learned task. We observed specific learning and memory impairments in the MWM upon long inter-training-interval conditions. Interestingly, upon intensive training, the deficits in learning and memory in the water maze could be decreased in KO mice. These data indicate that mTORC1 very likely is a regulator of processes involved in protein synthesis-dependent neuronal plasticity and that the lack of mTORC1 signaling can be overcome under circumstances where the consolidation phase is within a short time window that presumably does not completely rely on *de novo* protein synthesis. These findings resemble the phenotype of CREB-mutant mice (Gass et al., 1998). Interestingly, the *R*cKO mice exhibit a specific fear-extinction learning deficit without showing alterations in the other fear conditioning parameters. This observation points towards a role of mTORC1 in this specific type of NMDA-R-dependent form of plasticity. Further investigations will be carried out to clarify the underlying mechanism of this interesting phenotype.

Further, our results together with the data from Antion *et al.* provide evidence that mTORC1 mainly contributes to long-term plasticity via its regulation of 4E-BP and that activation of S6K is probably not involved in L-LTP but rather in E-LTP. While S6K1 knockout mice show impaired E-LTP but do not display a L-LTP deficit in electrophysiological experiments, *rptor* deletion results in reduced S6 and 4E-BP activity and *R*cKO mice exhibit an impairment in both forms of LTP. Thus, our data for the first time provide electrophysiological and behavioral evidence that mTORC1 signaling is critical for learning and memory performance.

In addition to deficits in neuronal plasticity and learning and memory, we found a reduction in synaptic efficiency in *R*cKO mice that is potentially due to a reduced availability of GluR2 in raptor deficient neurons. In line with this observation, the overexpression of PTEN (a mTORC1 suppressor) in hippocampal slices results in depressed synaptic transmission (Jurado et al., 2010). The opposite phenotype is observed in 4E-BP2$^{-/-}$ mice, in which Bidinosti *et al.* showed an increase in mEPSC amplitude (Bidinosti et al., 2010). Together with our data, this indicates that the regulation of mTORC1 signaling in neurons is critical for both specific protein synthesis-dependent plasticity processes (such as L-LTP) and for the maintenance of basal synaptic functions. To date, this aspect of the mTORC1 signaling has not been intensively discussed. It could well be that mTORC1 activity is regulating the basal synthesis-level of AMPA receptors and other synaptic proteins and upon further stimulation of mTORC1 by increased synaptic activity mTORC1 additionally contributes to the L-LTP-specific *de novo* protein synthesis. In line with this hypothesis, the study by Auerbach *et al.* provides evidence that diseases such as fragile X syndrome or TSC, both of which are associated with increased mTORC1 activity, are potentially based on alterations in the control of basal protein synthesis (Auerbach et al., 2011). Furthermore, several studies report a conversion of E-LTP to L-LTP under conditions of constant mTORC1 hyperactivity (Banko et al., 2005; Ehninger et al., 2008). In combination with our observations, these data point towards an important role of mTORC1 in protein synthesis homeostasis in adult neurons and indicate that unbalanced mTORC1 signaling can have detrimental effects on brain functioning and the coordination of plasticity-related processes.

To date, we cannot explicitly assign the plasticity-related phenotypes we observed in the *R*cKO mice to one (control of basal protein synthesis-level) or the other (*de novo* protein synthesis) role of mTORC1 only. It is very likely, though, that both mechanisms are displayed synergistically in the observed LTP characteristics of *R*cKO mice. It remains to be further analyzed whether the repression of mTORC1 in postnatal brain structures affects other aspects of neuronal function and processes associated with neurodegenerative diseases.

Our data so far indicate that basal mTORC1 activity is crucial for the regulation of postnatal neuron size, synaptic function and plasticity and thus ultimately for learning and memory. Therefore, in the view of the fact that rapamycin is prescribed to patients as an immunosuppressive drug for a prolonged time period, our results also shed new light onto potential side effects of this drug in the central nervous system.

Figure 1

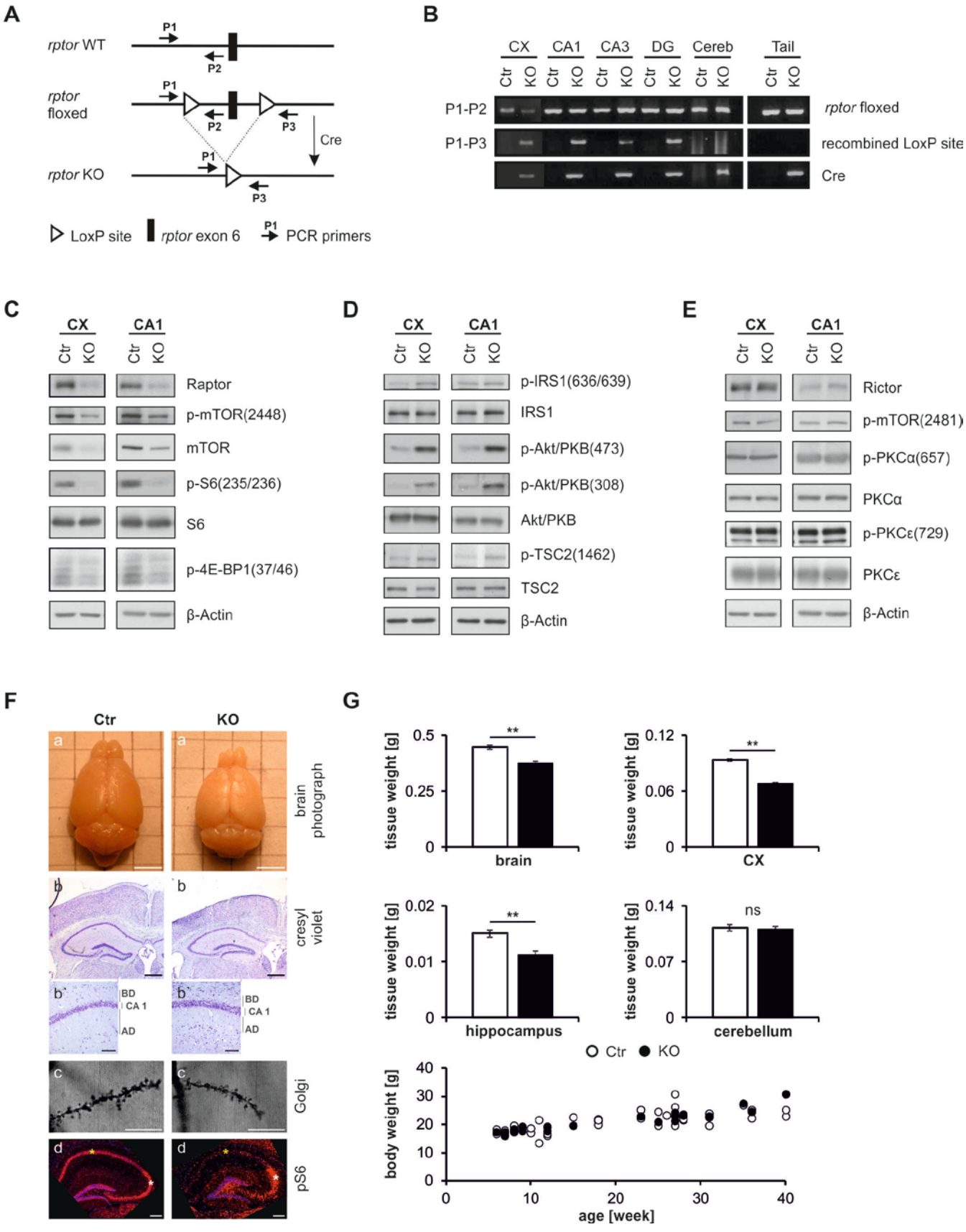
A
rptor WT
rptor floxed
rptor KO
P1
P2
P3
Cre
LoxP site
rptor exon 6
PCR primers
B
CX
CA1
CA3
DG
Cereb
Tail
Ctr
KO
P1-P2
P1-P3
rptor floxed
recombined LoxP site
Cre
C
Raptor
p-mTOR(2448)
mTOR
p-S6(235/236)
S6
p-4E-BP1(37/46)
β-Actin
D
p-IRS1(636/639)
IRS1
p-Akt/PKB(473)
p-Akt/PKB(308)
Akt/PKB
p-TSC2(1462)
TSC2
β-Actin
E
Rictor
p-mTOR(2481)
p-PKCα(657)
PKCα
p-PKCε(729)
PKCε
β-Actin
F
Ctr
KO
brain photograph
cresyl violet
BD
CA 1
AD
Golgi
pS6
G
tissue weight [g]
brain
CX
hippocampus
cerebellum
ns
Ctr
KO
body weight [g]
age [week]

Figure 1. Selective depletion of raptor in the forebrain results in diminished mTORC1 activity and reduced brain size.

(A) Schematic presentation of the localization of the LoxP sites in the *rptor* gene in the wild-type allele (WT) and the targeted allele (floxed) before and after (KO) recombination. Positioning of the primers P1-P3 used in (B) are indicated.

(B) PCR identification of *rptor* floxed alleles, alleles from recombined LoxP sites and Cre in DNA extracts from cortex (CX), CA1, CA3, dentate gyrus (DG), cerebellum (Cereb) and the tail from control (Ctr) and *R*cKO (KO) mice. P1, P2 and P3 represent primers indicated in (A).

(C-E) Western blot analysis showing protein and phosphorylation levels of the indicated targets in lysates from cortex (CX) and CA1 tissue. For quantification see Supplementary Table 1.

(F) Representative photographs of whole brain, cresyl violet stained cross-sections, Golgi-stained cross-sections and immunohistochemical pS6-staining of cross-sections from adult control (left) and *R*cKO (right) mice. Total brain size, hippocampal size, length of basal dendrites (BD) and apical dendrites (AD) are reduced in *R*cKO. pS6 staining in CA1 neurons (yellow asterisk) of *R*cKO mice is strongly reduced. No difference in pS6 staining in CA2 area (white asterisk) is observed.

(G) Quantification of specific tissue weight from total brain, cortex (CX), hippocampus, cerebellum and whole body weight of control (white) and *R*cKO (black) mice. *R*cKO mice show reduced weight of total brain, CX and hippocampus (Ctr: n = >3; KO: n = >6).

Data represent mean ± SEM. Statistics: ** $p<0.01$, two-tailed t-test. Scale bars: 4 mm (F,a), 0.5 mm (F,b), 0.1 mm (F,b`), 5 µm (F,c), 0.2 mm (F,d).

Figure 2

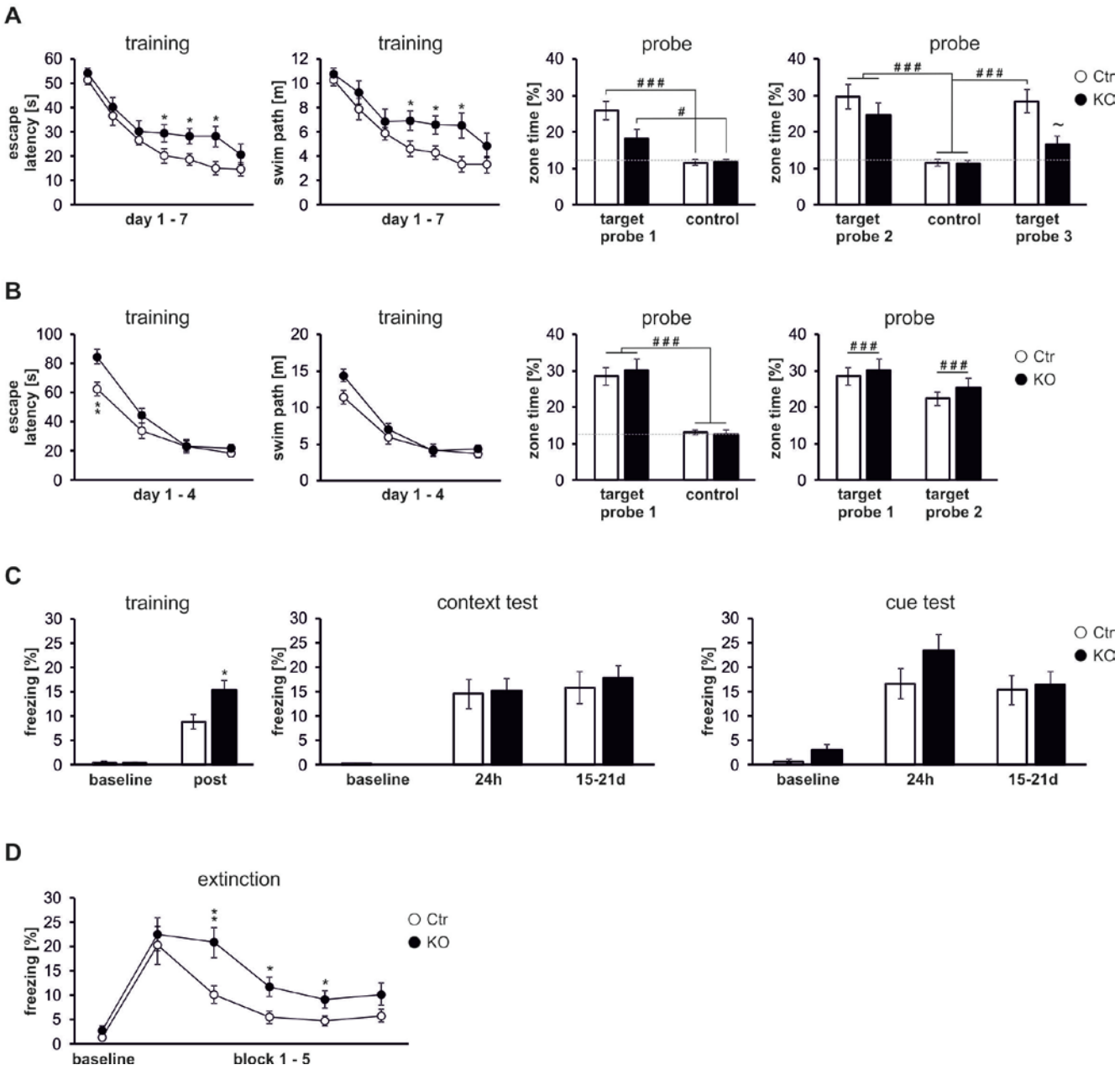

Figure 2. Task-specific impairment of learning and memory in *R*cKO mice.

(A) Left: escape latency and swim path during the training phase of 14 days in the MWM. Each point represents average across 4 sessions of 2 days. KO took on average significantly longer to reach the platform. Right: time spent in the target zone versus average of control zones in the other quadrants (probe 1: at day 10 of training; probe 2: 24 h post training; probe 3: 14 days post training). KO showed a weaker preference for the target zone during probe trial 1 and no preference for the target zone at probe trial 3 while no difference could be detected in probe trial 2 (Ctr: n = 17; KO: n = 17).

(B) Left: escape latency and swim path during the training phase of 4 days in the MWM. Each point represents average across the 6 sessions per day. Both genotypes show overall robust learning. Right: time spent in the target zone versus average of control zones in the other quadrants (probe 1: 24 h post training) or time in target zone of probe 1 versus time spent in target zone during probe 2 (probe 2: 14 days post training). Independent of genotype mice showed strong preference for the target zone (Ctr: n = 18; KO: n = 17).

(C) Cued and contextual fear conditioning. Left: freezing in the training chamber before and immediately after training. KO froze more after training. Middle: context test shows freezing in the training chamber before training, 24 h and 15-21 days after training. Independently of genotype, mice showed significant retention. Right: cued test shows freezing in a new context before and during representation of the tone (24 h and 15-21 days after conditioning). Both genotypes showed robust freezing to the tone.

(D) Freezing during 1 min baseline and 15 min of extinction. Blocks 1-5 represent average across 5 consecutive tone presentations (25 s each). Both groups reduced freezing in response to extinction training but reduction was less in *R*cKO mice (Ctr: n = 35; KO: n = 35).

Data points of control mice are shown in white, data points of *R*cKO are shown in black. Data represents mean ± SEM. Statistics: follow-up one-sample t-test versus chance: ### $p<0.001$, ## $p<0.01$, # $p<0.05$, ~ $p<0.1$. Follow-up unpaired t-test KO versus Ctr: ** $p<0.01$, * $p<0.05$.

Figure 3

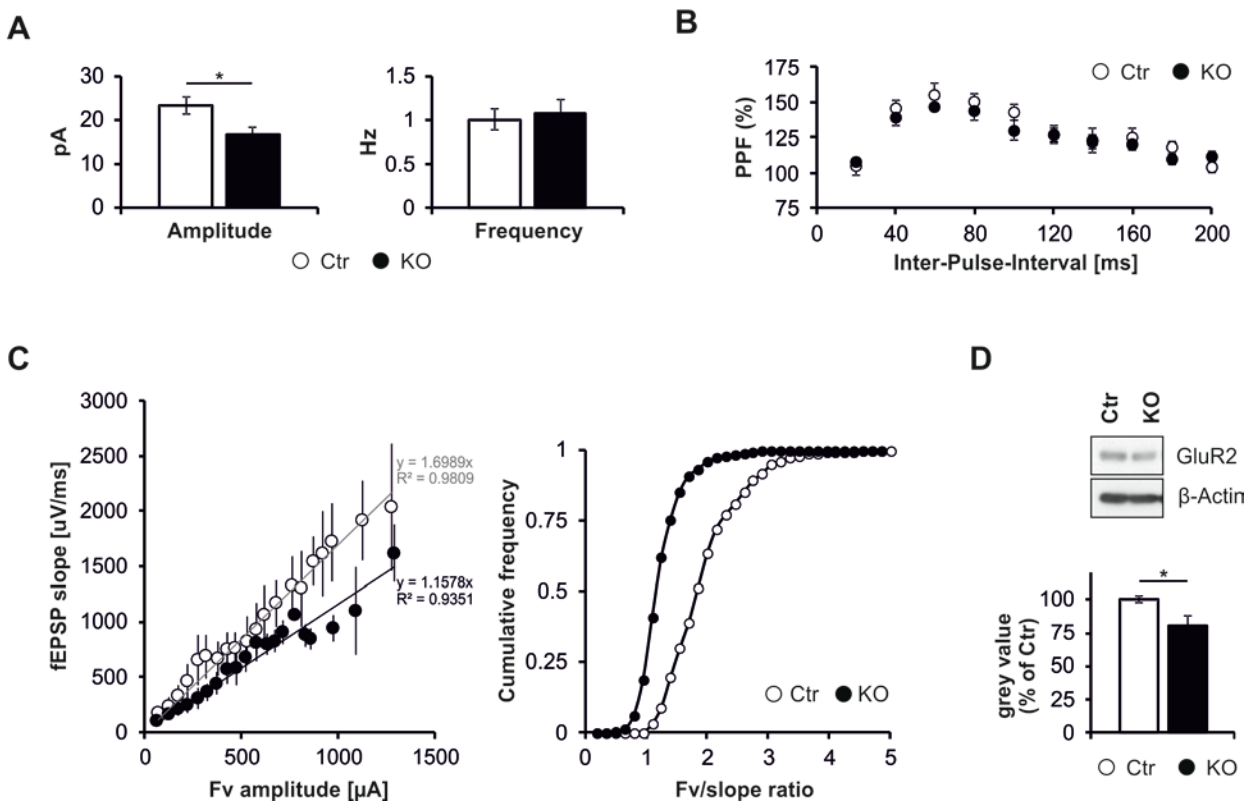

Figure 3. Reduced synaptic efficiency in *R*cKO mice.

(A) Quantification of mEPSC recordings in CA1 neurons of 3 months old control (Ctr) and *R*cKO (KO) mice. Bars represent mean amplitude and mean frequency of mEPSCs. Amplitude of mEPSCs in *R*cKO mice was significantly reduced (Ctr: n = 9; KO: n = 11).

(B) PPF measured in CA1 field recordings from adult control and *R*cKO mice. The percentage of facilitation, determined by the ratio of the second fEPSP to the first fEPSP, is shown at interpulse intervals from 20 to 200 ms. *R*cKO mice show normal PPF (Ctr: n = 10; KO: n = 9).

(C) Input (fibervolley (Fv) amplitude) versus output (fEPSP slope) plot (left) and cumulative frequency plot of Fv/slope ratios (right) are depicted. A shifted input-output relationship towards smaller Fv/slope ratios is observed in KO (Ctr: n = 13; KO: n = 17).

(D) Representative western blot of GluR2 of CA1 lysates from control (Ctr) and *R*cKO (KO) mice and quantification of grey values normalized to β-Actin. The abundance of GluR2 is reduced in *R*cKO lysates (Ctr: n = 7; KO: n = 7).

Data represents mean ± SEM. Statistics: two-tailed t-test, * $p<0.05$; Kolmogorov-Smirnov-test, * $p<0.05$.

Figure 4

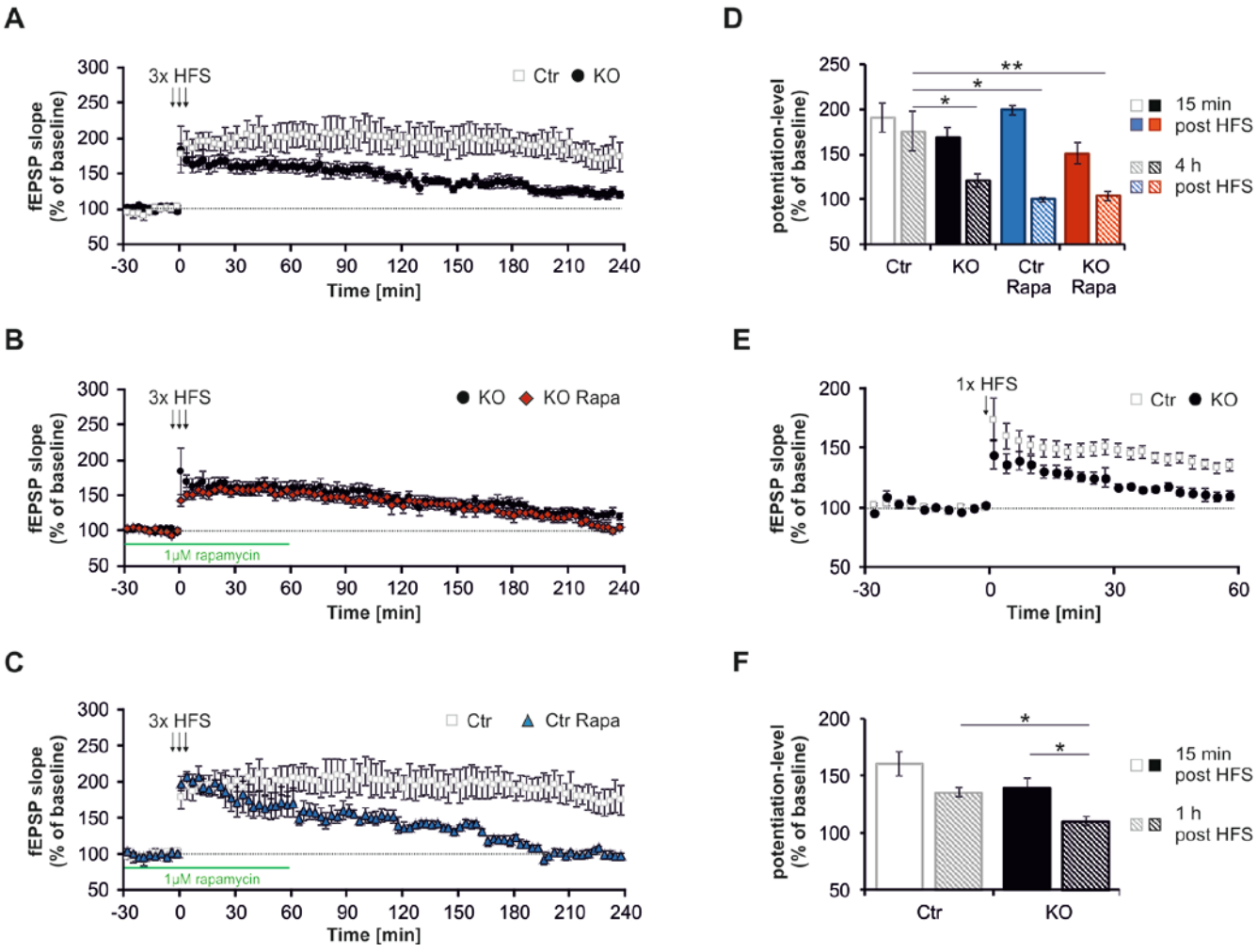

Figure 4. Impaired E-LTP and L-LTP in RcKO mice.

(A) Three trains of HFS (100 Hz, 1 s, 4 min inter-train-interval) induced L-LTP in control (Ctr) and *R*cKO (KO) slices. Graph shows fEPSP slope as percentage of mean baseline values. Each data point represents average of recordings during a time interval of 3 min. L-LTP maintenance is reduced in KO slices (Ctr: n = 9; KO: n = 9). (B) L-LTP recording in *R*cKO mice as described in (A) compared to measurements of KO slices treated with 1 µM rapamycin (KO Rapa) during baseline measurements and for 1 h post induction. No difference between the two groups is observable (KO Rapa: n = 6). (C) L-LTP recording in control mice as described in (A) compared to measurements of control slices treated with 1 µM rapamycin (Ctr Rapa) during baseline measurements and for 1 h post induction. rapamycin treatment impaired L-LTP maintenance in Ctr slices (Ctr Rapa: n = 3). (D) Quantified levels of potentiation during the first 15 min (filled bars) and after 4 h (striped bars) post L-LTP induction. *R*cKO slices, control and *R*cKO slices treated with rapamycin showed significantly reduced potentiation levels after 4 h recording (color code is as follows: Ctr: white; KO: black; Ctr Rapa: blue;

KO Rapa: red). (E) One train of HFS (100 Hz, 1 s) was applied to Ctr and KO slices and E-LTP progression was measured for 1 h. Graph shows fEPSP slope as percent of mean baseline values. Each data point represents average of recordings during a time interval of 3 min. LTP progression in KO slices was affected compared to Ctr (Ctr: n = 7; KO: n = 6). (F) Graph shows level of potentiation during the first 12 min (filled bars) and after 1 h (striped bars) post E-LTP induction for Ctr (white) and KO (black). The level of potentiation in KO slices 1 h post LTP induction was significantly reduced compared Ctr. Data represents mean ± SEM. Statistics: two-tailed t-test, ** $p<0.01$, * $p<0.05$.

Supplementary Figure S1

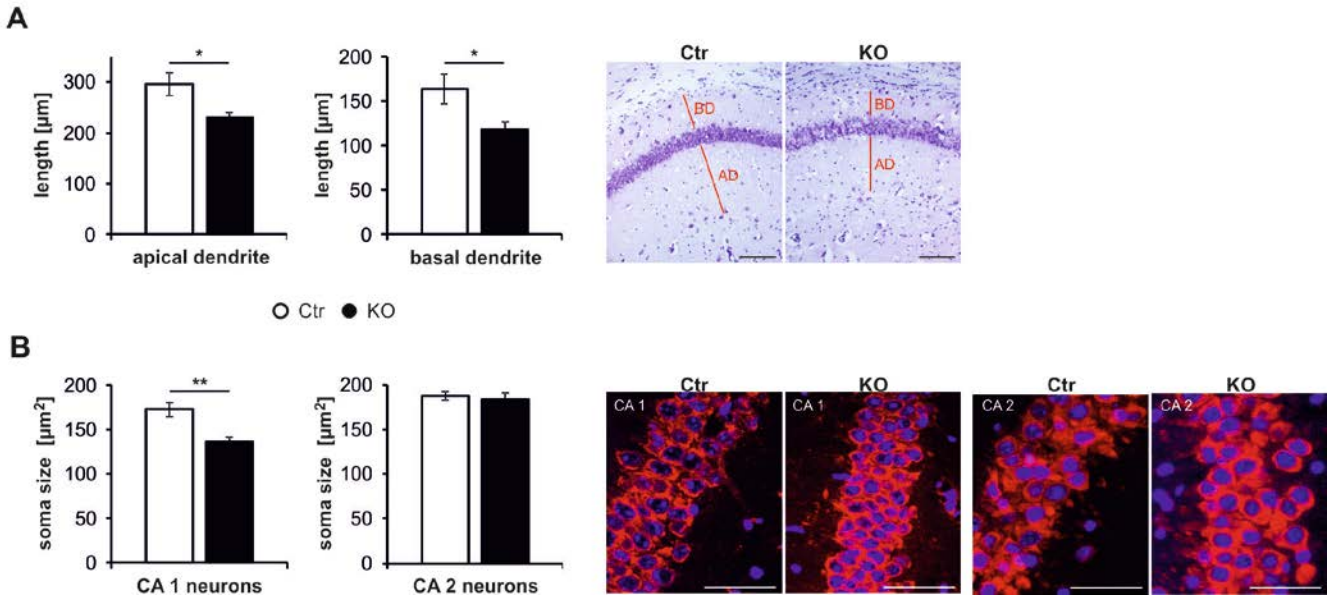

Supplementary Figure S1. Reduced dendritic length and soma size of CA1 neurons in *R*cKO mice.

(A) Analysis of dendritic length based on cresyl violet stained tissue sections from control (Ctr) and *R*cKO (KO) mice. Graphs on the left show quantification of apical dendritic length and basal dendritic length in the CA1 region of Ctr (white bars) and *R*cKO (black bars) mice. Representative photographs of the CA1 region of cresyl violet stained coronal cross sections from KO and Ctr mice are depicted on the right. Both dendritic areas showed reduced length in KO sections (Ctr: n = 5; KO: n = 5).

(B) Analysis of the soma size of CA1 and CA2 neurons based on tissue sections from control (Ctr) and *R*cKO (KO) mice that were stained for S6. Graphs on the left show quantification of soma size of Ctr (white bars) and KO (black bars) from CA1 neurons and CA2 neurons, respectively. Representative photographs of CA1 and CA2 neurons from cross sections stained against S6 (red) are depicted on the right. Soma size of CA1 neurons in KO sections is reduced, whereas no difference was observed in soma size of CA1 neurons (Ctr: n = 5; KO: n = 5).

Data represents mean ± SEM. Statistics: two-tailed t-test, ** $p<0.01$, * $p<0.05$. Scale bars: 200 µm (A); 50 µm (B).

Supplementary Figure S2

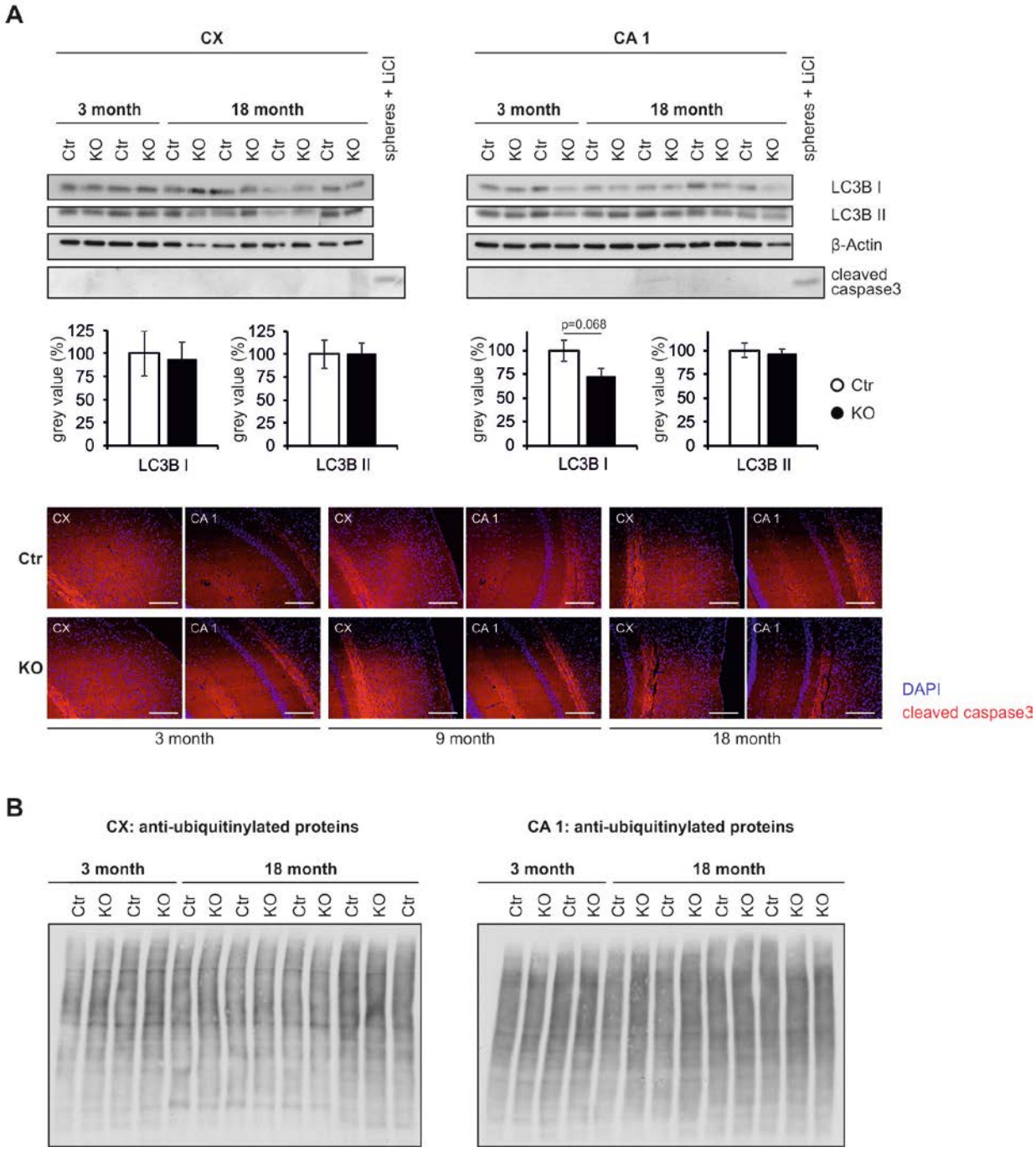

Supplementary Figure 2. No pronounced apoptosis and autophagy alterations in *R*cKO mice. (A) Western blot analysis showing LC3B I and LC3B II protein levels in cortex (CX) and CA1 lysates from 3 months and 18 months old mice. No significant difference in LC3B I and LC3B II was detected neither in CX lysates nor in CA1. Probing against cleaved caspase3 did not reveal any signal in control (Ctr) and *R*cKO (KO) mice (Ctr: n<5; KO: n<5). As positive control for the probing against cleaved caspase3 a protein sample of apoptotic primary mouse neurospheres was used.

Representative microscope pictures showing cleaved caspase3 staining (red) and DAPI (blue) are depicted on the right. No positive staining for cleaved caspase3 could be detected in sections from 3-18 month old mice.

(B) Western blot analysis of lysates from cortex (CX) and CA1 region from Ctr and KO mice of different ages probing against ubiquitinylated proteins (Ctr: n<5; KO: n<5). No difference in signal intensity could be detected between Ctr and KO.

Data represents mean ± SEM. Statistics: two-tailed t-test, * p<0.05. Scale bar: 0.2 mm (A).

Supplementary Figure S3

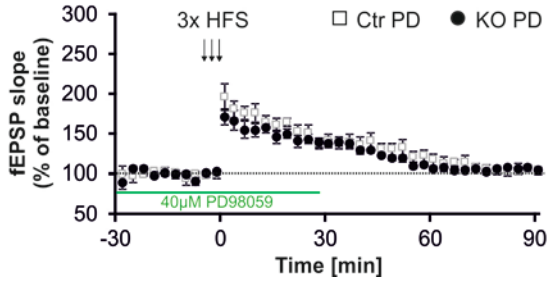

Supplementary Figure 3. Control and *R*cKO mice show similar LTP progression in response to PD98059.

Three trains of HFS (100 Hz, 1 s, 4 min inter-train-interval) induced L-LTP in control (Ctr) and *R*cKO (KO) slices. Graph shows fEPSP slope as percentage of mean baseline values. Each data point represents average of recordings during a time interval of 3 min. L-LTP maintenance is impaired in Ctr (white) and KO (black) slices (Ctr: n = 5; KO: n = 5).

Supplementary Table 1

Protein	CA1			CX		
	Ctr	KO (% of Ctr)	n (Ctr) / n (KO)	Ctr	KO (% of Ctr)	n (Ctr) / n (KO)
Raptor	100 ± 8.99	59.83 ± 4.43 **	5 / 7	100 ± 4.58	41.11 ± 2.74 ***	5 / 6
Rictor	100 ± 5.89	89.13 ± 9.11	4 / 6	100 ± 22.11	93.53 ± 14.85	5 / 5
p-mTOR(2448)	100 ± 14.01	52.38 ± 6.30 **	5 / 6	100 ± 6.66	38.41 ± 7.40 **	3 / 4
p-mTOR(2481)	100 ± 21.43	291 ± 185.76	5 / 7	100 ± 31.71	102.83 ± 35.57	4 / 4
mTOR	100 ± 5.33	61.26 ± 12.28 *	5 / 7	100 ± 14.94	49.12 ± 4.24 **	4 / 5
p-S6(235/236)	100 ± 10.19	57.63 ± 9.37 *	6 / 7	100 ± 16.05	42.88 ± 12.41 *	5 / 5
S6	100 ± 3.59	101.79 ± 6.61	4 / 6	100 ± 3.99	100.90 ± 4.37	3 / 4
p-4E-BP(37/46)	100 ± 3.65	69.18 ± 5.85 **	6 / 7	100 ± 1.95	76.19 ± 14.12 ~	5 / 5
p-Akt/PKB(308)	100 ± 9.09	425.05 ± 52.13 ***	5 / 7	100 ± 8.34	351.19 ± 41.26 ***	4 / 4
p-Akt/PKB(473)	100 ± 13.63	292.28 ± 34.78 **	4 / 5	100 ± 8.52	360.30 ± 53.64 **	4 / 4
Akt/PKB	100 ± 8.47	103.29 ± 2.52	5 / 7	100 ± 4.09	93.92 ± 7.97	4 / 5
p-IRS1(636/639)	100 ± 0.52	159.36 ± 55.13 *	6 / 7	100 ± 7.79	140.21 ± 3.4 **	3 / 4
IRS1	100 ± 11.41	127.01 ± 14.72	5 / 6	100 ± 3.08	98.09 ± 14.08	3 / 4
p-TSC2(1462)	100 ± 10.25	174.68 ± 16.23 **	7 / 7	100 ± 9.48	150.18 ± 23.13 ~	4 / 3
TSC2	100 ± 111.38	111.38 ± 11.63	4 / 5	100 ± 3.19	105.68 ± 21.90	4 / 4
p-PKCα(657)	100 ± 5.62	116.25 ± 12.41	5 / 6	100 ± 3.34	110.49 ± 30.58	4 / 4
PKCα	100 ± 3.15	122.32 ± 10.73	4 / 5	100 ± 2.30	108.38 ± 14.38	4 / 5
p-PKCε(729)	100 ± 2.02	129.66 ± 12.34	3 / 3	100 ± 12.80	86.98 ± 23.37	3 / 3
PKCε	100 ± 1.08	102.29 ± 10.86	4 / 4	100 ± 17.91	91.48 ± 25.59	4 / 4

Supplementary Table 1. Quantification of Western blot analysis.

Table shows quantified grey values of representative Western blots from Figure 1. All values were normalized to the β-Actin signal of the corresponding sample. The mean intensity for each individual target of interest from control lysates was set as 100%. The mean values from *R*cKO are indicated as percentage of control. In the right column, the targets and phosphorylation sites which were probed for are indicated. In the middle column, the results from Western blot analysis of CA1 lysates from control (Ctr) and *R*cKO (KO) are depicted. The right column shows the results from Western blot analysis of cortex (CX) lysates. Number of samples used for each target are indicated as n (Ctr) / n (KO). Data represent mean ± SEM. Statistics: two-tailed t-test, *** $p<0.001$, ** $p<0.01$, * $p<0.05$, ~ $p<0.075$.

MATERIAL AND METHODS

Raptor cKO Mice: *R*cKO

Mice were maintained in a conventional facility with a fixed day-night cycle. Studies were carried out according to criteria outlined for the care and use of laboratory animals and with approval of the Swiss authorities. Mice with floxed *rptor* alleles ($R^{fl/fl}$) were generated as described previously (Bentzinger et al., 2008). For the generation of forebrain-specific *rptor* knockout, mice homozygously floxed for the *rptor* allel were crossed to T29-1 α-CamKII-Cre mice (from The Jackson Laboratory). All mice were bread in a clean C57BL/6J background. For genotyping, tail lysates were analyzed with Cre specific primers and primers identifying the floxed *rptor* allel (P1, P2). Cre fw: 5'-TGT GGC TGA TGA TCC GAA TA; Cre bw: 5'-GCT TGC ATG ATC TCC GGT AT; P1: 5'-ATG GTA GCA GGC ACA CTC TTC ATG; P2: 5'-GCT AAA CAT TCA GTC CCT AAT C. Successful recombination of the LoxP sites in knockout mice was tested using P1 and an additional primer P3: 5'-CAG ATT CAA GCA TGT CCT AAG C. Control mice used in this study carried the genotype α-CamKII-Cre^{-}/$R^{fl/fl}$ and *R*cKO mice carried the genotype α-CamKII-Cre^{+}/$R^{fl/fl}$. Only female α-CamKII-Cre^{+} mice were used for the *R*cKO breedings. If not specifically indicated, adult mice (2-12 month) were used for all the experiments.

Protein lysate preparation and immunoblotting

Mice were deeply sedated with Isoflurane (Attane^{TM}) and decapitated. After removal of the brain, the hippocampus as well as the frontal cortex was rapidly dissected. Cortices were immediately frozen in liquid nitrogen. The hippocampi were further cut into 400 µm thick slices with the tissue chopper (McIlwain). Microdissection of the CA1, CA3 and DG was performed in ice cold PBS and tissue fragments were subsequently frozen in liquid nitrogen. Tissue samples were homogenized in protein lysis buffer (50 mM Tris pH 8, 150 mM NaCl, 1 mM EDTA, 1% Triton-X100, protease inhibitor cocktail (Roche), phosphatase inhibitor cocktail (Roche)) using a 1 ml syringe. Homogenates were centrifuged at 13'600 rpm for 20 min at 4 °C and the supernatant was harvested. Total protein concentration was measured using BCA protein assay kit (Pierce). Protein sample buffer was added and samples were cooked at 95 °C for 15 min. The positive control for the cleaved caspase3 was kindly provided by Dr. M. Tome, Group of Prof. B. Bettler, Pharmazentrum, University of Basel, and contained lysed primary mouse neurospheres treated with 20 µM Etoposide for 6 h before lysis. For western blot analysis, equal amount of protein was loaded on SDS gels and subsequently transferred onto nitrocellulose membranes and subsequently probed for the specific proteins and phosphorylation sites indicated. All primary antibodies were diluted in PBST (PBS, 5 % BSA (Sigma), 0.1 % Tween (Sigma)) and incubated over night at 4 °C. The following primary antibodies were used: rabbit anti: Raptor, Rictor, p-mTOR(2448), p-mTOR(2481), mTOR, p-S6(235/236), S6, p-4E-BP(37/46), p-Akt/PKB(308), p-Akt/PKB(473), Akt/PKB, p-IRS1(636/639), IRS1, p-TSC2(1462), TSC2, PKCα, PKCε, LC3B, cleaved Caspase3 and β-Actin from Cell Signaling; rabbit anti p-PKCα(657) from Santa Cruz; rabbit anti p-

PKCε(729) from Abcam; mouse anti ubiquitinylated proteins from Millipore; mouse anti GluR2 from BD Biosciences. Secondary antibodies were as follows: goat anti-mouse HRP and goat anti-rabbit HRP from Nordic Immunology.

Immunohistochemistry

Adult mice were deeply anesthetized with Esconarkon (Streuli Pharma) and transcardially perfused with 4 % PFA. Brains were removed and either embedded in Paraffin (Merck) and subsequently cut with a microtome (Microm) or froze in Tissue-Tek® (Sakura) and cut with a cryostat (Leica), respectively. Before starting the staining procedure, paraffin sections were deparaffinated by backing the slides for 20 min at 60 °C, followed by dehydration steps (xylol, 100 % EtOH, 98 % EtOH, 96 % EtOH, 70 % EtOH, H_2O). For cresyl violet staining, the sections were incubated for 15 min in cresyl violet and afterwards dehydrated (70 % EtOH, 96 % EtOH, 100 % EtOH, xylol) and mounted with toluol-based medium. For antibody stainings, the sections were washed in PBS, cooked in citrate buffer (0.1 M sodium-citrate, pH 6) and blocked for 30 min in blocking buffer (PBS, 5 % BSA, 0.1 % TritonX). Primary antibodies were diluted in blocking buffer or PBS (cleaved caspase 3) and incubated over night at 4 °C. Secondary antibodies combined with Dapi were applied for 1 h at room temperature. After washing with PBS, sections were mounted with Kaisers glycerol gelatin (MERCK). The following antibodies were used: rabbit anti-pS6 (Cell Signaling, 1:200), rabbit anti-S6 (Cell Signaling, 1:250), rabbit anti-cleaved caspase 3 (Cell Signaling, 1:200), DAPI (1:1000), goat anti-rabbit Cy3 (Jackson Immunoresearch, 1:500). For microscopic analysis, a Leica microscope (Leica DM 5000 B) and the Analysis software (analySIS Pro 3.2) were used.

Morris Water Maze

Spatial learning and memory performance was tested in the Morris water maze (MWM) according to previous publication (Morris, 1984). In brief, a round white poly-propylene swim tank with a diameter of 150 cm, was filled with water (temperature 24-26 ° C, depth 15 cm) and made opaque by addition of 1 l of milk. The white quadratic goal platform (14x14 cm) was hidden 0.5 cm below the water surface. Salient distant cues were available in the indirectly illuminated room (4 40W bulbs, 12 lux). Animals were video-tracked at 4.2 Hz and 576x768 pixel spatial resolution using a Noldus EthoVision 3.00 system (Noldus Information Technology, Wageningen NL). Raw data were then transferred to public domain software Wintrack 2.4 (www.dpwolfer.ch/wintrack) for further analysis. The short version of the MWM consisted of 6 trainings per day over 4 consecutive days and a probe trial (removal of the platform) at 1 day or 14 days after training, respectively. The long version of the MWM consisted of 2 trainings per day over 14 consecutive days with one probe trial at day 10 as well as at day 1 and day 14 after the training session, respectively.

Fear Conditioning

Four mice were tested in parallel in an Actimetrics FreezeFrame video-based Conditioned Fear System (www.actimetrics.com). The conditioning chambers (175 mm deep x 180 mm wide x 280 mm high) were enclosed in ventilated and sound-attenuated cabinets and had a floor consisting of stainless steel rods permitting the application of current. The conditional stimulus (CS) was a 2500 Hz 85 dB tone lasting 30 s, co-terminating with a 2 s 0.25 A foot shock (US). Freezing (absence of movement aside from respiration) was quantified automatically by the FreezeFrame software subtracting subsequent images recorded by the ceiling-mounted IR video cameras in the conditioning chambers. Bouts of 1.0 s were used to define % freezing and movement thresholds were set at 20 (training and context test) or 8 units (tone test). The conditioning consisted of 1min baseline measurement followed by three CS with 30 sec of CS-CS interval. The cue-test was performed in modified cabinets for 2 min (1min baseline followed by 1 min CS representation). The context-test was performed in the same cabinets as during the training session for 2 min. For both, cue- and context-test, a short-term and long-term testing was executed at day 1 and day 14 after the training, respectively. For the extinction test, mice were placed in a modified cabinet and after 1 min of baseline recording, the CS was represented 25 times for 30 s with a 5s CS-CS interval. The delayed extinction test was performed 1 day after.

Golgi staining

Adult mice were deeply deeply anesthetized with Esconarkon (Streuli Pharma) and transcardially perfused with 4 % PFA. Further procedure was according to the manual of the FD Rapid GlogiSatin^{TM} Kit (FD Neuro Technologies, Inc.).

Electrophysiology

For patch clamp recordings, mice at the age of 8 to 12 weeks were deeply sedated with isofluran (Attane^{TM}). After decapitation, the brain was rapidly removed and immediately transferred into ice cold oxygenated (95 % O_2, 5 % CO_2) low-calcium artificial cerebrospinal fluid (low-Ca^{2+}-ACSF) containing: 119 mM NaCl, 1 mM NaH_2PO_4, 2.5 mM KCl, 0.125 mM $CaCl_2$, 3.3 mM $MgCl_2$, 11 mM D-glucose and 26.2 mM $NaHCO_3$. Brains were cut with a vibratome (Leica) into 300 µm coronal sections and retained at least for 1 h at room temperature in oxygenated ACSF (119 mM NaCl, 1 mM NaH_2PO_4, 2.5 mM KCl, 2.5 mM $CaCl_2$, 1.3 mM $MgCl_2$, 11 mM D-glucose and 26.2 mM $NaHCO_3$) before recording. Miniature events were recorded using an Axonpatch Multiclamp 700B amplifier and borosilicate glass pipettes (4-8 mΩ) filled with intracellular solution (135 mM $CsMeSO_4$, 8 mM NaCl, 10 mM HEPES, 0.5 mM EGTA, 4 mM Mg-ATP, 0.3 mM Na-GTP, 5 mM Lidocaine-N-ethylbromid). For mEPSC recording, the holding potential was set to -70 mV. The postsynaptic current was recorded for 10 min in the presence of 0.5 µM TTX. Traces were further analyzed with Mini Analysis Program v6 (Synaptosoft).

For field recordings, brain slices of 400 µm thickness were obtained as described and transferred into oxygenated ACSF at 30 °C for 30 min before placing them in an interface chamber (house made) perfused with oxygenated ACSF at least 1 h prior to recording. For all recordings, a Pt-Ir electrode (25 µm in diameter) was used to stimulate the Schaffer collaterals and field responses of CA1 neurons were measured with a glass pipette (1-6 MΩ) filled with ACSF. Extracellular postsynaptic field potentials (fEPSP) were evoked by test stimuli applied at 0.33 Hz with an intensity to induce 40-50 % of maximal fEPSP. After 30 min of baseline recording, E-LTP (1x HFS: 100Hz, 1 s duration) or L-LTP (3x HFS: 100 Hz, 1 s, 4 min inter-train-interval) was induced. Stimulus intensity of the HFS was matched the intensity during baseline recording. When indicated, slices were perfused with ACSF containing 1 µM rapamycin (LC Laboratories) or 40 µM PD98059 (Tocris), respectively. Signals were averaged over 3 min and normalized to baseline recordings. Paired-pulse facilitation was analyzed in the range of inter-pulse-intervals from 20 ms to 200 ms and the slope response of the second stimuli was calculated relatively to the first response. For input-output relationship assessment, slices were stimulated in the range of 20 µA - 9 mA and fibervolley amplitude and fEPSP slope were analyzed.

Quantifications and statistics

Quantification of Western blots was performed using the ImageJ software. Background-corrected grey values were normalized to β-Actin levels and the mean value of Ctr was set to 100 %. For quantification of soma size as well as apical and basal dendritic length of CA1 neurons the software Analysis (analySIS Pro 3.2) was used. For soma size quantification, the area of positive S6 staining surrounding CA1 nuclei was measured. The length of apical and basal dendritic area was measured based on cresyl violet stainings. If not otherwise indicated, data are expressed as mean ± SEM. For statistical analysis of the MWM and FC data, mixed ANOVA models were used with follow-up one-sample t-test versus chance and follow-up unpaired t-test Ctr versus *R*cKO. The cumulative frequency of Fv/slope ratio was analyzed using Kolmogorov-Smirnov test. For all other statistical comparisons of two genotypes or conditions, the Student's t-test was used. Levels of significance are as indicated in the figure legends.

Acknowledgments

This work was supported by grants to MAR from the Novartis Research Foundation, the Swiss National Science Foundation and the Cantons of Basel-Stadt and Baselland. We thank the members of the laboratory for critical discussions. Behavioral testing was supported by the NCCR Neural Plasticity and repair. DPW is member of the Zurich Centers for Neuroscience (ZNZ) and Integrative Human Physiology (ZIHP).

REFERENCES

Antion, M.D., Merhav, M., Hoeffer, C.A., Reis, G., Kozma, S.C., Thomas, G., Schuman, E.M., Rosenblum, K., and Klann, E. (2008). Removal of S6K1 and S6K2 leads to divergent alterations in learning, memory, and synaptic plasticity. Learn Mem *15*, 29-38.

Auerbach, B.D., Osterweil, E.K., and Bear, M.F. (2011). Mutations causing syndromic autism define an axis of synaptic pathophysiology. Nature *480*, 63-68.

Banko, J.L., Poulin, F., Hou, L., DeMaria, C.T., Sonenberg, N., and Klann, E. (2005). The translation repressor 4E-BP2 is critical for eIF4F complex formation, synaptic plasticity, and memory in the hippocampus. J Neurosci *25*, 9581-9590.

Bartsch, D., Casadio, A., Karl, K.A., Serodio, P., and Kandel, E.R. (1998). CREB1 encodes a nuclear activator, a repressor, and a cytoplasmic modulator that form a regulatory unit critical for long-term facilitation. Cell *95*, 211-223.

Bentzinger, C.F., Romanino, K., Cloetta, D., Lin, S., Mascarenhas, J.B., Oliveri, F., Xia, J., Casanova, E., Costa, C.F., Brink, M.*, et al.* (2008). Skeletal muscle-specific ablation of raptor, but not of rictor, causes metabolic changes and results in muscle dystrophy. Cell Metab *8*, 411-424.

Bidinosti, M., Ran, I., Sanchez-Carbente, M.R., Martineau, Y., Gingras, A.C., Gkogkas, C., Raught, B., Bramham, C.R., Sossin, W.S., Costa-Mattioli, M.*, et al.* (2010). Postnatal deamidation of 4E-BP2 in brain enhances its association with raptor and alters kinetics of excitatory synaptic transmission. Mol Cell *37*, 797-808.

Cammalleri, M., Lutjens, R., Berton, F., King, A.R., Simpson, C., Francesconi, W., and Sanna, P.P. (2003). Time-restricted role for dendritic activation of the mTOR-p70S6K pathway in the induction of late-phase long-term potentiation in the CA1. Proc Natl Acad Sci U S A *100*, 14368-14373.

Campbell, D.S., and Holt, C.E. (2001). Chemotropic responses of retinal growth cones mediated by rapid local protein synthesis and degradation. Neuron *32*, 1013-1026.

Chen, X.G., Liu, F., Song, X.F., Wang, Z.H., Dong, Z.Q., Hu, Z.Q., Lan, R.Z., Guan, W., Zhou, T.G., Xu, X.M.*, et al.* (2010). Rapamycin regulates Akt and ERK phosphorylation through mTORC1 and mTORC2 signaling pathways. Mol Carcinog *49*, 603-610.

Davis, M. (2011). NMDA receptors and fear extinction: implications for cognitive behavioral therapy. Dialogues Clin Neurosci *13*, 463-474.

Ehninger, D., Han, S., Shilyansky, C., Zhou, Y., Li, W., Kwiatkowski, D.J., Ramesh, V., and Silva, A.J. (2008). Reversal of learning deficits in a Tsc2+/- mouse model of tuberous sclerosis. Nat Med *14*, 843-848.

Frey, U., Krug, M., Reymann, K.G., and Matthies, H. (1988). Anisomycin, an inhibitor of protein synthesis, blocks late phases of LTP phenomena in the hippocampal CA1 region in vitro. Brain Res *452*, 57-65.

Frey, U., and Morris, R.G. (1997). Synaptic tagging and long-term potentiation. Nature *385*, 533-536.

Gafford, G.M., Parsons, R.G., and Helmstetter, F.J. (2011). Consolidation and reconsolidation of contextual fear memory requires mammalian target of rapamycin-dependent translation in the dorsal hippocampus. Neuroscience *182*, 98-104.

Gass, P., Wolfer, D.P., Balschun, D., Rudolph, D., Frey, U., Lipp, H.P., and Schutz, G. (1998). Deficits in memory tasks of mice with CREB mutations depend on gene dosage. Learn Mem *5*, 274-288.

Gelinas, J.N., Banko, J.L., Hou, L., Sonenberg, N., Weeber, E.J., Klann, E., and Nguyen, P.V. (2007). ERK and mTOR signaling couple beta-adrenergic receptors to translation initiation machinery to gate induction of protein synthesis-dependent long-term potentiation. J Biol Chem *282*, 27527-27535.

Hoeffer, C.A., Tang, W., Wong, H., Santillan, A., Patterson, R.J., Martinez, L.A., Tejada-Simon, M.V., Paylor, R., Hamilton, S.L., and Klann, E. (2008). Removal of FKBP12 enhances mTOR-Raptor interactions, LTP, memory, and perseverative/repetitive behavior. Neuron *60*, 832-845.

Jaworski, J., Spangler, S., Seeburg, D.P., Hoogenraad, C.C., and Sheng, M. (2005). Control of dendritic arborization by the phosphoinositide-3'-kinase-Akt-mammalian target of rapamycin pathway. J Neurosci *25*, 11300-11312.

Jurado, S., Benoist, M., Lario, A., Knafo, S., Petrok, C.N., and Esteban, J.A. (2010). PTEN is recruited to the postsynaptic terminal for NMDA receptor-dependent long-term depression. Embo J *29*, 2827-2840.

Kang, H., and Schuman, E.M. (1996). A requirement for local protein synthesis in neurotrophin-induced hippocampal synaptic plasticity. Science *273*, 1402-1406.

Kelleher, R.J., 3rd, Govindarajan, A., Jung, H.Y., Kang, H., and Tonegawa, S. (2004). Translational control by MAPK signaling in long-term synaptic plasticity and memory. Cell *116*, 467-479.

Kim, D.H., Sarbassov, D.D., Ali, S.M., King, J.E., Latek, R.R., Erdjument-Bromage, H., Tempst, P., and Sabatini, D.M. (2002). mTOR interacts with raptor to form a nutrient-sensitive complex that signals to the cell growth machinery. Cell *110*, 163-175.

Klann, E., Chen, S.J., and Sweatt, J.D. (1991). Persistent protein kinase activation in the maintenance phase of long-term potentiation. J Biol Chem *266*, 24253-24256.

Klann, E., Chen, S.J., and Sweatt, J.D. (1993). Mechanism of protein kinase C activation during the induction and maintenance of long-term potentiation probed using a selective peptide substrate. Proc Natl Acad Sci U S A *90*, 8337-8341.

Kumar, V., Zhang, M.X., Swank, M.W., Kunz, J., and Wu, G.Y. (2005). Regulation of dendritic morphogenesis by Ras-PI3K-Akt-mTOR and Ras-MAPK signaling pathways. J Neurosci *25*, 11288-11299.

Lang, U.E., Heger, J., Willbring, M., Domula, M., Matschke, K., and Tugtekin, S.M. (2009). Immunosuppression using the mammalian target of rapamycin (mTOR) inhibitor everolimus: pilot study shows significant cognitive and affective improvement. Transplant Proc *41*, 4285-4288.

Low, P. (2011). The role of ubiquitin-proteasome system in ageing. Gen Comp Endocrinol *172*, 39-43.

Malinow, R., Schulman, H., and Tsien, R.W. (1989). Inhibition of postsynaptic PKC or CaMKII blocks induction but not expression of LTP. Science *245*, 862-866.

Morris, R. (1984). Developments of a water-maze procedure for studying spatial learning in the rat. J Neurosci Methods *11*, 47-60.

Panja, D., Dagyte, G., Bidinosti, M., Wibrand, K., Kristiansen, A.M., Sonenberg, N., and Bramham, C.R. (2009). Novel translational control in Arc-dependent long term potentiation consolidation in vivo. J Biol Chem *284*, 31498-31511.

Piper, M., Anderson, R., Dwivedy, A., Weinl, C., van Horck, F., Leung, K.M., Cogill, E., and Holt, C. (2006). Signaling mechanisms underlying Slit2-induced collapse of Xenopus retinal growth cones. Neuron *49*, 215-228.

Santini, E., and Klann, E. (2011). Dysregulated mTORC1-Dependent Translational Control: From Brain Disorders to Psychoactive Drugs. Front Behav Neurosci *5*, 76.

Sarbassov, D.D., Ali, S.M., Kim, D.H., Guertin, D.A., Latek, R.R., Erdjument-Bromage, H., Tempst, P., and Sabatini, D.M. (2004). Rictor, a novel binding partner of mTOR, defines a rapamycin-insensitive and raptor-independent pathway that regulates the cytoskeleton. Curr Biol *14*, 1296-1302.

Shima, H., Pende, M., Chen, Y., Fumagalli, S., Thomas, G., and Kozma, S.C. (1998). Disruption of the p70(s6k)/p85(s6k) gene reveals a small mouse phenotype and a new functional S6 kinase. Embo J *17*, 6649-6659.

Sperow, M., Berry, R.B., Bayazitov, I.T., Zhu, G., Baker, S.J., and Zakharenko, S.S. (2012). Phosphatase and tensin homologue (PTEN) regulates synaptic plasticity independently of its effect on neuronal morphology and migration. J Physiol *590*, 777-792.

Steward, O., and Schuman, E.M. (2003). Compartmentalized synthesis and degradation of proteins in neurons. Neuron *40*, 347-359.

Stoica, L., Zhu, P.J., Huang, W., Zhou, H., Kozma, S.C., and Costa-Mattioli, M. (2011). Selective pharmacogenetic inhibition of mammalian target of Rapamycin complex I (mTORC1) blocks long-term synaptic plasticity and memory storage. Proc Natl Acad Sci U S A *108*, 3791-3796.

Stolovich, M., Tang, H., Hornstein, E., Levy, G., Cohen, R., Bae, S.S., Birnbaum, M.J., and Meyuhas, O. (2002). Transduction of growth or mitogenic signals into translational activation of TOP mRNAs is fully reliant on the phosphatidylinositol 3-kinase-mediated pathway but requires neither S6K1 nor rpS6 phosphorylation. Mol Cell Biol *22*, 8101-8113.

Swiech, L., Perycz, M., Malik, A., and Jaworski, J. (2008). Role of mTOR in physiology and pathology of the nervous system. Biochim Biophys Acta *1784*, 116-132.

Tang, S.J., Reis, G., Kang, H., Gingras, A.C., Sonenberg, N., and Schuman, E.M. (2002). A rapamycin-sensitive signaling pathway contributes to long-term synaptic plasticity in the hippocampus. Proc Natl Acad Sci U S A *99*, 467-472.

Tavazoie, S.F., Alvarez, V.A., Ridenour, D.A., Kwiatkowski, D.J., and Sabatini, B.L. (2005). Regulation of neuronal morphology and function by the tumor suppressors Tsc1 and Tsc2. Nat Neurosci *8*, 1727-1734.

Tokuda, S., Mahaffey, C.L., Monks, B., Faulkner, C.R., Birnbaum, M.J., Danzer, S.C., and Frankel, W.N. (2011). A novel Akt3 mutation associated with enhanced kinase activity and seizure susceptibility in mice. Hum Mol Genet *20*, 988-999.

Tsien, J.Z., Chen, D.F., Gerber, D., Tom, C., Mercer, E.H., Anderson, D.J., Mayford, M., Kandel, E.R., and Tonegawa, S. (1996). Subregion- and cell type-restricted gene knockout in mouse brain. Cell *87*, 1317-1326.

Tsokas, P., Grace, E.A., Chan, P., Ma, T., Sealfon, S.C., Iyengar, R., Landau, E.M., and Blitzer, R.D. (2005). Local protein synthesis mediates a rapid increase in dendritic elongation factor 1A after induction of late long-term potentiation. J Neurosci *25*, 5833-5843.

Tsokas, P., Ma, T., Iyengar, R., Landau, E.M., and Blitzer, R.D. (2007). Mitogen-activated protein kinase upregulates the dendritic translation machinery in long-term potentiation by controlling the mammalian target of rapamycin pathway. J Neurosci *27*, 5885-5894.

von der Brelie, C., Waltereit, R., Zhang, L., Beck, H., and Kirschstein, T. (2006). Impaired synaptic plasticity in a rat model of tuberous sclerosis. Eur J Neurosci *23*, 686-692.

Wang, X., and Proud, C.G. (2011). mTORC1 signaling: what we still don't know. J Mol Cell Biol *3*, 206-220.

Wullschleger, S., Loewith, R., and Hall, M.N. (2006). TOR signaling in growth and metabolism. Cell *124*, 471-484.

4.2 Paper 2 (submitted)

Deletion of mTORC1 in the developing brain causes microcephaly and affects glial differentiation

Dimitri Cloëtta[1*], Venus Thomanetz[1*], Regula M. Lustenberger[1], Constanze Baranek[2], Shuo Lin[1], Filippo Oliveri[1], Suzana Atanasoski[2], and Markus A. Rüegg[1]

[*] These authors equally contributed to the study.

[1]Biozentrum, University of Basel, CH-4056 Basel, Switzerland

[2]Institute of Physiology, Department of Biomedicine, University of Basel, CH-4056 Basel, Switzerland and Institute of Anatomy and Cell Biology, Albert-Ludwigs-University Freiburg, D-79104 Freiburg, Germany

Key words: raptor, mTORC1, brain development, gliogenesis

Send correspondence to:
Markus A. Rüegg, Ph.D.
Biozentrum, University of Basel
Klingelbergstrasse 70
CH-4056 Basel, Switzerland
Phone: +41 61 267 22 23
Fax: +41 61 267 22 08
email: markus-a.ruegg@unibas.ch

SUMMARY

The mammalian target of rapamycin (mTOR) regulates cell growth in response to various intracellular and extracellular signals. It assembles into two multiprotein complexes, the rapamycin-sensitive mTOR complex 1 (mTORC1) and the rapamycin-insensitive mTORC2. In this study, we inactivated mTORC1 in mice by deleting the gene encoding raptor in the progenitors of the developing central nervous system. Mice are born but never feed and die within a few hours because of respiratory difficulties. The brains deficient for mTORC1 show a strong microcephaly which becomes visible at E17.5, and is the consequence of reduced cell number and cell size. The reduced cell number is due, at least in part, to specific changes in cell cycle phases during late cortical development and increased cell death. Depletion of raptor in vitro inhibits differentiation of neural progenitors into glia but not neurons. The differentiation defect is paralleled by decreased Stat3 signaling, which is a target of mTORC1 and has been implicated in gliogenesis. Taken together, our results show that postnatal survival, overall brain growth and specific aspects of brain development critically depend on mTORC1 function.

INTRODUCTION

In eukaryotes, cell growth is regulated by the TOR pathway (Hay and Sonenberg, 2004; Laplante and Sabatin, 2012; Wullschleger et al., 2006). The mammalian ortholog mTOR assembles into two distinct multiprotein complexes referred to as mTORC1 and mTORC2 (Jacinto et al., 2004; Sarbassov et al., 2004). mTORC1 consists of mTOR, raptor (gene abbreviated as *rptor*), mLST8 and PRAS40 and is sensitive to acute treatment with the immunosuppressant rapamycin (Wullschleger et al., 2006). mTORC1 has been implicated in the control of metabolism, protein translation, ribosome biogenesis, autophagy and transcription (Wullschleger et al., 2006). However, analysis of the physiological function of mTORC1 *in vivo* was for a long time restricted to early embryonic development, due to the lethality of mTOR-, raptor- and mLST8-deficient embryos. *mTOR*$^{-/-}$ and *rptor*$^{-/-}$ embryos die shortly after implantation due to proliferation defects (Gangloff et al., 2004; Guertin et al., 2006; Murakami et al., 2004). Because of this early lethality of the constitutive mutants, none of these studies have addressed the role of mTOR in brain development.

The role of mTOR in the brain has so far mainly been studied using cultured cells. A few studies addressed differentiation of neural stem cells and came to the seemingly conflicting conclusions that mTORC1 is either crucial for commitment into the neuronal (Han et al., 2008) or into the glial lineage (Rajan et al., 2003; Wang et al., 2008). Different conditions may explain these alterations, thus posing the question to which extent the chosen conditions reflect the physiological situation. A large set of studies addressed consequences of mTOR inhibition or knockdown for growth of postmitotic neurons (Swiech et al., 2008). Based on those studies, mTOR has been postulated to be important for polarization, dendrite development and axonal growth and guidance. Moreover, it has been shown that the complexity of the dendritic tree is reduced upon mTORC1 inhibition (Jaworski et al., 2005; Kumar et al., 2005). For axons, some studies have shown that local translation in growth cones that mediates axon guidance or regrowth after axotomy, is rapamycin-sensitive (Campbell and Holt, 2001; Park et al., 2008; Verma et al., 2005). Other studies have shown that axon specification and elongation is mTORC1-dependent (Li et al., 2008). In summary, *in vitro* data have resulted in a panoply of potential functions of mTORC1. However, the role of mTORC1 *in vivo* has not been addressed.

The only study that has addressed the role of mTOR in brain development has characterized the flat-top mutant (Hentges et al., 1999) caused by a mutation in the *mTOR* gene that results in a splicing defect (Hentges et al., 2001). Mutant embryos lack telencephaly and die at midgestation. Interestingly, this effect is phenocopied by prolonged application of rapamycin to pregnant mice (Hentges et al., 2001). Interpretation of these results is difficult because mTOR null embryos die in a much earlier developmental stage (Gangloff et al., 2004; Murakami et al., 2004) and because the prolonged treatment with rapamycin is likely to inhibit both mTORC1 and mTORC2. The generation of floxed alleles for *rptor* and *rictor* (Bentzinger et al., 2008; Cybulski et al., 2009; Polak et al., 2008) has

allowed to study the specific role of mTORC1 and mTORC2 in the developing brain. Here, we addressed the physiological function of mTORC1 in brain development by mating *rptor*-floxed mice with mice expressing Cre under the control of the nestin promoter (Tronche et al., 1999). We find that raptor-deficient brains are uniformly smaller than control brains due to decreased cell size and reduced cell number. Moreover, we show that differentiation into the glial but not the neuronal lineage is impaired and that the development of the hippocampal layering is affected.

RESULTS

mTORC1 controls embryonic brain size and is required for postnatal survival

To address the role of mTORC1 in brain development, we conditionally inactivated *rptor* in nestin-expressing neural progenitors using *rptor* floxed mice (Bentzinger et al., 2008) and the well-described nestin-Cre mice (Graus-Porta et al., 2001; Tronche et al., 1999). In those *rptor*$^{fl/fl}$;*nestin-Cre* (RAbKO) mice (Fig. S1A), *rptor* was successfully deleted as verified by the elimination of exon 6 in genomic DNA from brain but not from tails (Fig. S1B). Deletion of exon 6 resulted in the almost complete loss of raptor protein (Fig. 1A). Consistent with a complete loss of mTORC1 activity, phosphorylation of the mTORC1-dependent site serine 2448 in mTOR (Copp et al., 2009; Jastrzebski et al., 2007) and of the downstream substrate S6 was strongly decreased in the brains of RAbKO mice (Fig. 1A, Table S1 for quantification). In contrast, abrogation of mTORC1 did not affect the function of mTORC2 as the protein level of rictor and phosphorylation of mTOR at the mTORC2-specific phosphorylation site at serine 2481 (Copp et al., 2009), and of Akt/PKB at serine 473 (Sarbassov et al., 2005) was not abrogated. To the contrary, phosphorylation at both sites was rather increased in RAbKO mice (Fig. 1A, right), consistent with previous results from mice in which raptor was conditionally deleted in other tissues (Bentzinger et al., 2008; Godel et al., 2011; Inoki et al., 2011; Polak et al., 2008; Shende et al., 2011). These data are strong evidence that mTORC1 activity had been eliminated by loss of raptor and that mTORC2 activity was not impaired. Although RAbKO mice were born at the expected Mendelian ratio (Table 1) and their body weight was normal (Fig. 1B), they became cyanotic and died within a few hours after birth (data not shown). Their stomachs never contained milk and their breathing was often irregular (gasping), suggesting that the mice died of respiratory failure. The respiratory difficulties seemed not to be due to malformations of the neuromuscular junctions as revealed by the staining of presynaptic motor nerves with antibodies to neurofilament and postsynaptic acetylcholine receptors with α-bungarotoxin in the diaphragm (Fig. S2). Rather, higher brain centers involved in respiratory control might be affected.

The brains of RAbKO mice appeared smaller and their brain weight was reduced to 54% of that in control animals (Fig. 1C) even though the body weight was not changed (Fig. 1B). The difference in brain size could be caused by a decrease in cell number or cell size, both processes that have been reported to be influenced by mTOR (Laplante and Sabatini, 2012; Wullschleger et al., 2006). Comparative analysis of cell number by quantification of the DNA content indicated a more than 30% reduction in the number of cells in the brains of E19.5 RAbKO mice (Fig. 1D, upper part). Together with the reduced brain weight, these data suggest that the DNA amount/g brain tissue (reflecting cell density) was increased to more than 120% in the brains of RAbKO mice compared to controls (Fig. 1D, lower part). Moreover, the ratio of protein to DNA amount was decreased to 71 ± 10% (mean ± SEM; N ≥ 3) (data not shown) consistent with the concept that the cells in RAbKO brains are smaller. Together, these results indicate that a decrease in cell number and a decrease in cell size (resulting in

higher cell density) contribute to the microcephaly observed in newborn RAbKO mice. Although brain size was reduced, the overall structure was normal at birth (Fig. 1E). The difference in brain size became obvious at E17.5 (Fig. 1F, lower part) but could not be detected earlier (Fig. 1F, upper part). Although there was a trend in E17.5 RAbKO mice for an increased cell density compared to control mice, this difference did not reach significance (Fig. 1G), indicating that the smaller size of RAbKO brains at this developmental period was mainly due to changes in cell number. In summary, these data indicate that the size difference becomes manifest between E15.5 and E17.5 and increases progressively until birth.

Raptor deficiency increases apoptosis and affects cell cycle duration

To address the mechanism involved in the loss of cells in RAbKO mice, the presence of apoptotic cells was assessed by staining brain sections with antibodies to cleaved Caspase 3. Apoptotic, cleaved Caspase 3-positive cells were not increased in E15.5 or E17.5 RAbKO mice compared to controls (Fig. 2A,C). However, the appearance of apoptotic cells was strongly increased in RAbKO mice at E19.5 (Fig. 2A,C) and the vast majority of the dying cells were NeuN-positive neurons (Fig. 2B). Apoptotic cells were not unique to cortical regions but could also be found at E19.5 in other brain regions, such as the hippocampus (Fig. 7C) or the thalamus (data not shown). This suggests that the reduced brain size and the decreased cell number at E17.5 is not a consequence of cell death. However, neuronal cell death contributes to the reduced cell number in the brain of RAbKO mice at late developmental stages.

To search for the mechanism involved in the earlier brain size reduction, we next assessed cell cycle kinetics and cell differentiation. As mTORC1 has been implicated in controlling G2/M phase transition during the cell cycle (Ramirez-Valle et al., 2010) we analyzed proliferation in embryonic RAbKO mice by BrdU labeling *in utero*. Radial glial cells in the ventricular zone of the developing cortex display phase-related interkinetic nuclear migration during cell cycle progression (Gotz and Huttner, 2005; Sargeant et al., 2008). DNA replication takes place in the basal and mitosis in the apical region of the ventricular zone. In order to determine nuclear position, we divided the developing cortex into three progenitor regions R1 to R3, based on Sox2 and Tbr2 staining. R1 covered the apical VZ, R2 the basal VZ and the subventricular zone and R3 the intermediate zone (Fig. S3). E15.5 RAbKO embryos labeled with BrdU 3 hours prior to sacrifice did not show differences in the distribution of BrdU-labeled cells in the developing cortex compared to controls (Fig. 3A,B). When RAbKO mice were pulsed with BrdU at E15 and analyzed 12 hours later, a significantly larger proportion of the BrdU-labeled cells was detected in R1 and this was at the expense of labeled cells in R2 (Fig. 3C,D). Following one pulse of BrdU at E14.5 and analysis 24 hours later showed that roughly a quarter of the BrdU-positive nuclei in control mice were located in R1 whereas in RAbKO mice, only very few BrdU-positive cells were found in R1 (Fig. 3E,F). In contrast, significantly more BrdU-positive

cells were present in R2 in the RAbKO mutants (Fig. 3E,F). This nuclear localization phenotype was also observed when BrdU was injected at E16.5 and mice were analyzed at E17.5 (Fig. 3G).

Moreover, the total number of BrdU-positive cells per ventricular surface length was reduced in RAbKO mice at E17.5 but was not changed at E15.5 and E19.5 (Fig. 3H). Thus, labeling of cells in S-phase by one pulse of BrdU at E16.5 results in fewer BrdU-positive cells 24 hours later. To address the proportion of cortical cells within the cell cycle, we also performed cumulative labeling of cells by repetitive administration of BrdU for up to 12 hours (Fig. S4). Analysis of mice at E15.5 showed that more than 50% of the cortical cells were BrdU-positive after 8 hours of cumulative labeling (Fig. S4) and there was no significant difference in the labeling index (number of BrdU-positive cells/total cell number) between control and RAbKO mice (Fig. 3I; Fig. S4). When the same cumulative labeling studies were performed at E17.5, only approximately 8% of the cells incorporated BrdU after 8 hours, consistent with the view that peak neurogenesis occurs at E15.5 and decreases thereafter. Also at E17.5, the relative labeling index of BrdU-positive cells was the same in RAbKO and control mice (Fig. 3I). Since after a 24 hour BrdU pulse, E17.5 RAbKO mice have approximately 15% fewer BrdU-positive cells, it is possible that labeling during one cell cycle is not sufficient to obtain a detectable difference in the number of cumulatively labeled cells. The finding that fewer cells entered the S-phase at E16.5 in the RAbKO mice (Fig. 3H) indicates that the cell number reduction occurs in a narrow time window between E15.5 and E17.5 and is due, at least in part, to defects in proliferation.

Loss of Raptor affects neurosphere formation and growth

Neurosphere formation and maintenance is a surrogate assay for neural stem cells (Reynolds and Weiss, 1996). Thus, we isolated and cultured spherogenic neural stem/progenitor cells from the telencephalon of P0 mice. The number of secondary neurospheres generated from RAbKO and control animals was similar (control: 10.9 ± 3.04; RAbKO: 12.7 ± 5.29; $N \geq 15$; $p > 0.05$), whereas the size of RAbKO-derived neurospheres was strongly reduced (Fig. 3J,K). Compared to control cultures, the size distribution in RAbKO spheres was shifted towards smaller diameters ($p < 1.384 \times 10^{-12}$; Wilcoxon two sample test). Thus, spherogenic stem cells seemed not to be affected by loss of raptor but the proliferative capacity of cells within the neurospheres was decreased. Interestingly, a similar proliferation defect was reported for embryonic stem cells deficient for raptor or mTOR (Gangloff et al., 2004; Guertin et al., 2006; Murakami et al., 2004).

Cell cycle exit and proliferation are reduced in raptor-deficient neural progenitor cells

The changes in tempospatial distribution of progenitor cells and the reduction of cells in S-phase indicated potential defects in specific periods of the cell cycle. Therefore, we addressed whether loss of raptor affected cell cycle exit of progenitors. We administered BrdU to pregnant mice at E14.5, E16.5 or E18.5 of gestation and examined progenitor cell cycle exit by co-staining for BrdU and Ki67

24 hours later (Fig. 4A,B). The proportion of BrdU-positive progenitors that exited the cell cycle (i.e. became Ki67 negative) was not affected at E15.5 but was reduced by approximately 50% in E17.5 and E19.5 RAbKO cortices (Fig. 4A,B). Hence, precursor cells in the cortex of RAbKO mice in late embryonic development remain longer in the cell cycle. We also examined cells in mitosis by immunostaining for phosphorylated histone 3 (PH3). The number of PH3-positive cells was not changed in the cortex of E15.5 RAbKO mice (Fig. 4D) but there was a significant reduction at E17.5 (Fig. 4C,D). These data suggested that a prolongation of the cell cycle time and delayed cell cycle exit affect brain size in RAbKO mice.

Because the above data can also be interpreted as a sign for changes in the differentiation of neural precursors, we then determined the number of Sox2-positive neural progenitors and Tbr2-positive basal progenitors in the cortex of control and RAbKO mice. Both, the number of Sox2-positive cells and the number of Tbr2-positive cells when determined above a specific ventricular surface area were reduced in RAbKO mice at E17.5 but were not changed at E15.5 (Fig. 4E-G). Consistent with our finding that the total cell number is already reduced at E17.5 (Fig. 1G), we calculated the number of Sox2- and Tbr2-positive cells relative to the total cell number and found a significant reduction of Sox2 progenitors but only a trend to reduced Tbr2 cell numbers (Fig. 4H). Therefore, these findings together support a reduced expansion of the Sox2 progenitor pool due to a prolonged cell cycle and exclude a precocious differentiation to Tbr2-positive, committed basal progenitors in RAbKO mice.

During cortical development, radial glial cells are highly polarized and possess specialized apical endfeet that form the lining of the ventricle and basal processes stretching to the pial surface. The apical cell surface of the radial glial cells contains important fate determinants. Loss of cell polarity or detachment from the apical membrane following mitosis results in proliferation defects (Loulier et al., 2009). We therefore examined the structure of radial glial cells in the cortex of RAbKO embryos. Like in control embryos, radial glia in the ventricular zone of RAbKO mutants showed a continuous and apical staining for the adhesion complex protein β-catenin (Fig. 4I) and for F-actin at E15.5 and E17.5 (Fig. S5). Moreover, the radial glia morphology appeared normal following immunostaining for nestin (Fig. S5). Thus, a disturbed radial glial morphology and polarity cannot explain the observed changes in progenitor proliferation and differentiation in the cortex of RAbKO brains.

Effect of raptor deficiency on cortical layering

Cortical precursor proliferation, differentiation and migration of neurons are intimately linked (Gotz and Huttner, 2005). We examined the production of differentiated cells in the cortical plate from E12.5 and E14.5 progenitors by BrdU label and chase experiments. When progenitors were labeled at E12.5, no differences in BrdU-labeled progeny in the cortical plate at E19.5 could be observed and BrdU-labeled cells were distributed throughout all cortical layers in both genotypes (Fig. 5A). However, when labeled at E14.5, cortical progenitor derived cells showed a different cellular distribution in RAbKO mice

compared to controls at E19.5. Whereas in control mice most BrdU-positive cells populated the upper cortical plate (Fig. 5B), the labeled cells in RAbKO mice remained concentrated in the ventricular zone/subventricular zone/intermediate zone (VZ/SVZ/IZ) and fewer cells reached the cortical plate (Fig. 5B). As a consequence, the ratio between BrdU-positive cells in the cortical plate and in the VZ/SVZ/IZ was significantly reduced in RAbKO mice (Fig. 5C). Therefore, fewer cells generated after E14.5 reached the cortical plate in RAbKO mice but were in a location more reminiscent of less mature cells. These data are in agreement with a previous study showing that rapamycin does not interfere with preplate splitting and early cortical plate formation (Jossin and Goffinet, 2007).

Despite the change in size and proliferation, the gross organization of cells within the cortex of RAbKO mice seemed normal at E19.5 (Fig. 5D). In addition, NeuN-positive neurons were present in the cortex and the subplate appeared to have been normally formed (Fig. 5E). However, Map2 staining (a dendritic marker) revealed that although preplate splitting and subplate formation was normal in RAbKO mice (Fig. 5F), expression was weak compared to controls indicative of a reduction of neuropil or a decrease in the number of neurons in the cortical plate of raptor-deficient mice. To test whether the low Map2 signal in RAbKO cortex was the consequence of a reduced dendritic complexity, we also examined neurite outgrowth in raptor-deficient neurons *in vitro*. We deleted *rptor* from E16.5 primary hippocampal neurons of floxed raptor mice after 4 days *in vitro* by transfection with a Cre-expression vector. Transfected neurons were visualized by co-transfection with a GFP-expressing vector (Fig. 5G). Sholl blot analysis 10 days post transfection showed a significant decrease in the complexity of the neurites compared to control-transfected neurons (Fig. 5G,H). These results are also in agreement with previous work using rapamycin or RNAi against mTOR (Jaworski et al., 2005; Kumar et al., 2005). Thus, the decreased Map2 staining in cortical sections of RAbKO mice could have been due to a reduction in the neuronal complexity.

Effect of raptor deficiency on hippocampal layering

In contrast to the normal layering of the cortex, layering of the hippocampus was altered in RAbKO mice. At E19.5, the CA regions and the dentate gyrus were less structured in RAbKO mice (Fig. 6A, 1st row). Map2 staining was reduced in the cortical plate and in the hippocampus of E19.5 RAbKO mice (Fig. 6A, 2nd row, left) and this difference was already obvious at E15.5 (Fig. 6A, 2nd row, right). Because cell density is not changed in E15.5 RAbKO cortices this indicates a defect in neurite elaboration. Examination of neuronal layer formation revealed that NeuN-positive neurons in the CA regions of the hippocampus did not form a proper pyramidal layer in RAbKO mice (Fig. 6A, 3rd row, open arrowhead). In the dentate gyrus, which contains a secondary proliferation zone distinct from the VZ, neurons did not form the C-shaped structure in the hilus (Fig. 6A, arrow) and did not show the initial signs of a granule cell layer (Fig. 6A, asterisk). These changes were not observed in E15.5 RAbKO brains. We also analyzed the formation of hippocampal layering by BrdU label and chase

experiments of E14.5 progenitors. At E19.5, BrdU-labeled progenitors were still near or within the VZ in RAbKO mice (Fig. 6C) whereas in control mice those progenitors were integrated into the pyramidal cell layer. These results show that mTORC1 strongly contributes to the formation of a pyramidal layer in the CA regions and to a defined granule cell layer in the dentate gyrus.

Glial differentiation is impaired in raptor-deficient brains

mTORC1 is important for neural stem/progenitor cell differentiation into neurons and glia (Han et al., 2008; Rajan et al., 2003; Wang et al., 2008). Thus, we analyzed the expression of neuronal and glial proteins in the brains of E19.5 control and RAbKO mice by Western blot analysis. We did not detect significant changes in the expression of the neuron-specific isoform β-tubulinIII, or GAD65/67, a marker for a subpopulation of inhibitory interneurons (Zhu et al., 1999), or brain lipid-binding protein (BLBP), a radial glia marker reflecting the number of neuronal precursors (Hartfuss et al., 2001) (Fig. 7A). In contrast, the astrocytic marker glial fibrillary acidic protein (GFAP) was strongly reduced in RAbKO brain lysates (Fig. 7A; Table S1). In newborn mice, when GFAP+ cells start to populate the brain (Sancho-Tello et al., 1995; Shu et al., 2003), GFAP immunostaining in RAbKO brains was weaker compared to controls in the granule cell layer of the dentate gyrus and in the midline glial stuctures: the indusium griseum glia, the midline zipper glia and the glial wedge (Fig. 7B). Although apoptosis was increased in the hippocampus of RAbKO mice at E19.5, the cells positive for Caspase 3 were not GFAP-positive (Fig. 7C). We also examined expression of S100β, a marker of postmitotic astrocytes. RAbKO mice showed a trend to have fewer S100β-positive cells but this was not significant (Fig. S6). In summary, these results indicate that mTORC1 is also important for the generation of glial cells.

mTOR signaling has been linked to glial differentiation via its ability to phosphorylate Stat3 (Rajan et al., 2003; Yokogami et al., 2000), which regulates astrocyte development (Bonni et al., 1997; Johe et al., 1996). Hence, Stat3 could provide a potential explanation on how glial differentiation is regulated by mTORC1. Thus, we studied the expression and phosphorylation state of Stat3 in brain lysates of newborn RAbKO mice. Indeed, the level of Stat3 protein as well as its phosphorylation was decreased in RAbKO compared to control mice (Fig. 7D; Table S1). This result suggests that failure of mTORC1-mediated activation of Stat3 may be the cause for the decrease in GFAP-positive cells.

We addressed whether the reduction in GFAP expression in RAbKO mice was due to a reduced ability for RAbKO progenitors to differentiate into the astroglial lineage. Thus, we induced differentiation in dissociated neurosphere cultures from RAbKO and control mice. Whereas the number of β-tubulinIII neurons was not changed, the number of GFAP-positive cells was much lower in 5 day old cultures of RAbKO mice (Fig. 7E,F). In addition, Western blot analysis confirmed that GFAP levels were lower in RAbKO-derived cell cultures (Fig. 7G).

To examine whether the changes in glial differentiation were due to inherent differences in the stem cell pool of RAbKO mice, we ablated raptor from neural stem cells, derived from heterozygously or homozygously floxed *rptor* mice in culture by using a Cre-expressing adenovirus. This acute removal of raptor also resulted in fewer GFAP-positive cells (Fig. S7A,B). In addition, an increase in the number of β-tubulinIII-positive immature neurons was observed (Fig. S7A,B). Western blot analysis of such cultures showed that the state of phosphorylation of Stat3 was lower in RAbKO-derived neural progenitors (Fig. S7D) as was also observed in brain lysates. In conclusion, these results indicate that mTORC1 is important for the proper differentiation of neural progenitor cells into the glial lineage and that this function is mediated by activation of the Stat3 pathway.

DISCUSSION

Raptor is required for CNS development

We addressed the role of raptor in brain development by conditional inactivation of *rptor* in nestin-expressing progenitor cells, which is known to be expressed as early as E10.5 (Graus-Porta et al., 2001). Consistent with the concept that mTORC1 controls organismal size as shown in other species (Long et al., 2002; Oldham et al., 2000), RAbKO mice show microcephaly and die shortly after birth with signs of cyanosis. In agreement, rapamycin treatment of developing embryos revealed that mTOR is essential for the development of the telencephalon and the survival after midgestation (Hentges et al., 2001). Thus, the prolonged survival of RAbKO mice compared to rapamycin-treated embryos suggests that rapamycin-treated embryos may die due to mTORC1 inhibition in non-CNS cells and /or to loss of activity of both mTOR complexes.

Raptor regulates progenitor cell proliferation in the telencephalon and affects survival

Inactivating *rptor* in neural progenitors caused aberrations in the cell cycle and in cell differentiation that resulted in the thinning of the telencephalic cortex and in a reduced brain size. Although differences in brain size and cellularity of the cortex were not obvious before peak neurogenesis at E15.5, during late embryonic and early postnatal stages the number of progenitors and differentiated cells was strongly reduced in RAbKO mice. These data are in agreement with slice culture studies where rapamycin had no effect on preplate splitting and the layering of the early cortical plate (Jossin and Goffinet, 2007). The RAbKO phenotype corresponded with a slowing of the cell cycle, supporting the described role for mTORC1 in cell cycle regulation (Ramirez-Valle et al., 2010). We also provide evidence for a cell autonomous effect of raptor on proliferation by showing that raptor-deficient stem/progenitor cells in neuroshpere cultures are able to be maintained but generate smaller clones. This reduction in neurosphere size but not number is probably a reflection of mitotic expansion within the cultures. Hence, we propose that raptor controls neural progenitor proliferation and loss of raptor results in an extended cell cycle. Our cumulative BrdU labeling experiments also indicate a trend towards a lengthening of the cell cycle. We think that small differences in cell cycle length might not be detectable by cumulative BrdU labeling because small aberrations in proliferative cell number might have to add up to a cumulative effect that becomes only significant when a higher proportion of cells is lost. This might only be the case after more than one cell cycle which is also supported by our data. Progenitor cell cycle and differentiation are interconnected in the developing nervous system (Calegari and Huttner, 2003). Interestingly, extension of the cell cycle, particularly G1 is often associated with differentiation. Recent evidence suggests that proliferation depends on mTORC1-mediated activation of 4E-BP proteins (Dowling et al., 2010). However, raptor-deficient neural progenitors show not only a longer cell cycle time but also reduced differentiation. The effect of raptor on differentiation of neurosphere cells into neurons *in vitro* was less apparent and rather the formation of astroglia was

affected. It will be interesting to establish the exact mechanism of raptor function in cell cycle progression and to determine whether raptor and mTORC1 are required in a separate differentiation mechanism *in vivo.*

Our work also provides evidence that mTORC1 function is important to warrant survival of cells at late stages of embryonic development as we observed a substantial extent of apoptosis at E19.5. These apoptotic events may also contribute to the small size of the brains in RAbKO mice at birth. The apoptotic cells were positive for the neuronal marker NeuN but not for GFAP, indicating that this process affects mostly neuronal cells and not glia. However, we do not know if prevention of apoptosis is a cell autonomous function of mTORC1 or a consequence of a failure of neurons to connect to their targets. Indeed, cultured neurons that lack raptor show deficits in neurite outgrowth.

Raptor promotes gliogenesis by regulating the Jak-Stat signaling pathway

It is possible that raptor is responsible for maintaining neural progenitors in a multipotent state through regulation of the Jak/Stat pathway. We found a reduction in early populations of GFAP-positive cells in RAbKO brains suggesting that glial differentiation was affected *in vivo*. The Jak-Stat pathway controls astrocytic differentiation (Bonni et al., 1997; Johe et al., 1996) and mTORC1 has been implicated in this Stat3-dependent function (Rajan et al., 2003; Wang et al., 2008). Phosphorylation of Stat3 at Ser727 is rapamycin-sensitive and phosphorylation of Stat3 at Tyr705 and Ser727 is essential for maximal activation (Wen et al., 1995; Yokogami et al., 2000). We show that Stat3 phosphorylation is strongly reduced in the brains of RAbKO mice. The reduced phosphorylation likely results in the reduced amounts of Stat3 protein that we also observed (He et al., 2005). Interestingly, deletion of the mTORC1 inhibitor TSC, a model for the genetic disease tuberous sclerosis in humans, increased Stat3 phosphorylation and GFAP expression (Onda et al., 2002).

mTORC1 pathway is a key controller of neural development and brain size

mTORC1 can be activated by Akt3/PKBγ. The role of raptor in controlling brain size was similar to the function described for the mTORC1-upstream molecule Akt3/PKBγ (Easton et al., 2005; Tschopp et al., 2005). As in RAbKO mice, cell number was reduced in the brains of Akt3/PKBγ -deficient mice (Tschopp et al., 2005). Together, these findings suggest that Akt3/PKBγ acts through mTORC1 during brain development. On the other hand S6K, one of the main targets of mTORC1 has been shown to affect cell size when deleted *in vivo* (Montagne et al., 1999; Shima et al., 1998). The lack of phosphorylation of S6K in the RAbKO brains likely affects cell size resulting in an increase in cell density and reduced complexity of the raptor-deficient neurons.

Deletion of mTORC1 causes a more severe phenotype than deletion of its upstream activator Rheb1. Rheb1 and not Rheb2 is the upstream GTPase responsible for the activation of mTORC1 (Zou et al., 2011). Mice in which *Rheb1* was ablated from neural progenitors (using the same nestin-Cre

driver that we used to delete *rptor*) did not die and their brains were not smaller than controls at birth. However, postnatal brain size and myelination was strongly affected later and the mice died at 5 to 6 weeks of age. Hence, deletion of *rptor* and inactivation of mTORC1 causes a more severe phenotype than deletion of *Rheb1* suggesting the existence of either a functional redundancy in the GTPases that activate mTORC1 during brain development, or of alternative pathways that can activate mTORC1 in neural progenitors independent of Rheb1. In this context it is interesting that phosphorylation of Akt at serine 473 was increased in *Rheb1*-deficient mice as it is in RAbKO mice. These data show that in both mice mTORC1 activity is diminished and that the absence of the S6K-mediated feedback inhibition and/or an increase in mTORC2 activity is responsible for the increased phosphorylation of Akt at serine 473. Consistent with the notion that mTORC2 activity is increased, we also observed increased phosphorylation of mTOR at the mTORC2-specific site serine 2481.

Role of mTORC1 in hippocampal layering

Ablation of mTORC1 may affect granule cell migration in the dentate gyrus by affecting glial differentiation. In our mouse model, the malformation of the granule cell layer coincides with a generally decreased GFAP signal in the dentate gyrus. The glial scaffold in the dentate gyrus starts to express GFAP during late embryonic development (Forster et al., 2002; Rickmann et al., 1987). Granule cell migration originates from the hilus of the dentate gyrus and involves a highly organized glial network. A decrease in the organization of this scaffold causes malformations of the granule cell layer (Zhao et al., 2004). In addition, elongation and organization of glia in the dentate gyrus was reported to depend on reelin and some of its functions are rapamycin sensitive (Jossin and Goffinet, 2007). In raptor-deficient hippocampi, both, the developing granule cell layer of the dentate gyrus and the pyramidal cell layer of the CA regions were perturbed, which also correlated with an impaired, Stat3-dependent glial differentiation.

Concluding remarks

Our data show that mTORC1 is crucial for normal brain growth and postnatal survival. Several aspects of brain development are affected by ablation of mTORC1 function and may in sum be responsible for the death of the newborn mice. Regulation of cell morphology (size) and division, which are both affected in RAbKO mice, are processes that are well known to be associated with mTORC1 signaling. Our data also strongly indicate that Stat3 is an important downstream target of mTORC1 that is required for normal differentiation of precursor cells into GFAP-positive glia. In summary, the multiple phenotypes of RAbKO mice described here show that mTORC1 has a central role in the integration of the inputs from several signaling pathways and that it activates various downstream effectors.

Acknowledgements

We thank Dr. J. S. Tchorz and F. Schatzmann for providing a Cre-expressing adenovirus and Prof. V. Taylor and Dr. M. Gassmann for their comments to the manuscript. This work was supported by the Cantons of Basel-Stadt and Baselland and grants from the Swiss National Science Foundation to MAR. The work in the laboratory of SA was supported by the Swiss National Science Foundation, the Novartis Foundation (Novartis Stiftung für medizinisch-biologische Forschung), the Botnar Foundation, and Swiss Life (Jubiläumsstiftung für Medizinische Forschung).

Figure 1

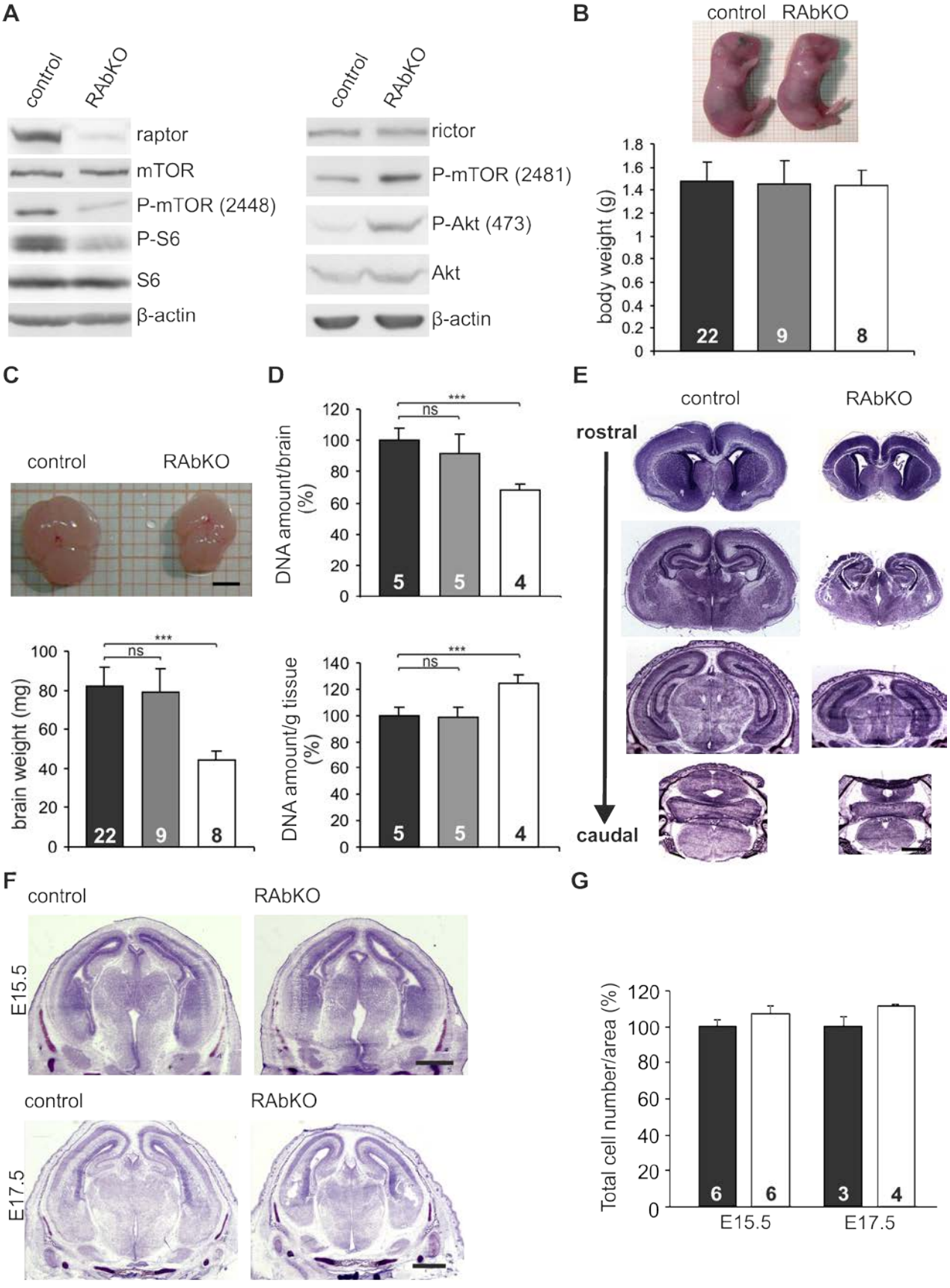
A
control
RAbKO
raptor
mTOR
P-mTOR (2448)
P-S6
S6
β-actin
rictor
P-mTOR (2481)
P-Akt (473)
Akt
β-actin
B
control RAbKO
body weight (g)
22
9
8
C
control RAbKO
brain weight (mg)
DNA amount/brain (%)
DNA amount/g tissue (%)
ns
***
5
4
D
E
control
RAbKO
rostral
caudal
F
control
RAbKO
E15.5
E17.5
G
Total cell number/area (%)
6
3
E15.5
E17.5

Fig. 1. *Nestin-Cre*-mediated deletion of *rptor* causes microcephaly and perinatal death.

(A) Western blot analysis for the indicated proteins with whole brain lysates of E19.5 control and RAbKO mice. The presence of remaining raptor protein is probably due to meninges and blood vessels, which both do not express Cre in our mouse model (see Graus-Porta et al., 2001).

(B) Photographs of newborn control and RAbKO mice (top) and body weight of E19.5 mice (bottom).

(C) The brain from E19.5 RAbKO mice is considerably smaller (top) and weighs less (bottom).

(D) Relative DNA amount per brain (top) and relative DNA amount per gram wet weight (bottom). Note that the DNA amount per brain in RAbKO mice is lower, indicative of lower number of cells whereas the DNA/g weight is increased indicative of a higher cell density.

(E) Cresyl violet-stained sections of E19.5 control and RAbKO brains at different levels in the rostro-caudal axis.

(F) Cresyl violet-stained sections at E15.5 (top) and E17.5 (bottom). Note, that the brain of RAbKO mice is smaller at E17.5.

(G) Quantification of the cell number in the cortex of control and RAbKO mice as measured in Hoechst staining.

Bars in B, C, D represent means ± standard deviation; bar in G represents ± sem; number in the bars are the number of animals measured. Black bars: control; grey bars: heterozygous RAbKO; open bars: RAbKO mice. p-values (two-tailed t-Test) are: *** $p < 0.001$; * $p < 0.05$; ns $p > 0.05$. Scale bars: (E) and (F) = 1 mm.

Figure 2

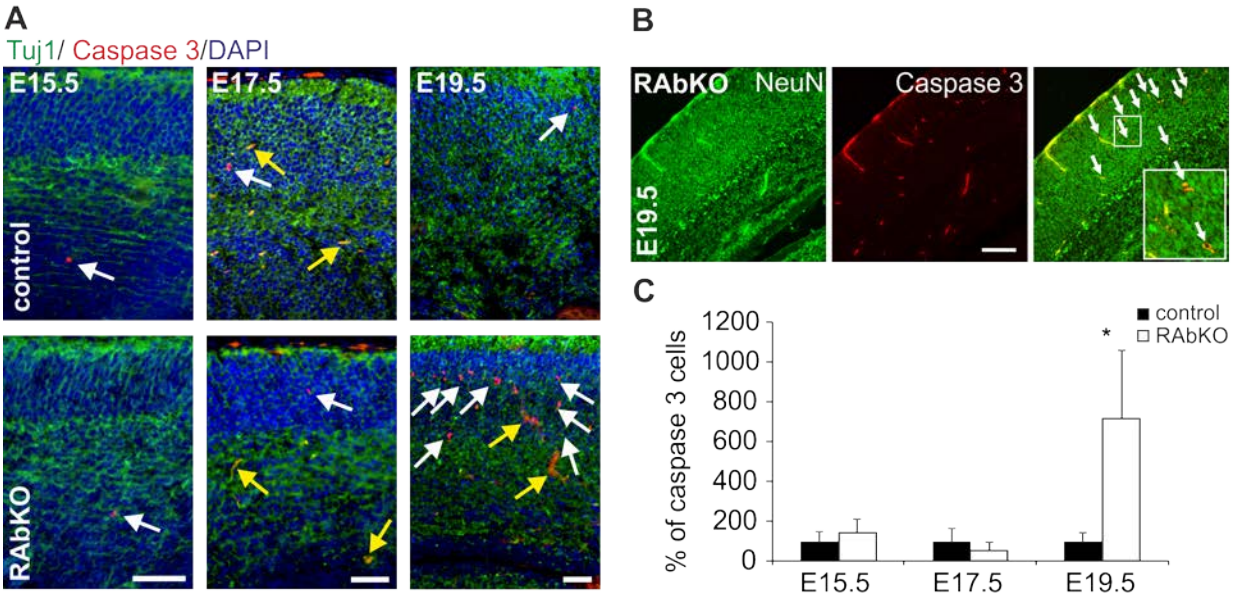

Fig. 2. Loss of raptor leads to increased cell death during late brain development.

(A) Examination of apoptosis at different developmental time points by staining for cleaved Caspase3 (red) in conjunction with antibodies to β-tubulin III (Tuj1; green) and DAPI (blue). While no or only little apoptotic nuclei were detected at E15.5 and E17.5, RAbKO mice show a strong increase of apoptosis at E19.5 (white arrows). Yellow arrows indicate background staining in blood vessels.

(B) Most of those apoptotic nuclei at E19.5 are also positive for the neuronal maker NeuN (arrows).

(C) Histograms represent mean ± standard deviation using at least 3 animals for each genotype. p-values (from two-tailed t-Test); * $p < 0.05$. Scale bars = 50 µm.

Figure 3

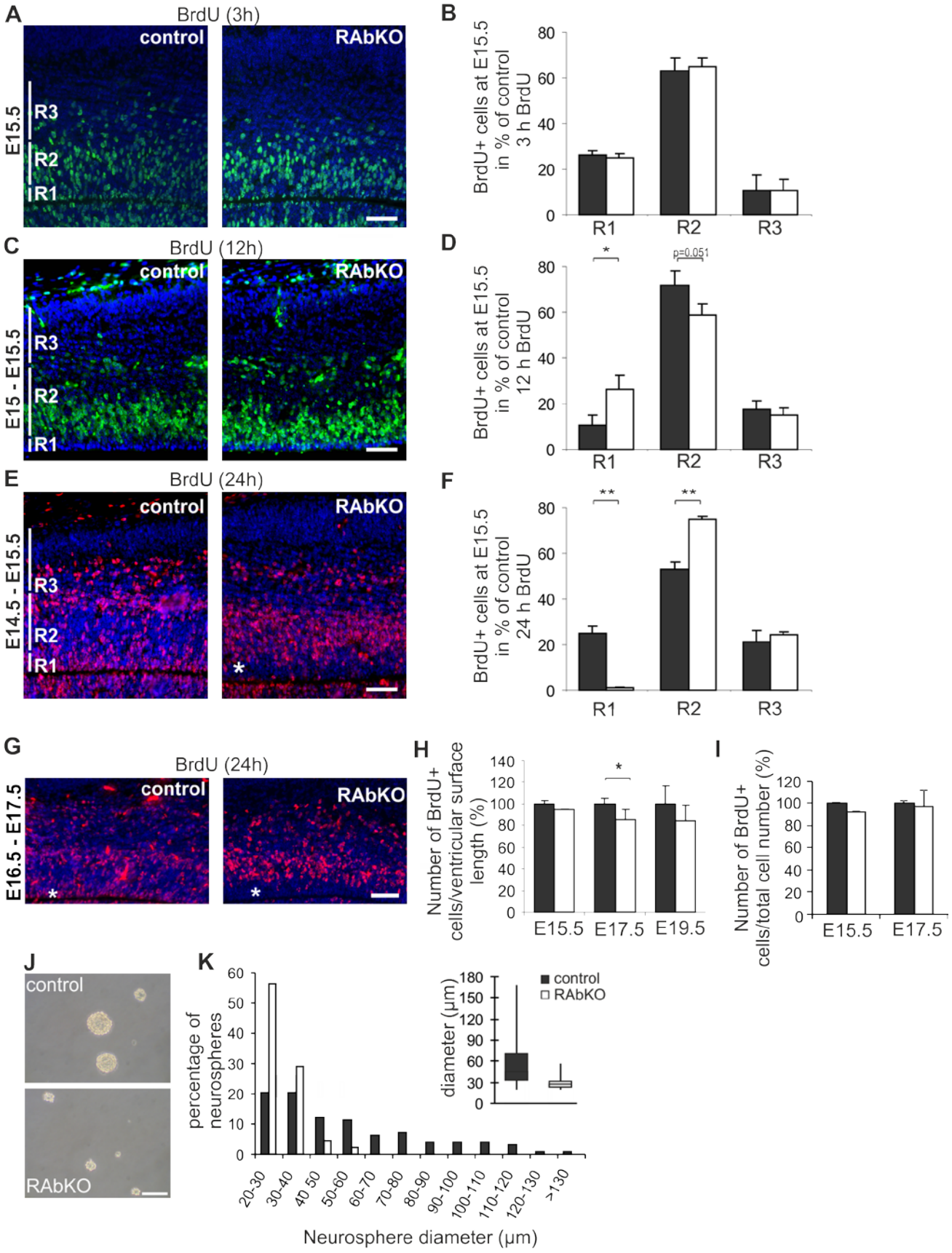
A
BrdU (3h)
control
RAbKO
E15.5
R3
R2
R1
B
BrdU+ cells at E15.5 in % of control 3 h BrdU
R1
R2
R3
C
BrdU (12h)
E15 - E15.5
D
BrdU+ cells at E15.5 in % of control 12 h BrdU
p=0.051
E
BrdU (24h)
E14.5 - E15.5
F
BrdU+ cells at E15.5 in % of control 24 h BrdU
G
E16.5 - E17.5
H
Number of BrdU+ cells/ventricular surface length (%)
E15.5
E17.5
E19.5
I
Number of BrdU+ cells/total cell number (%)
J
K
percentage of neurospheres
diameter (µm)
control
RAbKO
20-30
30-40
40 50
50-60
60-70
70-80
80-90
90-100
100-110
110-120
120-130
>130
Neurosphere diameter (µm)

Fig. 3. Depletion of raptor alters location and number of proliferating precursor cells.

Regions used for counting proliferating cells are indicated in the picture as R1 to R3 and are explained in Fig.S3. Sections were stained for BrdU (green in A,C; red in E, G) and DAPI (blue). Developmental time points are indicated in the picture.

(A, B) Mice were sacrificed three hours after BrdU injection. There is no significant difference in the number of BrdU+ cells in R1 to R3.

(C, D) Mice were sacrificed twelve hours after BrdU injection. The number of BrdU+ cells in the RAbKO mice is increased in R1 but decreased in R2.

(E, F) Mice were sacrificed 24 hours after BrdU injection. RAbKO mice had almost no BrdU+ cells in R1 (asterisk) but most in R2.

(G) Injection of BrdU at E16.5 and analysis at E17.5. Note that RAbKO mice do not have many BrdU+ cells in the deepest layer, corresponding to R1 (asterisk).

(H) Quantification of BrdU+ cells in comparable cortex regions normalized to ventricular surface length.

(I) Percentage of BrdU+ cells per total cell number in comparable cortex sections. Mice were sacrificed after 8 hours of cumulative BrdU injections that were given every 2 hours.

(J) Micrographs of secondary neurospheres derived from E19.5 brains. Note the pronounced difference in size.

(K) Distribution of the diameters of secondary neurospheres derived from control (black) or RAbKO (white) brain. Size distribution of RAbKO neurospheres is shifted to the left. Inset: box plot of the median size of the neurospheres. N = 100 (control) or 91 (RAbKO) Neurospheres.

Bars in B, D, F, H, I represent means ± standard deviation. For each experiment, at least 3 mice per genotype were analyzed. p-values (from two-tailed t-Test) are: n.s. $p > 0.05$*; $p < 0.05$, ** $p < 0.01$. Scale bars = 100 µm. Black bars: control; open bars: RAbKO mice.

Figure 4

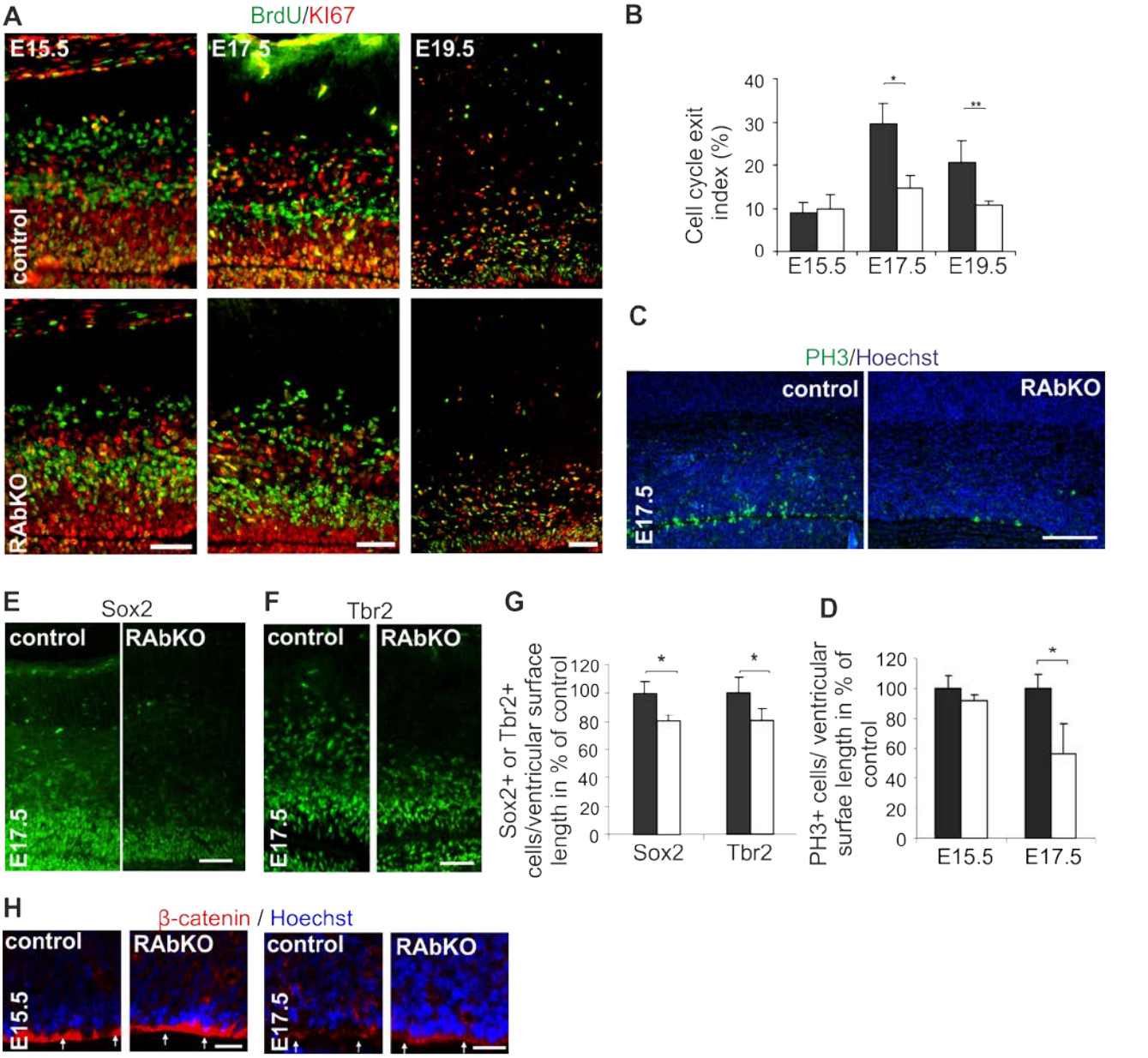

Fig. 4. Deficiency for raptor in the brain causes aberrant cell cycle exit and leads to decreased progenitor cell number.

(A) Staining of brain sections for BrdU and Ki67 at indicated time points.

(B) Quantification of BrdU+/Ki67- as percentage of all BrdU+ cells (cell cycle exit index). Note that at E17.5 viewer cells leave the cell cycle.

(C) Analysis of mitosis at E17.5 by staining for PH3 and

(D) corresponding quantification of mitotic nuclei at E15.5 and E17.5.

(E) Staining of E17.5 brain sections with antibodies to Sox2 or (F) Tbr2.

(G) Quantification of the number of Sox2+ and Tbr2+ cells per ventricular surface length at E17.5.

(H) Quantification of the number of Sox2+ and Tbr2+ cells per total cell number. (I) Staining for β-catenin in the ventricular zone of cortical sections from E15.5 and E17.5 control and RAbKO mice. Error bars in B and H represent means ± STDV, bars in D and G represents ± sem. For each experiment, at least 3 mice per genotype were analyzed. p-values (from two-tailed t-Test) are: * $p < 0.05$, ** $p < 0.01$. Scale bars in A, C and E = 100 µm. Scale bar in H = 20 µm. Black bars: control; open bars: RAbKO mice.

Figure 5

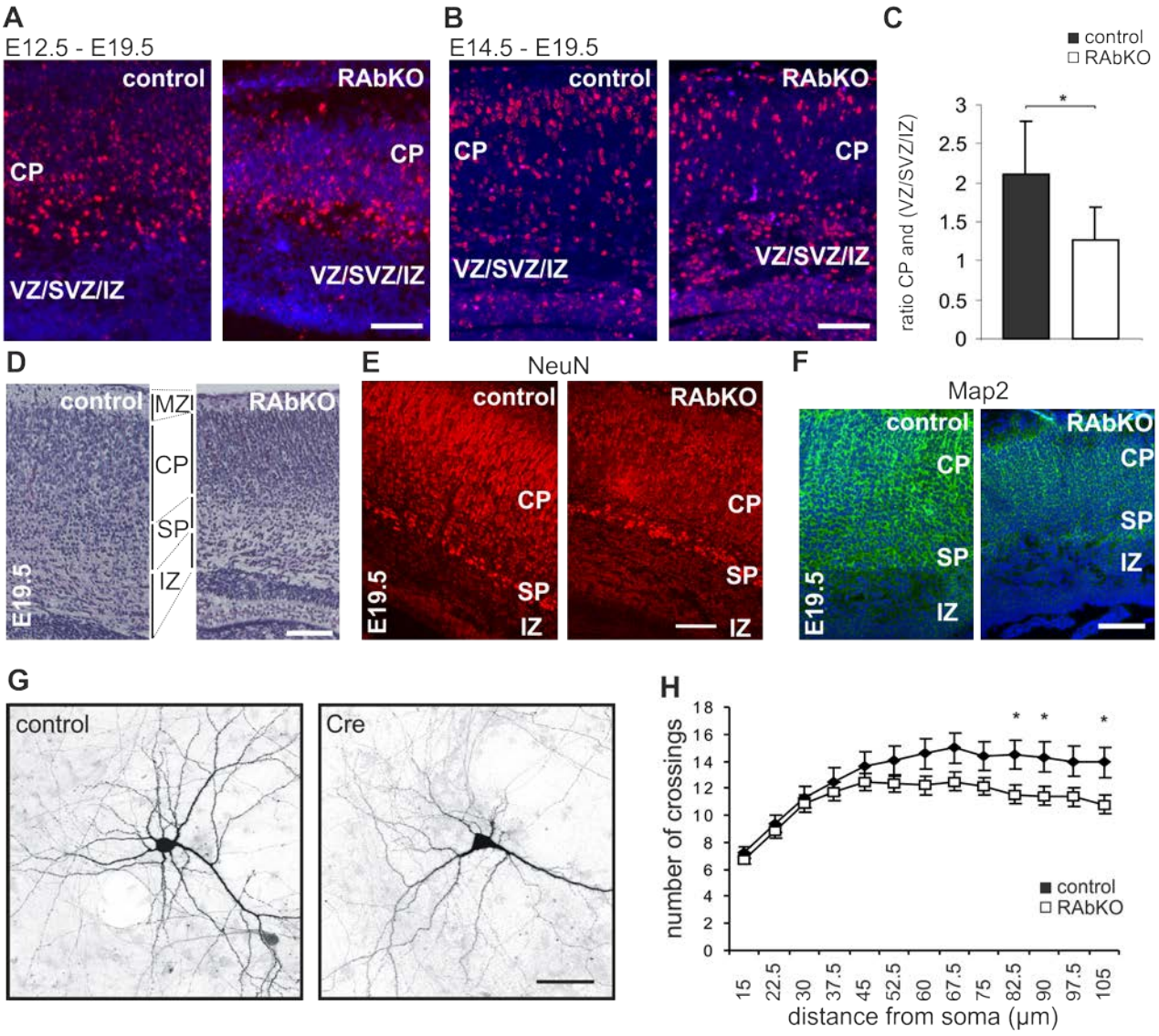

Fig. 5. RAbKO mice show changes in the localization of late generated neurons without affecting overall cortical layering.

(A, B) BrdU was injected into pregnant dams at E12.5 (A) or at E14.5 (B) of embryonic development and brain sections were prepared from E19.5 embryos. BrdU (red)/DAPI (blue) staining shows a difference in the distribution of BrdU-labeled cells when labeled at E14.5 but not at E12.5. Note, that viewer cells reach the CP.

(C) Quantification of the distribution of BrdU-labeled cells in the cortex of mice in which BrdU was administered at E14.5. Results are presented as the ratio between the number of BrdU+ cells localized to the CP and those remaining in the VZ/SVZ/IZ.

(D) Cortical sections of E19.5 control and RAbKO mice stained with cresyl violet. Abbreviations: MZ: marginal zone; CP: cortical plate; SP: subplate; IZ: intermediate zone; SVZ: subventricular zone; VZ: ventricular zone.
(E) Cortical sections of E19.5 control and RAbKO mice stained with antibodies to NeuN (red) and (F) Map2 (green) and Hoechst (blue).
(G) Confocal picture of cultured hippocampal neurons isolated from *rptor*$^{fl/fl}$ mice that were transfected with control plasmid (control) or a Cre-expressing construct (Cre). To visualize the transfected neurons, cells were co-transfected with a GFP-expression plasmid. Neurons were transfected at DIV 4 and analyzed at DIV 14.
(H) Sholl analysis of Cre-expressing and control neurons.
Sample number N in (C) is 5 mice per genotype. Number of samples in (H) is 5 control mice and 4 RAbKO mice. p-values (from two-tailed t-Test): * $p < 0.05$. Error bar in C represents mean ± STDV, error bar in H represents confidence intervals. Scale bar in (A, B, D-F) = 100 µm. Scale bar in (G) = 50 µm.

Figure 6

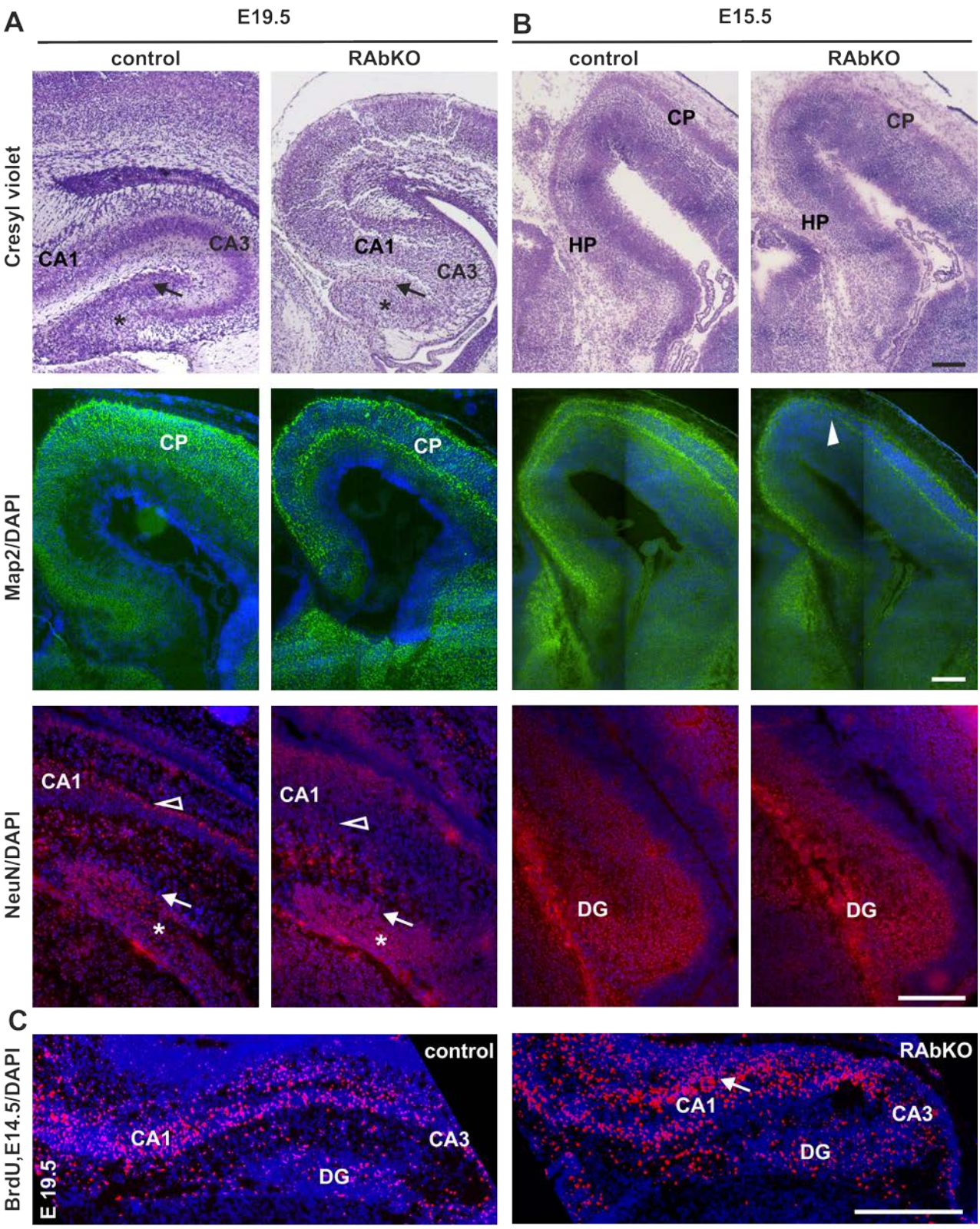
A
E19.5
control
RAbKO
B
E15.5
control
RAbKO
Cresyl violet
CA1
CA3
CP
HP
Map2/DAPI
NeuN/DAPI
DG
C
BrdU,E14.5/DAPI
E 19.5
control
RAbKO

Fig. 6. RAbKO mice display defects in hippocampal layering.

(A) Sections from E19.5 hippocampi with indicated stainings. RAbKO mice show a deficit in the CA region and the dentate gyrus (DG). Map2 (green) and DAPI (blue) stainings reveal changes in hippocampus and cortical plate (CP). NeuN+ neurons (red) accumulate in the hilus (asterisk) and do not form a distinct granular cell layer (arrow) in RAbKO mice. Note that staining for NeuN in the pyramidal layer (open arrowhead) is also missing in RAbKO mice.

(B) Hippocampal sections of E15.5 embryos. There is no large difference in cresyl violet-stained sections between genotypes. The subplate neuron-specific staining visualized with antibodies to Map2 (green) fades off before it reaches the hippocampus (arrowhead). Neuron specific staining (visualized by NeuN) is normal in the dentate gyrus of E15.5 RAbKO brains.

(C) Hippocampal sections from E19.5 embryos that were labeled at E14.5 with BrdU (red). BrdU-labeled cells are more broadly distributed in RAbKO mice (arrow). Scale bars = 200 µm.

Figure 7

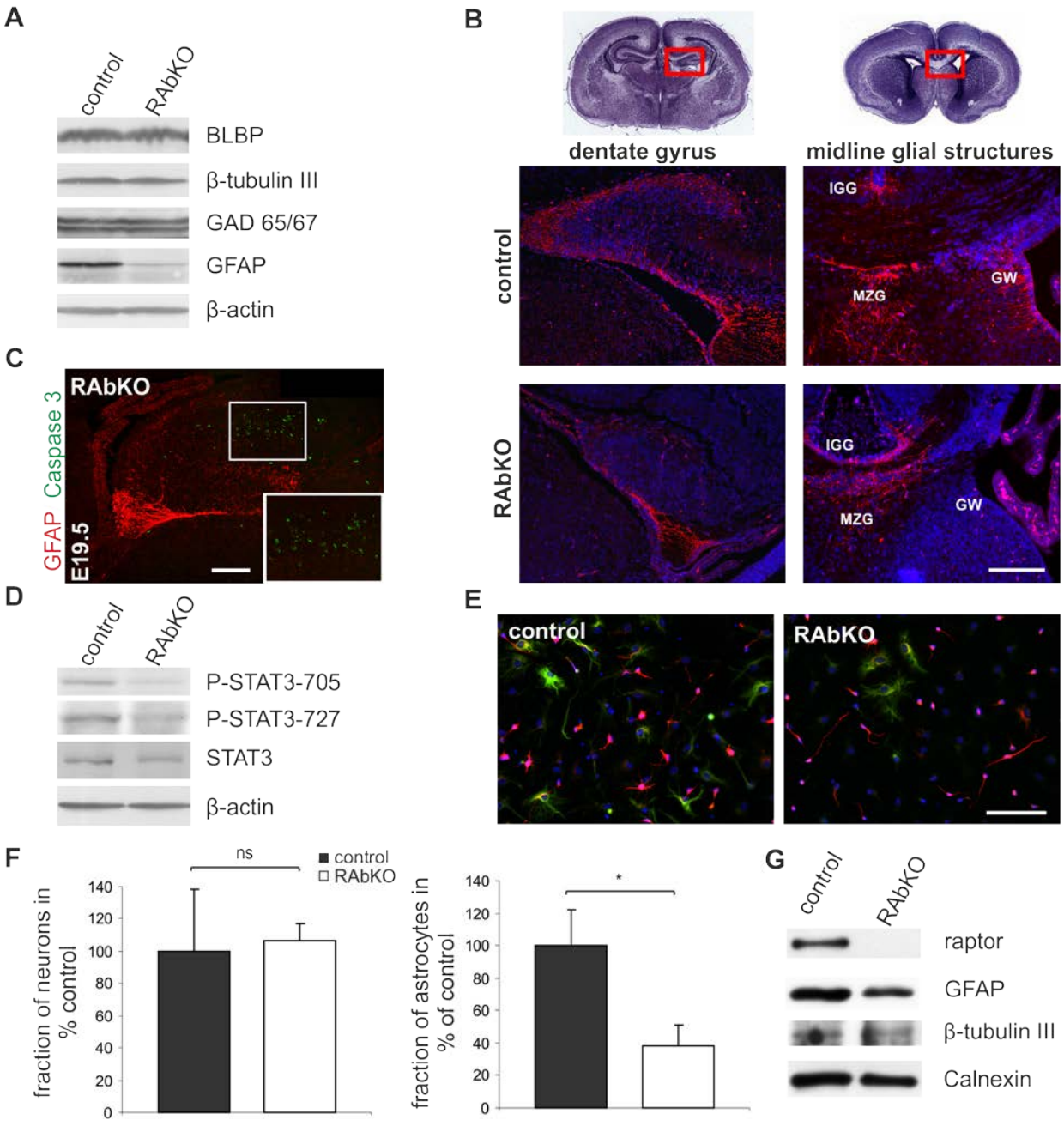

Fig. 7. Astrocytic differentiation is impaired in RAbKO brains.

(A) Western blot analysis of E19.5 brain lysates probed for indicated markers of neural development.

(B) Upper part: Cresyl violet stainings of brain sections from E19.5 mice. Red boxes represent regions shown below: Sections of dentate gyrus and midline glial structure regions stained with antibody to GFAP (red) and DAPI (blue).

IGG: indusium griseum glia; MZG: midline zipper glia; GW: glial wedge.

(C) Analysis of apoptotic cells in E19.5 hippocampus of RAbKO mice stained for GFAP (red) and Caspase 3 (green). Note that the apoptotic cells are not GFAP+. The white frame indicates the magnified inset.

(D) Western blot analysis of E19.5 brain lysates probed for Stat3 and its phosphorylated forms.

(E) Cells from dissociated neurospheres that have differentiated for 5 days. Cells were stained with antibodies against β-tubulin III (red), GFAP (green) and with DAPI (blue). There are fewer GFAP+ cells in RAbKO cultures whereas the number of β-tubulin III+ cells is the same.

(F) Relative number of neurons (left) and astrocytes (right) derived from neurospheres from control or RAbKO mice. Bars represent mean ± standard deviation. N = 3 independent experiments.

(G) Western blot analysis of lysates from cultures grown under the same conditions as in (E) probed with antibodies against the proteins indicated.

Bars represent means ± standard deviation. p-values (from t-Test): * $p < 0.05$. Scale bars: (B, C) = 200 µm, (E) = 100 µm.

Table 1

Table 1. Number and percentage of E19.5 embryos or newborns of indicated genotype.

	rptor$^{fl/+}$ *or* *rptor*$^{fl/fl}$	*rptor*$^{fl/+}$; *nestin-Cre*	*rptor*$^{fl/fl}$; *nestin-Cre*
Number per genotype	56	27	24
Percentage of total	52.3	25.2	22.4

Genotyping reveals that RAbKO mice are born with the expected Mendelian frequency.

Supplementary Figure S1

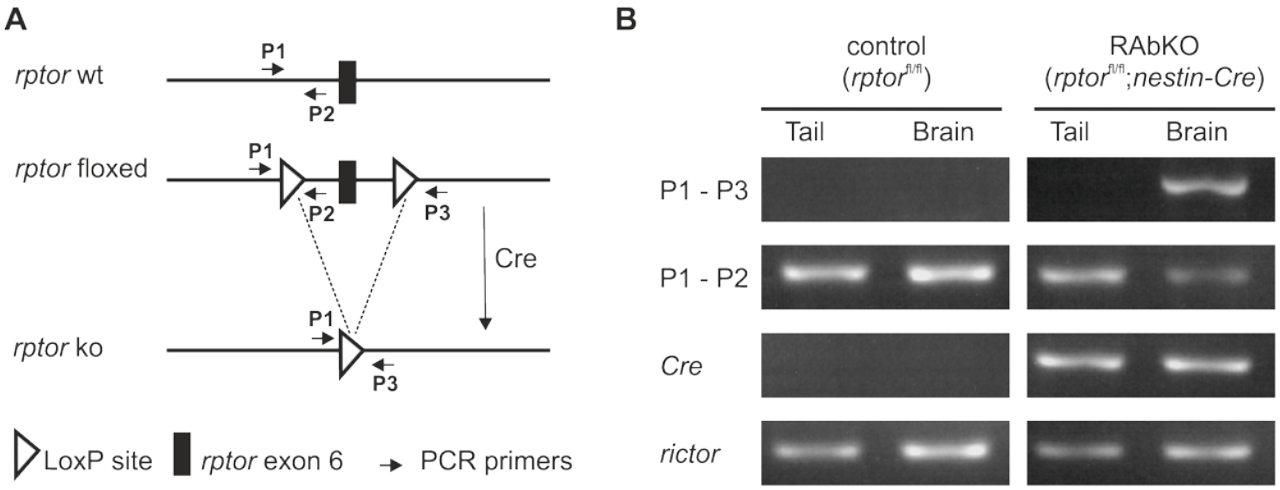

Fig. S1. Generation of CNS-specific raptor knockout mice.

(A) Schematic representation of the wild-type (*rptor* floxed) and after (*rptor* ko) recombination. Position of PCR primers P1, P2 and P3 used in (B) are indicated.

(B) PCR analysis of genomic DNA isolated from brains or the tails of newborn control (*rptorfl/fl*) and RAbKO (*rptorfl/fl;nestin*-Cre) mice. PCR using primers within the *rictor* allele served as control.

Supplementary Figure S2

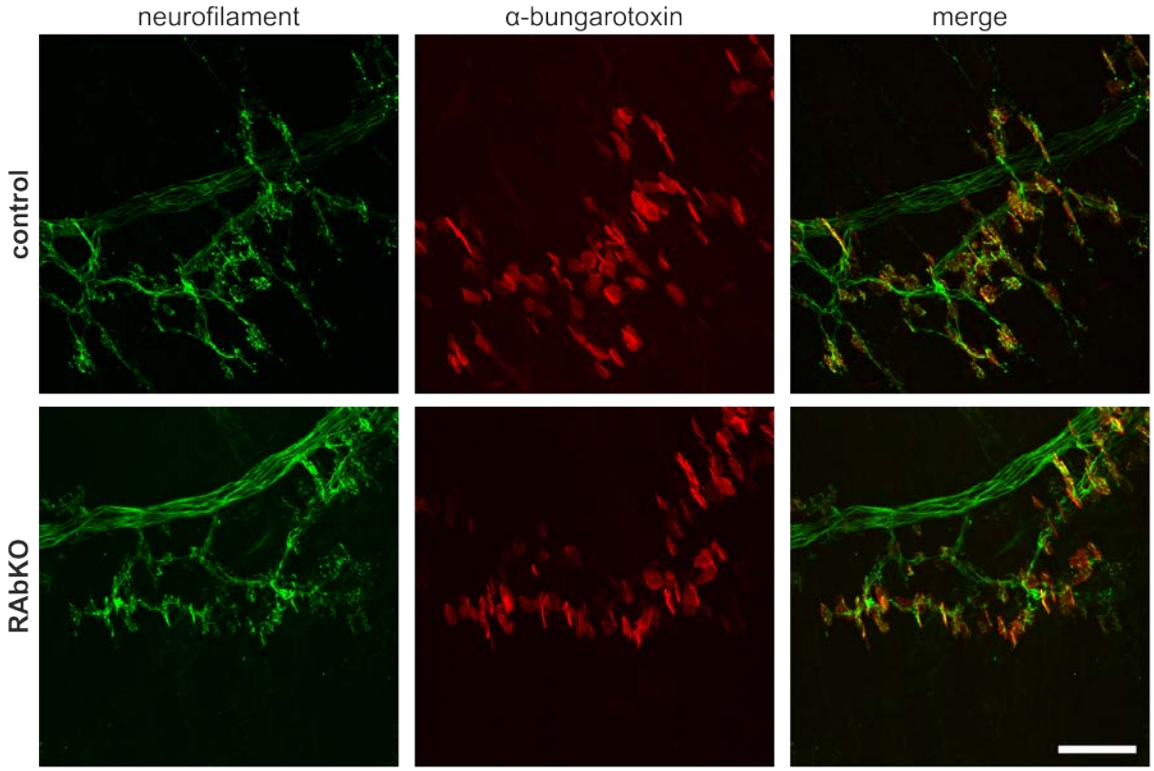

Fig. S2. Neuromuscular junctions are properly formed in RAbKO mice.

Micrographs of whole-mount preparations of diaphragms of E19.5 control (upper panels) and RAbKO (lower panels) mice stained with neurofilament antibody (green) and α-bungarotoxin (red).

Scale bar = 50 µm.

Supplementary Figure S3

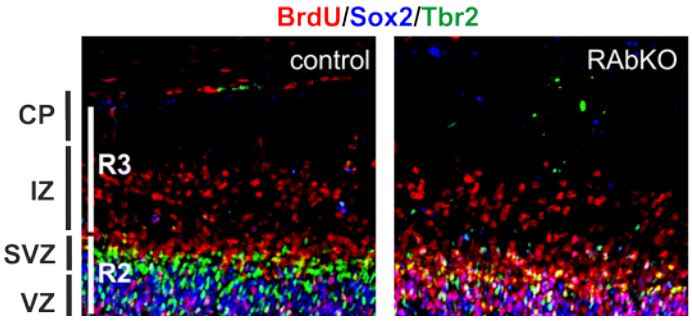

Fig. S3. Staining of E15.5 cortical sections from control and RAbKO mice with antibodies to BrdU, Sox2 and Tbr2.

Region R1 spanned the most apical part of the ventricular zone (VZ) and was defined by the exclusive presence of Sox2-positive (Sox+) but Tbr2-negative (Tbr2-) cells. Region R2 harbored the basal VZ and the sub-ventricular zone (SVZ) containing all Tbr2+ cells (but also Sox2+ cells). Finally, region R3 covered the intermediate zone (IZ) and the cortical plate (CP) and was defined by the absence of both Sox2+ and Tbr2+ cells.

Abbreviations are: VZ: ventricular zone; SVZ: subventricular zone; IZ: intermediate zone; CP: cortical plate. Scale bar = 100 mm.

Supplementary Figure S4

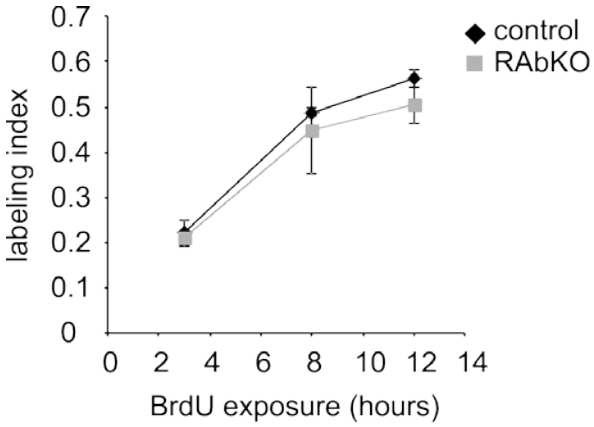

Fig. S4. Labeling index.

Labeling index in E15.5 control and RAbKO embryos as defined by the number of BrdU positive cells per total cell number. BrdU was cummulatively injected for 3, 8 and 12 hours. After 8 hours 50 % of the cells are BrdU positive. There is no significant difference in the number of BrdU positive cells per total cell number. Data represent mean +- sem. $p > 0.05$, N = 3 mice per genotype and time point.

Supplementary Figure S5

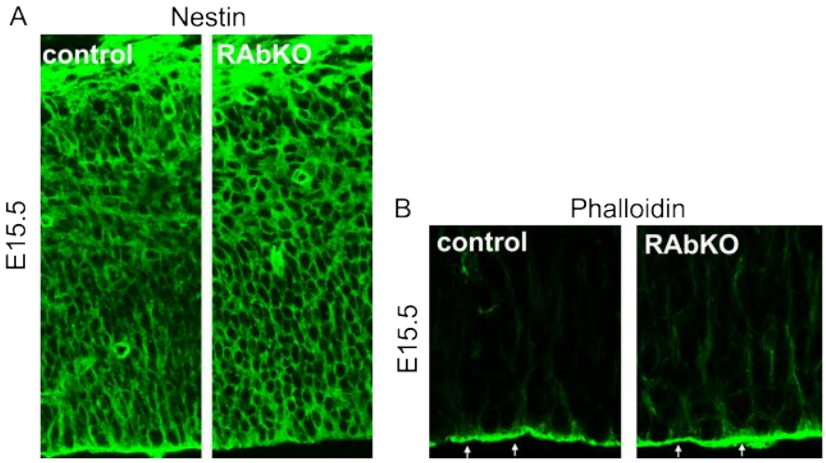

Fig. S5. Analysis of the morphology and attachment of radial glia in E15.5 RAbKO mice.

(A) Staining for Nestin in cortical sections of E15.5 control and RAbKO mice.

(B) Staining of actin filaments with Phalloidin in cortical sections of E15.5 control and RAbKO mice.

Supplementary Figure S6

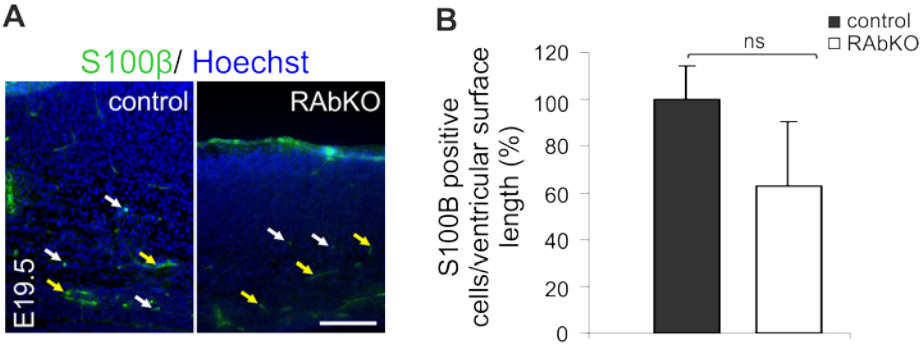

Fig. S6. Determination of S100β-positive cells in E19.5 RAbKO cortex.

(A) Cortical sections of E19.5 control and RAbKO mice stained for S100β (green) and Hoechst (blue). White arrows indicate S100β-positive cells, yellow arrows indicate blood vessels.

(B) Quantification of S100β-positive cells in the two genotypes. Although viewer S100β-positive cells were detected in RAbKO mice, the difference was not significant. $p > 0.05$, N = 3 mice. Scale bar = 100 µm.

Supplementary Figure S7

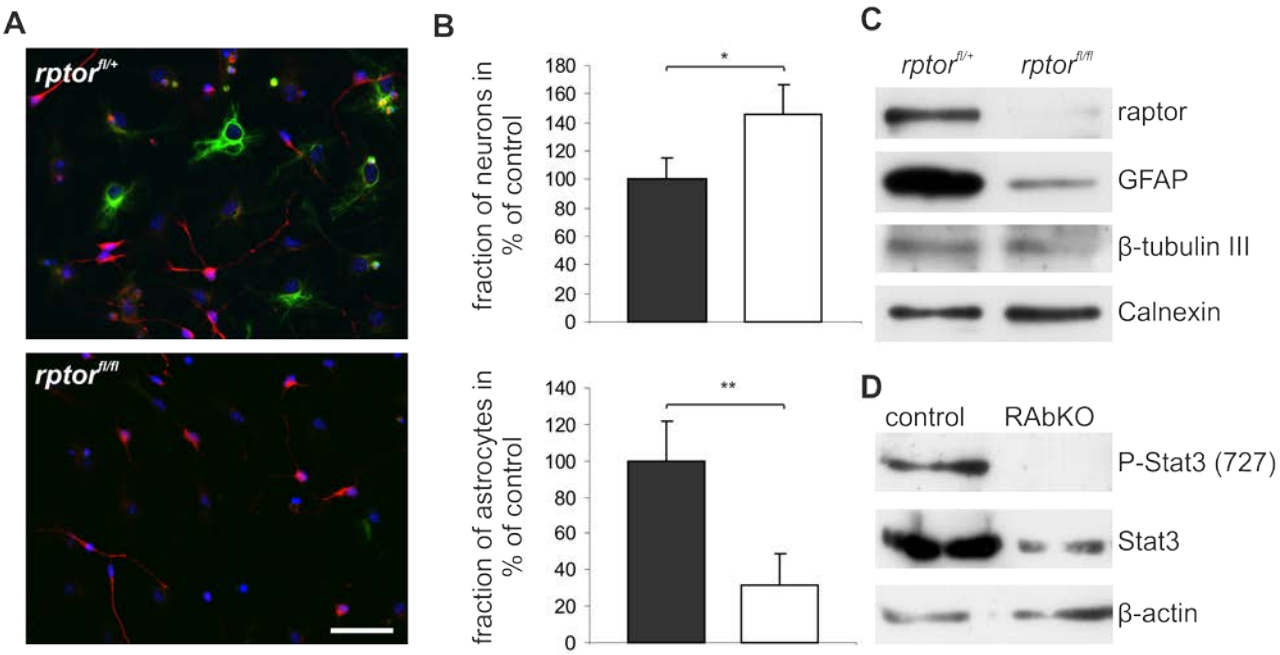

Fig. S7. Analysis of differentiation in E19.5 rptorfl/+ and rptorfl/fl neurospheres transduced with Cre-expressing adenoviruses.

(A) Micrographs of neurosphere-derived cells after differentiation. Dissociated cells from the spheres were transduced at a density of 106 cells/ml and at an MOI of 500 for 1 hour and then plated. After 5 days, cultures were stained with anti-β-tubulin III antibody (red), anti-GFAP antibody (green) and DAPI (blue).

(B) Quantification of the fraction of neurons (upper panel) and astrocytes (lower panel) in percent of control. Bars represent mean ± standard deviation.

(C) Western blot analysis of lysates from cultures grown under the same conditions as in (A) probed for the indicated marker proteins.

(D) Western blot analysis of lysates from RAbKO and control cultures with antibodies against the proteins indicated.

Sample number in (B) are 4 (control) and 4 (RAbKO). p-values (from t-Test): * $p < 0.05$, ** $p < 0.01$. Scale bar = 100 µm.

MATERIALS AND METHODS

Brain-specific *rptor* knockout mice

Mice that lack mTORC1 in the brain were generated by crossing mice in which exon 6 of the gene encoding raptor (*rptor*) was flanked by loxP sites (Bentzinger et al., 2008) with mice that express Cre under control of the central nervous system (CNS) stem cell-specific enhancer of the nestin promoter (Bentzinger et al., 2008; Graus-Porta et al., 2001; Tronche et al., 1999; Zimmerman et al., 1994). In the resulting *rptor*$^{fl/fl}$; *nestin-Cre* (herein called RAbKO for raptor brain knockout) mice, Cre-mediated recombination induces a frame shift that causes a precocious stop of translation (Fig. S1A). Time matings were made and E15.5, E17.5 and E19.5 embryos or newborns were taken for analysis. Genotyping was performed on tail or brain lysates using primers depicted in Fig. S1A. P1: 5'-ATG GTA GCA GGC ACA CTC TTC ATG; P2: 5'-GCT AAA CAT TCA GTC CCT AAT C; P3: 5'-CAG ATT CAA GCA TGT CCT AAG C; Cre-forward: 5'-TGT GGC TGA TGA TCC GAA TA; Cre-backward: 5'-GCT TGC ATG ATC TCC GGT AT. Mice that were heterozygous or homozygous for the floxed *rptor* allele and were negative for Cre were used as control.

Antibodies

The following rabbit polyclonal antibodies were used: mTOR, S6 Ribosomal Protein, P-S6 Ribosomal Protein (Ser235/236), P-mTOR (Ser2448), P-mTOR (2481), Akt, P-Stat3 (Ser727), cleaved Caspase 3, from Cell Signaling; BLBP and Map2 from Chemicon; GAD65/67 and neurofilament from Sigma; Ki-67 from Novocastra; and Tbr2 from Abcam. Rabbit monoclonal antibodies were as follows: raptor, rictor, P-Akt (Ser473), P-Stat3 (Tyr705) and β-actin from Cell Signaling. Mouse monoclonal antibodies were as follows: Stat3 from Cell Signaling; NeuN and GFAP from Chemicon; β-Tubulin III (also called Tuj1) from Sigma. Goat polyclonal antibodies to Sox2 were from Santa Cruz. Rat monoclonal antibodies to BrdU were from AbD Serotec.

Brain lysates for Western blots

Brains were dissected, washed in ice-cold PBS and combined with 10x (volume/weight) lysis buffer (50 mM Tris at pH 8, 150 mM NaCl, 1 mM EDTA, 1% Triton-X100) supplemented with protease inhibitor cocktail tablets (Roche) and phosphatase inhibitor cocktail I and II (Sigma). Brains were passed several times through a 1 ml pipette tip and homogenized with a glass-teflon homogenizer by using 12 strokes at 800 rpm. After lysate clearing, protein levels were determined using the BCA protein assay (Pierce). Equal amounts of protein were loaded onto SDS gels, transferred to nitrocellulose membranes and probed for indicated antibodies.

Brain sections, histochemistry and immunohistochemistry

For immunohistochemistry, the heads of the embryos were fixed in 4% PFA in PBS overnight and then cryoprotected in 30% sucrose in PBS. Brains were embedded in OCT reagent and frozen on dry ice. For fresh frozen sections (size comparison, cresyl violet), heads were directly frozen in OCT on dry ice. 10 or 12 µm-thick brain sections were prepared with a cryostat. Fresh frozen sections were post-fixed for 20 min with 4% PFA. For paraffin sections, brains were fixed for at least two days in 4% PFA in PBS, then dehydrated in a graded alcohol series and paraffin embedded. 4 µm sections were prepared on a microtome. Mounted sections were deparaffinized by heating for 20 minutes at 65°C, immediately immersed twice in xylol for 5 min each. Sections were rehydrated and either directly subjected to cresyl violet staining or to antigen retrieval. For antigen retrieval, slides were boiled in sodium citrate buffer (10 mM sodium citrate, 0.05% Tween 20, pH 6) and allowed to cool slowly for another 20 minutes. For immunohistochemistry, sections were blocked for 30 minutes in PBS containing 5% BSA and 0.25% Triton-X100 or TSA Blocking reagent (Perkin Elmer lifescience) followed by washing in PBS. Slices were incubated overnight at 4°C in blocking buffer or in PBS (if TSA blocked) with following primary antibodies: GFAP (1:200), NeuN (1:200), Map2 (1:400), Sox2 (1:100), Tbr2 (1:200), Ki67 (1:200) BrdU (1:500). Subsequently, slides were washed 3 x with PBS for 5 min each and incubated with appropriate secondary antibodies and DAPI (0.2 µg/ml) for 1 hour at room temperature. After washing in PBS, coverslips were mounted with Kaiser's glycerol gelatin. For birthdating analysis, 50 mg BrdU/kg was applied by intraperitoneal injection to pregnant mice. Brain sections were incubated in 2 M HCl for 1h at 37°C. Subsequently, sections were washed 3 x in PBS, incubated for 10 minutes in borate buffer (0.1 M, pH 8.5) and processed for immunohistochemistry as described. Separation of cortical regions in R1, R2 and R3 were defined in stainings to BrdU, Sox2 and Tbr2 as described in Fig. S3. In this experiment BrdU injections were given 24 hours prior to analysis. To measure the cell cycle time, we injected pregnant mice cumulatively every 2 hours with BrdU for a period of up to 12 hours (E15.5) and up to 8 hours (E17.5).

Quantifications

For all experiments at least three mice per genotype were examined. For the BrdU pulse chase experiments, BrdU was administered to a pregnant mouse by a single intraperitoneal injection and the brains of the embryos were harvested 3, 12 or 24 hours later. For the cumulative BrdU experiments, BrdU was injected every 2 hours for a maximum time period of 12 hours. The brains of the embryos were removed and the tissue was then processed for immunostaining as described above. Quantification of BrdU-labeled cells was done by determining the number of BrdU-positive cells that were localized above a specifically-defined ventricular surface length. This allowed the detection of all newly generated cells originating from a defined length of the apical membrane. Similar quantification was applied for PH3-positive cells. All quantifications were carried out in anatomically-matched

regions. The total number of cells was determined by counting the number of Hoechst-stained nuclei in at least 3 sections per animal in a defined area that spanned from the ventricle up to the pial surface. The paired t-test was used for statistical analysis.

DNA quantification

DNA was quantified in tissue homogenates (Labarca and Paigen, 1980) as already characterize for the quantification of brain size in Akt3/PKBγ knockout mice (Easton et al., 2005; Tschopp et al., 2005). Briefly, brains were homogenized by Polytron in detection buffer (0.05 M sodium phosphate, 2.0 M NaCl, 2 mM EDTA, 1 µg/ml Hoechst 33258 (Sigma), pH 7.4), followed by sonication for 20 seconds. Samples were excited at 356 nm and emission at 492 nm was determined. DNA concentration of homogenates was determined relative to a standard curve using calf thymus DNA (Sigma).

Neurospheres

Neurospheres were prepared from P0 telencephali (Giachino et al., 2009). Briefly, telencephali were dissected in HBSS, the meninges and the olfactory bulbs were removed. The tissue was triturated with a 1 ml pipette tip in neurosphere medium consisting of DMEM/F12 (1:1), 0.2 mg/ml L-glutamine, 1% penicillin/streptomycin, 2% B27, 2 µg/ml heparin, 20 ng/ml EGF and 10 ng/ml FGF2. The homogenate was diluted twice in the ratio 1:1 with fresh medium and each time triturated shortly. 5×10^4 cells were plated in a 5 cm dish. After 7 days, cultures were split. For determination of the capacity of secondary neurosphere formation and growth, cells were plated at a clonal density of 3000 cells/ml (Sirko et al., 2007). Six representative images were taken for each well of a 6-well plate to determine neurosphere number and diameter. For differentiation, neurospheres were split after 5 to 6 days and plated on coverslips coated with 15 µg/ml Poly-L-ornithin and 40 µg/ml laminin (150,000 cells/cm²). The dispersed cultures were differentiated in neurosphere medium lacking FGF2, EGF and heparin and fixed after 5 days with 4% PFA (Giachino et al., 2009). For staining, cells were washed 3 x with PBS, incubated for 10 minutes in PBS containing 0.25% TritonX. Staining was performed with the same procedure as described above for the brain sections, β-tubulin III antibody was used 1:400 in stainings.

Hippocampal cultures

Hippocampi were dissected from E16.5 mice in HBSS and incubated for 10 minutes at 37°C in HBSS containing 0.05% Trypsin and 0.02% EDTA. Afterwards, hippocampi were gently washed twice with HBSS and then triturated in plating medium consisting of DMEM, 0.2 mg/ml L-glutamine, 1% penicillin/streptomycin and 10% FCS. Neurons were plated at a density of 100,000 cells/cm² on glass coverslips coated with 10 µg/ml Poly-D-Lysin. After 3 hours, this medium was replaced by growth medium consisting of Neurobasal medium (Invitrogen), 0.2 mg/ml L-glutamine, 1%

penicillin/streptomycin and 2% B27 (Invitrogen). After 4 days, the conditioned culture medium was decanted and kept and cells were cotransfected with a plasmid expressing GFP from the synapsin promoter and either a Cre- or a control plasmid which contain both the CMV promoter. Lipofectamine 2000 (Invitrogen) was used as transfection reagent according to the user manual. 0.5 µg total DNA and 1 µl Lipofectamine 2000 was used for transfection of 100,000 cells. After 3 hours, the transfection mix was exchanged for the conditioned medium. Cells were fixed after 14 days in culture and imaged by confocal microscopy.

REFERENCES

Bentzinger, C. F., Romanino, K., Cloetta, D., Lin, S., Mascarenhas, J. B., Oliveri, F., Xia, J., Casanova, E., Costa, C. F., Brink, M. et al. (2008). Skeletal muscle-specific ablation of raptor, but not of rictor, causes metabolic changes and results in muscle dystrophy. *Cell Metab* 8, 411-24.

Bonni, A., Sun, Y., Nadal-Vicens, M., Bhatt, A., Frank, D. A., Rozovsky, I., Stahl, N., Yancopoulos, G. D. and Greenberg, M. E. (1997). Regulation of gliogenesis in the central nervous system by the JAK-STAT signaling pathway. *Science* 278, 477-83.

Calegari, F. and Huttner, W. B. (2003). An inhibition of cyclin-dependent kinases that lengthens, but does not arrest, neuroepithelial cell cycle induces premature neurogenesis. *J Cell Sci* 116, 4947-55.

Campbell, D. S. and Holt, C. E. (2001). Chemotropic responses of retinal growth cones mediated by rapid local protein synthesis and degradation. *Neuron* 32, 1013-26.

Copp, J., Manning, G. and Hunter, T. (2009). TORC-specific phosphorylation of mammalian target of rapamycin (mTOR): phospho-Ser2481 is a marker for intact mTOR signaling complex 2. *Cancer Res* 69, 1821-7.

Cybulski, N., Polak, P., Auwerx, J., Ruegg, M. A. and Hall, M. N. (2009). mTOR complex 2 in adipose tissue negatively controls whole-body growth. *Proc Natl Acad Sci U S A* 106, 9902-7.

Dowling, R. J., Topisirovic, I., Alain, T., Bidinosti, M., Fonseca, B. D., Petroulakis, E., Wang, X., Larsson, O., Selvaraj, A., Liu, Y. et al. (2010). mTORC1-mediated cell proliferation, but not cell growth, controlled by the 4E-BPs. *Science* 328, 1172-6.

Easton, R. M., Cho, H., Roovers, K., Shineman, D. W., Mizrahi, M., Forman, M. S., Lee, V. M., Szabolcs, M., de Jong, R., Oltersdorf, T. et al. (2005). Role for Akt3/protein kinase Bgamma in attainment of normal brain size. *Mol Cell Biol* 25, 1869-78.

Forster, E., Tielsch, A., Saum, B., Weiss, K. H., Johanssen, C., Graus-Porta, D., Muller, U. and Frotscher, M. (2002). Reelin, Disabled 1, and beta 1 integrins are required for the formation of the radial glial scaffold in the hippocampus. *Proc Natl Acad Sci U S A* 99, 13178-83.

Gangloff, Y. G., Mueller, M., Dann, S. G., Svoboda, P., Sticker, M., Spetz, J. F., Um, S. H., Brown, E. J., Cereghini, S., Thomas, G. et al. (2004). Disruption of the mouse mTOR gene leads to early postimplantation lethality and prohibits embryonic stem cell development. *Mol Cell Biol* 24, 9508-16.

Giachino, C., Basak, O. and Taylor, V. (2009). Isolation and manipulation of mammalian neural stem cells in vitro. *Methods Mol Biol* 482, 143-58.

Godel, M., Hartleben, B., Herbach, N., Liu, S., Zschiedrich, S., Lu, S., Debreczeni-Mor, A., Lindenmeyer, M. T., Rastaldi, M. P., Hartleben, G. et al. (2011). Role of mTOR in podocyte function and diabetic nephropathy in humans and mice. *J Clin Invest* 121, 2197-209.

Gotz, M. and Huttner, W. B. (2005). The cell biology of neurogenesis. *Nat Rev Mol Cell Biol* 6, 777-88.

Graus-Porta, D., Blaess, S., Senften, M., Littlewood-Evans, A., Damsky, C., Huang, Z., Orban, P., Klein, R., Schittny, J. C. and Muller, U. (2001). Beta1-class integrins regulate the development of laminae and folia in the cerebral and cerebellar cortex. *Neuron* 31, 367-79.

Guertin, D. A., Stevens, D. M., Thoreen, C. C., Burds, A. A., Kalaany, N. Y., Moffat, J., Brown, M., Fitzgerald, K. J. and Sabatini, D. M. (2006). Ablation in mice of the mTORC components raptor, rictor,

or mLST8 reveals that mTORC2 is required for signaling to Akt-FOXO and PKCalpha, but not S6K1. *Dev Cell* 11, 859-71.

Han, J., Wang, B., Xiao, Z., Gao, Y., Zhao, Y., Zhang, J., Chen, B., Wang, X. and Dai, J. (2008). Mammalian target of rapamycin (mTOR) is involved in the neuronal differentiation of neural progenitors induced by insulin. *Mol Cell Neurosci* 39, 118-24.

Hartfuss, E., Galli, R., Heins, N. and Gotz, M. (2001). Characterization of CNS precursor subtypes and radial glia. *Dev Biol* 229, 15-30.

Hay, N. and Sonenberg, N. (2004). Upstream and downstream of mTOR. *Genes Dev* 18, 1926-45.

He, F., Ge, W., Martinowich, K., Becker-Catania, S., Coskun, V., Zhu, W., Wu, H., Castro, D., Guillemot, F., Fan, G. et al. (2005). A positive autoregulatory loop of Jak-STAT signaling controls the onset of astrogliogenesis. *Nat Neurosci* 8, 616-25.

Hentges, K., Thompson, K. and Peterson, A. (1999). The flat-top gene is required for the expansion and regionalization of the telencephalic primordium. *Development* 126, 1601-9.

Hentges, K. E., Sirry, B., Gingeras, A. C., Sarbassov, D., Sonenberg, N., Sabatini, D. and Peterson, A. S. (2001). FRAP/mTOR is required for proliferation and patterning during embryonic development in the mouse. *Proc Natl Acad Sci U S A* 98, 13796-801.

Inoki, K., Mori, H., Wang, J., Suzuki, T., Hong, S., Yoshida, S., Blattner, S. M., Ikenoue, T., Ruegg, M. A., Hall, M. N. et al. (2011). mTORC1 activation in podocytes is a critical step in the development of diabetic nephropathy in mice. *J Clin Invest* 121, 2181-96.

Jacinto, E., Loewith, R., Schmidt, A., Lin, S., Ruegg, M. A., Hall, A. and Hall, M. N. (2004). Mammalian TOR complex 2 controls the actin cytoskeleton and is rapamycin insensitive. *Nat Cell Biol* 6, 1122-8.

Jastrzebski, K., Hannan, K. M., Tchoubrieva, E. B., Hannan, R. D. and Pearson, R. B. (2007). Coordinate regulation of ribosome biogenesis and function by the ribosomal protein S6 kinase, a key mediator of mTOR function. *Growth Factors* 25, 209-26.

Jaworski, J., Spangler, S., Seeburg, D. P., Hoogenraad, C. C. and Sheng, M. (2005). Control of dendritic arborization by the phosphoinositide-3'-kinase-Akt-mammalian target of rapamycin pathway. *J Neurosci* 25, 11300-12.

Johe, K. K., Hazel, T. G., Muller, T., Dugich-Djordjevic, M. M. and McKay, R. D. (1996). Single factors direct the differentiation of stem cells from the fetal and adult central nervous system. *Genes Dev* 10, 3129-40.

Jossin, Y. and Goffinet, A. M. (2007). Reelin signals through phosphatidylinositol 3-kinase and Akt to control cortical development and through mTor to regulate dendritic growth. *Mol Cell Biol* 27, 7113-24.

Kumar, V., Zhang, M. X., Swank, M. W., Kunz, J. and Wu, G. Y. (2005). Regulation of dendritic morphogenesis by Ras-PI3K-Akt-mTOR and Ras-MAPK signaling pathways. *J Neurosci* 25, 11288-99.

Labarca, C. and Paigen, K. (1980). A simple, rapid, and sensitive DNA assay procedure. *Anal Biochem* 102, 344-52.

Laplante, M. and Sabatini, D. M. (2012). mTOR Signaling in Growth Control and Disease. *Cell* 149, 274-93.

Li, Y. H., Werner, H. and Puschel, A. W. (2008). Rheb and mTOR regulate neuronal polarity through Rap1B. *J Biol Chem* 283, 33784-92.

Long, X., Spycher, C., Han, Z. S., Rose, A. M., Muller, F. and Avruch, J. (2002). TOR deficiency in C. elegans causes developmental arrest and intestinal atrophy by inhibition of mRNA translation. *Curr Biol* 12, 1448-61.

Loulier, K., Lathia, J. D., Marthiens, V., Relucio, J., Mughal, M. R., Tang, S. C., Coksaygan, T., Hall, P. E., Chigurupati, S., Patton, B. et al. (2009). beta1 integrin maintains integrity of the embryonic neocortical stem cell niche. *PLoS Biol* 7, e1000176.

Montagne, J., Stewart, M. J., Stocker, H., Hafen, E., Kozma, S. C. and Thomas, G. (1999). Drosophila S6 kinase: a regulator of cell size. *Science* 285, 2126-9.

Murakami, M., Ichisaka, T., Maeda, M., Oshiro, N., Hara, K., Edenhofer, F., Kiyama, H., Yonezawa, K. and Yamanaka, S. (2004). mTOR is essential for growth and proliferation in early mouse embryos and embryonic stem cells. *Mol Cell Biol* 24, 6710-8.

Oldham, S., Montagne, J., Radimerski, T., Thomas, G. and Hafen, E. (2000). Genetic and biochemical characterization of dTOR, the Drosophila homolog of the target of rapamycin. *Genes Dev* 14, 2689-94.

Onda, H., Crino, P. B., Zhang, H., Murphey, R. D., Rastelli, L., Gould Rothberg, B. E. and Kwiatkowski, D. J. (2002). Tsc2 null murine neuroepithelial cells are a model for human tuber giant cells, and show activation of an mTOR pathway. *Mol Cell Neurosci* 21, 561-74.

Park, K. K., Liu, K., Hu, Y., Smith, P. D., Wang, C., Cai, B., Xu, B., Connolly, L., Kramvis, I., Sahin, M. et al. (2008). Promoting axon regeneration in the adult CNS by modulation of the PTEN/mTOR pathway. *Science* 322, 963-6.

Polak, P., Cybulski, N., Feige, J. N., Auwerx, J., Ruegg, M. A. and Hall, M. N. (2008). Adipose-specific knockout of raptor results in lean mice with enhanced mitochondrial respiration. *Cell Metab* 8, 399-410.

Rajan, P., Panchision, D. M., Newell, L. F. and McKay, R. D. (2003). BMPs signal alternately through a SMAD or FRAP-STAT pathway to regulate fate choice in CNS stem cells. *J Cell Biol* 161, 911-21.

Ramirez-Valle, F., Badura, M. L., Braunstein, S., Narasimhan, M. and Schneider, R. J. (2010). Mitotic raptor promotes mTORC1 activity, G(2)/M cell cycle progression, and internal ribosome entry site-mediated mRNA translation. *Mol Cell Biol* 30, 3151-64.

Reynolds, B. A. and Weiss, S. (1996). Clonal and population analyses demonstrate that an EGF-responsive mammalian embryonic CNS precursor is a stem cell. *Dev Biol* 175, 1-13.

Rickmann, M., Amaral, D. G. and Cowan, W. M. (1987). Organization of radial glial cells during the development of the rat dentate gyrus. *J Comp Neurol* 264, 449-79.

Sancho-Tello, M., Valles, S., Montoliu, C., Renau-Piqueras, J. and Guerri, C. (1995). Developmental pattern of GFAP and vimentin gene expression in rat brain and in radial glial cultures. *Glia* 15, 157-66.

Sarbassov, D. D., Ali, S. M., Kim, D. H., Guertin, D. A., Latek, R. R., Erdjument-Bromage, H., Tempst, P. and Sabatini, D. M. (2004). Rictor, a novel binding partner of mTOR, defines a rapamycin-insensitive and raptor-independent pathway that regulates the cytoskeleton. *Curr Biol* 14, 1296-302.

Sarbassov, D. D., Guertin, D. A., Ali, S. M. and Sabatini, D. M. (2005). Phosphorylation and regulation of Akt/PKB by the rictor-mTOR complex. *Science* 307, 1098-101.

Sargeant, T. J., Day, D. J., Miller, J. H. and Steel, R. W. (2008). Acute in utero morphine exposure slows G2/M phase transition in radial glial and basal progenitor cells in the dorsal telencephalon of the E15.5 embryonic mouse. *Eur J Neurosci* 28, 1060-7.

Shende, P., Plaisance, I., Morandi, C., Pellieux, C., Berthonneche, C., Zorzato, F., Krishnan, J., Lerch, R., Hall, M. N., Ruegg, M. A. et al. (2011). Cardiac raptor ablation impairs adaptive hypertrophy, alters metabolic gene expression, and causes heart failure in mice. *Circulation* 123, 1073-82.

Shima, H., Pende, M., Chen, Y., Fumagalli, S., Thomas, G. and Kozma, S. C. (1998). Disruption of the p70(s6k)/p85(s6k) gene reveals a small mouse phenotype and a new functional S6 kinase. *Embo J* 17, 6649-59.

Shu, T., Puche, A. C. and Richards, L. J. (2003). Development of midline glial populations at the corticoseptal boundary. *J Neurobiol* 57, 81-94.

Sirko, S., von Holst, A., Wizenmann, A., Gotz, M. and Faissner, A. (2007). Chondroitin sulfate glycosaminoglycans control proliferation, radial glia cell differentiation and neurogenesis in neural stem/progenitor cells. *Development* 134, 2727-38.

Swiech, L., Perycz, M., Malik, A. and Jaworski, J. (2008). Role of mTOR in physiology and pathology of the nervous system. *Biochim Biophys Acta* 1784, 116-32.

Tronche, F., Kellendonk, C., Kretz, O., Gass, P., Anlag, K., Orban, P. C., Bock, R., Klein, R. and Schutz, G. (1999). Disruption of the glucocorticoid receptor gene in the nervous system results in reduced anxiety. *Nat Genet* 23, 99-103.

Tschopp, O., Yang, Z. Z., Brodbeck, D., Dummler, B. A., Hemmings-Mieszczak, M., Watanabe, T., Michaelis, T., Frahm, J. and Hemmings, B. A. (2005). Essential role of protein kinase B gamma (PKB gamma/Akt3) in postnatal brain development but not in glucose homeostasis. *Development* 132, 2943-54.

Verma, P., Chierzi, S., Codd, A. M., Campbell, D. S., Meyer, R. L., Holt, C. E. and Fawcett, J. W. (2005). Axonal protein synthesis and degradation are necessary for efficient growth cone regeneration. *J Neurosci* 25, 331-42.

Wang, B., Xiao, Z., Chen, B., Han, J., Gao, Y., Zhang, J., Zhao, W., Wang, X. and Dai, J. (2008). Nogo-66 promotes the differentiation of neural progenitors into astroglial lineage cells through mTOR-STAT3 pathway. *PLoS ONE* 3, e1856.

Wen, Z., Zhong, Z. and Darnell, J. E., Jr. (1995). Maximal activation of transcription by Stat1 and Stat3 requires both tyrosine and serine phosphorylation. *Cell* 82, 241-50.

Wullschleger, S., Loewith, R. and Hall, M. N. (2006). TOR signaling in growth and metabolism. *Cell* 124, 471-84.

Yokogami, K., Wakisaka, S., Avruch, J. and Reeves, S. A. (2000). Serine phosphorylation and maximal activation of STAT3 during CNTF signaling is mediated by the rapamycin target mTOR. *Curr Biol* 10, 47-50.

Zhao, S., Chai, X., Forster, E. and Frotscher, M. (2004). Reelin is a positional signal for the lamination of dentate granule cells. *Development* 131, 5117-25.

Zhu, Y., Li, H., Zhou, L., Wu, J. Y. and Rao, Y. (1999). Cellular and molecular guidance of GABAergic neuronal migration from an extracortical origin to the neocortex. *Neuron* 23, 473-85.

Zimmerman, L., Parr, B., Lendahl, U., Cunningham, M., McKay, R., Gavin, B., Mann, J., Vassileva, G. and McMahon, A. (1994). Independent regulatory elements in the nestin gene direct transgene expression to neural stem cells or muscle precursors. *Neuron* 12, 11-24.

Zou, J., Zhou, L., Du, X. X., Ji, Y., Xu, J., Tian, J., Jiang, W., Zou, Y., Yu, S., Gan, L. et al. (2011). Rheb1 is required for mTORC1 and myelination in postnatal brain development. *Dev Cell* 20, 97-108.

4.3 Additional findings

Besides the conventional approach of a conditional knockout mouse model in which the Cre recombinase is under the control of a tissue-specific promoter (thus with a given expression pattern within a given timeframe), there exists a refined method that allows the temporal control for the onset of the recombination to take place. The time-specific induction of recombination can be achieved by the fusion of the Cre recombinase with a mutated ligand binding domain of the human estrogen receptor (ERT2) (Baumgartel et al., 2007). The ERT2 does not bind to endogenous estradiol, whereas it binds specifically to the synthetic estrogen receptor antagonist Tamoxifen. The inducible Cre-LoxP system is based on the fact that the chimeric recombinase CreERT2 is kept in the cytoplasm by heat-shock proteins (e.g. Hsp90) that interact with the ERT2 domain. Only upon Tamoxifen application the CreERT2 dissociates from Hsp90 and is able to enter the nucleus where it can combine with the DNA and exert its recombination-activity (Feil et al., 1997).

4.3.1 Results from α-CamKII-CreERT2 mediated *rptor* knockout

In order to more specifically control the recombination-pattern of the *rptor* knockout we originally intended to make use of an inducible Cre-LoxP system. The mice expressing CreERT2 under the control of the *αCamKII*-promoter were kindly provided by Isabelle Mansuy, Brain Research Institute, University of Zurich. A schematic illustration of the CreERT2-system is depicted in Supplementary Figure 1S, A and B. For the analysis of the recombination pattern we used a GFP-reporter mouse line that was provided by Matthias Müller, Novartis AG, Basel. In a first attempt, we injected Tamoxifen (1 mg) into a lactating mouse for 10 days (during the age P5 – P15 of the pups). The recombination efficiency of such an early induced Cre-activity was very low and only some single cells in the hippocampus and the hypothalamus showed recombination (data not shown). Also Western blot analysis of different tissue-fractions from homozygously floxed *rptor* mice that additionally were positive for CreERT2 revealed no substantial recombination upon Tamoxifen injections into the lactating mother. No detectable difference in raptor protein or phosphorylated S6 levels could be observed (Figure S1, E). Due to the failure of early recombination induction by Tamoxifen application via the lactation-path, we injected Tamoxifen (1 mg) into adult mice and analyzed the recombination pattern 3 month post induction. Main sites of recombination were found in the olfactory bulb, hippocampus and hypothalamus in the GFP-reporter mouse line (Figure S1, C). The same Tamoxifen administration was performed in mice carrying the GFP-reporter allele in addition to the floxed *rptor* alleles and the CreERT2 transgene. GFP-positive cells were considered as cells where recombination took place. However, immunohistochemical analysis of hippocampal CA1 neurons from such mice revealed no distinct difference in pS6 staining between GFP-positive and GFP-negative cells (Figure

S1, D). Furthermore, Western blot analysis of lysates from the olfactory bulbs, hippocampus and hypothalamus did not show reduced protein levels of raptor or phosphorylation level of S6 (Figure S1, F). Together, these results indicate that the used mouse model leads to minor recombination efficiency upon Tamoxifen injections in both young and adult mice. Therefore, it was not suitable for further experiments such as behavioral studies, field recordings or biochemical analysis.

4.3.2 Material and methods of α-CamKII-CreERT2 experiments

Tamoxifen (Sigma-Aldrich) was dissolved in 90% corn oil (Sigma-Aldrich), 10% EtOH (Sigma-Aldrich) to a final concentration of 10 mg/ml, and sonicated in a water bath during 5 min. Mice received intraperitoneal injections (1 mg) of freshly prepared Tamoxifen-solution. Injection-regimes were as follows: a) One Tamoxifen injection per day over 10 consecutive days into lactating mothers from P5 – P15 old pups. b) Two Tamoxifen injections per day over 5 consecutive days into adult mice. For immunohistochemical analysis, the procedures for perfusion, tissue processing and staining were as described in the chapter 4.1. Following antibodies were used: chicken anti-GFP (Invitrogen, 1:200), rabbit anti pS6 (Cell Signaling, 1:200), DAPI (1:1000), goat anti rabbit Cy3 (Jackson Immunoresearch, 1:500), goat anti chicken Alexa488 (Jackson Immunoresearch, 1:500). The procedure for Western blot analysis was as described in the chapter 4.1. Genotyping for floxed *rptor* alleles and Cre was performed as described in chapter 4.1. For detection of the *LoxPstopLoxPGFP* allele in the GFP-reporter mice the following primers were used: GFP for: TGA TAT TGC TGA AGA GCT TGG CGG C; GFP rev: TGT GTG TAT TCC TGG CTA TCC.

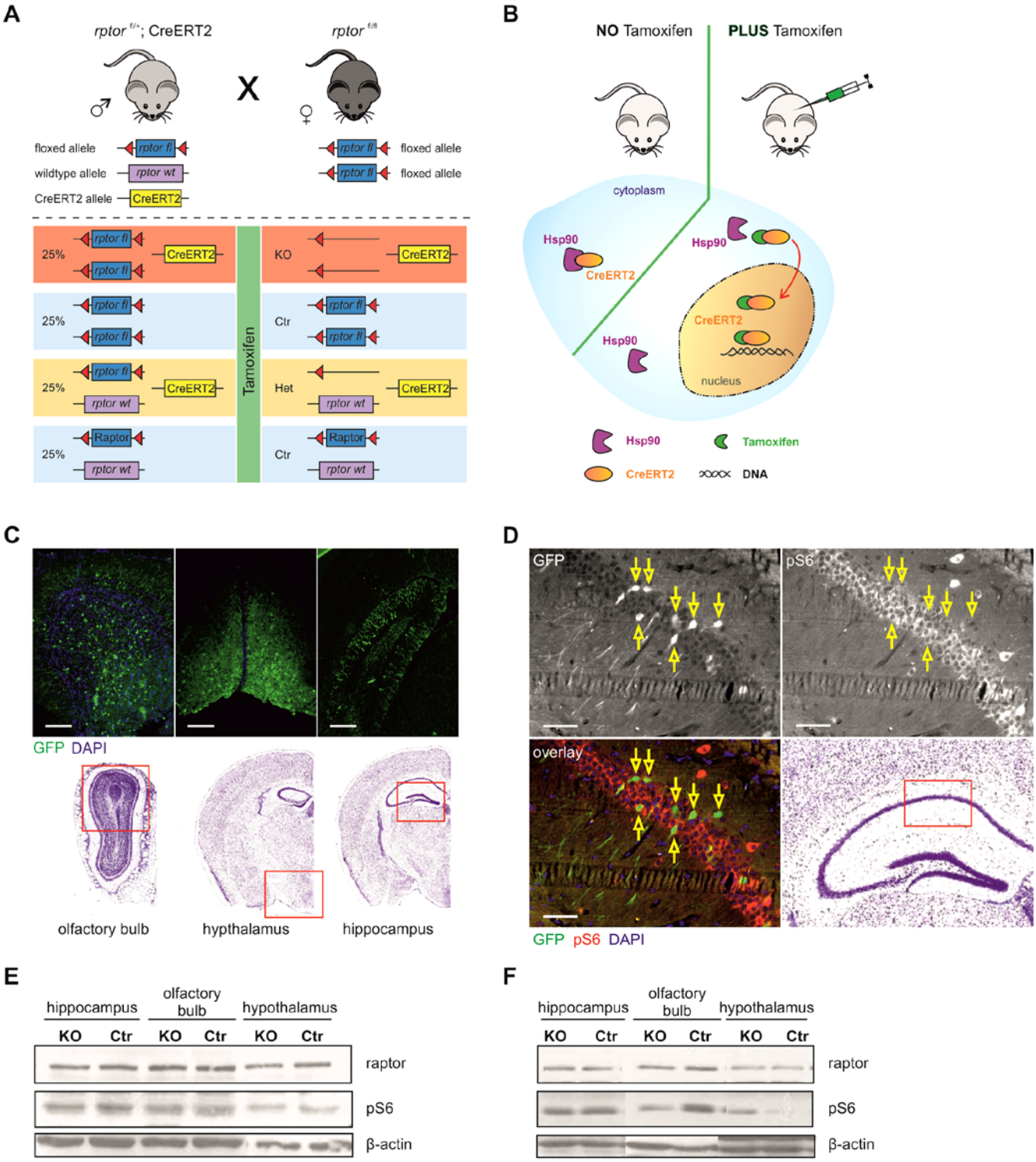

Additional findings. Analysis of αCamKII-CreERT2 mediated knockout. **A** Breeding scheme of inducible knockout mice. **B** Mechanism of Tamoxifen induced recombination. **C** Tissue analysis of GFP-reporter mice injected with Tamoxifen (1 mg, twice per day over 5 days) shows recombination in the olfactory bulb, hippocampus and hypothalamus (upper panel). Lower panel shows the according brain structure from Allen Brain Atlas. **D** Mice homozygous for the floxed *rptor* allele and the reporter allele and carrying the CreERT2-transgene were treated with the Tamoxifen-regime as in **C**. No distinct reduction of pS6 staining is observable in cells positive for the GFP-reporter (yellow arrows). **E** and **F** show representative Western blots of indicated tissue lysates probed for raptor, pS6 and β-actin. Lysates of mice with Tamoxifen application at P5 - P15 are depicted in **E**. Lysates of Tamoxifen application at adult stages are depicted in **F**. Abbreviations: Ctr, control; KO, knockout; Het, heterozygous; Hsp90, heat-shock protein 90. Scale bars: 200 µm (**C**); 50 µm (**D**).

5 CONCLUDING REMARKS

In this study, we report on two knockout mouse models and provide new insights into the function and importance of mTORC1 signaling in the developing and adult central nervous system. The conditional knockout of *rptor* at an early embryonic stage in all neuronal cells and in adult forebrain neurons, respectively, allowed us to specifically analyze the function of mTORC1 with regard to very distinct phases of a brain's or neuron's life.

The characterization of the RAbKO mice revealed a crucial role of mTORC1 for embryonic brain development, brain growth and ultimately for postnatal survival. As summarized in chapter 3.2.1, based on cell culture experiments the importance of mTORC1 signaling for axonal outgrowth and path-finding, dendritic arborization as well as for cell differentiation was suggested. Our data now provide first *in vivo* evidence that several of these aspects that are important during brain development are affected by ablation of mTORC1 activity. The most striking phenotypes observed in RAbKO mice are: hindered differentiation towards the glial lineage likely due to reduction of Stat3 signaling, deficits in cell proliferation and defective cortical as well as hippocampal layering. The molecular mechanisms behind these observations are – except for the Stat3-mediated triggering of glial differentiation – not clear yet. However, there are up- and downstream targets of mTORC1, which could serve as good candidates in regard to the mechanisms responsible for the observed phenotypes. The irregular cortical layering could be mediated via a disturbed nerve growth factor signaling or via a potential irresponsiveness to REDD1 signaling in the RAbKO mice. Furthermore, with reference to the overall reduced brain size the proteins Reelin and Ulk-1 were both associated with mTORC1 signaling and described as regulators of dendritic- and axonal outgrowth, respectively (Jossin and Goffinet, 2007; Zhou et al., 2007). Additionally, the alterations in proliferation and cell cycle length can largely (in addition to apoptosis) explain the reduction in brain size and besides possible intrinsic factors this may be due to a lack of response to EGF and BDNF signaling.

The examination of *R*cKO mice is the first study that investigated the direct role of mTORC1 in the adult brain by a genetic approach. In this work, we provide evidence that mTORC1 signaling in the adult brain is critical for postmitotic neuron cell size maintenance, synaptic efficiency and plasticity as well as specific forms of learning and memory. So far, only the consequences of enhanced mTORC1 activity have been discussed in quite some detail in literature but to date low focus – mainly by the use of rapamycin – was paid on hindered mTORC1 signaling.

Our data now suggest that well balanced mTORC1 signaling is crucial for basal synaptic efficiency. Besides the involvement of mTORC1 in basal synaptic functions, mTORC1 activity likely is further modulated in response to enhanced neuronal activity in order to trigger local protein synthesis

that is believed to be essential for L-LTP and long term memory. We found that both electrophysiological correlates to learning and short- and long-term memory, namely E-LTP and L-LTP, are altered in *R*cKO mice. This observation was accompanied by the finding that both the learning and the memory performance in the Morris water maze are markedly reduced in *R*cKO mice compared to control littermates. Interestingly, we found that in the same paradigm the learning and memory deficits can be bypassed upon a training scheme that is characterized by short inter-training-intervals. This observation indicates that several signaling pathways run in parallel to assemble in a complex network that finally accounts for the molecular requisite for synaptic plasticity. mTORC1 seems to be critical within this network, especially for tasks that include long time-intervals between individual trainings and thereby consolidation phases that are within a time frame where protein synthesis is crucial. Notably, upon intensive training in a time-setting that is characterized by short consolidation phases between individual trainings, the lack of mTORC1 signaling does not lead to learning or memory deficits.

Furthermore, we observed a specific deficit in the extinction test of the fear conditioning in *R*cKO mice whereas the learning and memory in the cue- and context test were not altered compared to control mice. It is well known that the mechanisms of the extinction learning do represent a distinct form of learning from the initial fear acquisition. Thus, our finding that mTORC1 deficiency specifically leads to an impairment of processes involved in extinction but not in the initial fear conditioning is very interesting. In summary, our observations on the learning and memory performance of *R*cKO mice in different behavioral paradigms suggest that mTORC1 is contributing to the complex molecular mechanisms that account for at least two distinct forms of learning and memory, namely spatial learning and memory and extinction learning, respectively. Other forms of plasticity-related learning and memory tests, such as fear conditioning and cue- and context-memory, are not dependent on mTORC1 activity.

Finally, we observed a striking reduction in neuronal cell size in the hippocampus as well as an overall reduced brain weight in *R*cKO mice compared to control mice. These data suggest that mTORC1 is critical for cell growth and proliferation and additionally plays an important role in cell size maintenance of postmitotic neurons.

As rapamycin is used in several indications, e.g. metabolic diseases, cancer, neurodegenerative diseases and mental disorders, our data are of general importance in respect to possible brain-specific side effects of prolonged mTORC1 inhibition.

6 OUTLOOK

The data presented here represent the first initial characterization of the RAbKO mice and *R*cKO mice, respectively. The reported phenotypes are of very interesting nature but the detailed mechanisms responsible for several findings are not understood in detail yet. Therefore, it will be important to further analyze the initially described phenotypes into depth with focus on the molecular mechanisms underlying the particular observations.

More precisely, the underlying mechanism for the disturbed cortical and hippocampal layering in RAbKO mice should be carefully analyzed. Birth-dating experiments in combination with immunohistochemistry as well as *in vitro* migrationassays could be performed. Furthermore, the proliferation capacity of the precursor cell pool at different embryonic stages as well as the features of axonal and dendritic outgrowth of newborn neurons are aspects for potential further investigations. It will be important to look for and identify signaling components which trigger axonal and dendritic outgrowth via mTORC1. One possible tool to achieve those goals would be the generation of an inducible knockout system with the additional possibility to track individual cells by a GFP-reporter. Such a mouse model would allow to differentiate between intrinsic mechanisms and environmental factors that possibly lead to the observed phenotypes. Furthermore, it could enable to more specifically define time-point specific effects of the mTORC1 inactivation.

With regard to *R*cKO mice, it will be interesting – although technically challenging – to examine the basal protein synthesis level and the protein synthesis level after LTP induction in the dendritic compartments as well as in the soma of CA1 neurons. Such investigations would provide more insight into the class of mRNA that is transcriptionally controlled by mTORC1 under basal and plasticity-related conditions. With regard to the L-LTP phenotype that was observed in *R*cKO mice it still remains unclear to what extent the decreased synaptic efficiency may also account for the L-LTP maintenance deficit. In order to more clearly separate the phenotype of synaptic efficiency and the phenotype of protein synthesis-dependent L-LTP progression, an excessive HFS paradigm could be applied to acute hippocampal slices. Assuming that such an LTP-induction protocol does obscure the differences in basal synaptic efficiency, the subsequent analysis of L-LTP progression would allow to make a more profound statement on the mTORC1 contribution to the protein synthesis-dependent phase of LTP.

In a broader point of view, the *R*cKO mice could serve as a useful model to study the contribution of mTORC1 signaling in various kinds of neurodegenerative diseases and mental disorders. The combination of different disease-related mouse models with *R*cKO mice could provide insight into the still open question about the cause or consequence of altered mTORC1 signaling in those diseases.

Such studies would improve the knowledge about brain specific mTOR signaling in general and the perception of disease-origins and progression in particular.

Furthermore, a very interesting topic that so far has not at all been approached is the phenomenon of long-term depression (LTD). In some aspects, such as kinase activation and protein synthesis dependence, L-LTD shares certain similarities with L-LTP. However, the molecular mechanisms that underlie the induction of LTD are regulated differently. Both, the induction phase and the maintenance phase are potentially dependent on mTORC1 signaling. E.g. GSK3α and GSK3β are well known components for LTD and at least GSK3α seems to be altered in *R*cKO mice (preliminary data, not shown). In respect of LTD, of course also mTORC2 should be taken into account. Based on the observation that several PKC isoforms are completely missing in rictor-deficient brains and in consideration of the well-known function of PKC in LTD and LTP, respectively, a detailed electrophysiological analysis of α-CamK2-Cre mediated *rictor* knockout would be worth to be carried out. The characterization of such a mouse model on the level of synaptic plasticity and learning and memory would further shed light of whether the synaptic plasticity-related effects that have been attributed to rapamycin are mTORC1 specific or involve further contributions by mTORC2.

7 REFERENCES

Abraham, W.C., and Williams, J.M. (2008). LTP maintenance and its protein synthesis-dependence. Neurobiol Learn Mem *89*, 260-268.

Altmann, M., Muller, P.P., Pelletier, J., Sonenberg, N., and Trachsel, H. (1989). A mammalian translation initiation factor can substitute for its yeast homologue in vivo. J Biol Chem *264*, 12145-12147.

An, W.L., Cowburn, R.F., Li, L., Braak, H., Alafuzoff, I., Iqbal, K., Iqbal, I.G., Winblad, B., and Pei, J.J. (2003). Up-regulation of phosphorylated/activated p70 S6 kinase and its relationship to neurofibrillary pathology in Alzheimer's disease. Am J Pathol *163*, 591-607.

Andrade, M.A., and Bork, P. (1995). HEAT repeats in the Huntington's disease protein. Nat Genet *11*, 115-116.

Antion, M.D., Merhav, M., Hoeffer, C.A., Reis, G., Kozma, S.C., Thomas, G., Schuman, E.M., Rosenblum, K., and Klann, E. (2008). Removal of S6K1 and S6K2 leads to divergent alterations in learning, memory, and synaptic plasticity. Learn Mem *15*, 29-38.

Asaki, C., Usuda, N., Nakazawa, A., Kametani, K., and Suzuki, T. (2003). Localization of translational components at the ultramicroscopic level at postsynaptic sites of the rat brain. Brain Res *972*, 168-176.

Auerbach, B.D., Osterweil, E.K., and Bear, M.F. (2011). Mutations causing syndromic autism define an axis of synaptic pathophysiology. Nature *480*, 63-68.

Banko, J.L., Poulin, F., Hou, L., DeMaria, C.T., Sonenberg, N., and Klann, E. (2005). The translation repressor 4E-BP2 is critical for eIF4F complex formation, synaptic plasticity, and memory in the hippocampus. J Neurosci *25*, 9581-9590.

Bartsch, D., Casadio, A., Karl, K.A., Serodio, P., and Kandel, E.R. (1998). CREB1 encodes a nuclear activator, a repressor, and a cytoplasmic modulator that form a regulatory unit critical for long-term facilitation. Cell *95*, 211-223.

Baumgartel, K., Fernandez, C., Johansson, T., and Mansuy, I.M. (2007). Conditional transgenesis and recombination to study the molecular mechanisms of brain plasticity and memory. Handb Exp Pharmacol, 315-345.

Bentzinger, C.F., Romanino, K., Cloetta, D., Lin, S., Mascarenhas, J.B., Oliveri, F., Xia, J., Casanova, E., Costa, C.F., Brink, M.*, et al.* (2008). Skeletal muscle-specific ablation of raptor, but not of rictor, causes metabolic changes and results in muscle dystrophy. Cell Metab *8*, 411-424.

Berger, Z., Ravikumar, B., Menzies, F.M., Oroz, L.G., Underwood, B.R., Pangalos, M.N., Schmitt, I., Wullner, U., Evert, B.O., O'Kane, C.J.*, et al.* (2006). Rapamycin alleviates toxicity of different aggregate-prone proteins. Hum Mol Genet *15*, 433-442.

Berry-Kravis, E., Knox, A., and Hervey, C. (2011). Targeted treatments for fragile X syndrome. J Neurodev Disord *3*, 193-210.

Bidinosti, M., Ran, I., Sanchez-Carbente, M.R., Martineau, Y., Gingras, A.C., Gkogkas, C., Raught, B., Bramham, C.R., Sossin, W.S., Costa-Mattioli, M.*, et al.* (2010). Postnatal deamidation of 4E-BP2 in

brain enhances its association with raptor and alters kinetics of excitatory synaptic transmission. Mol Cell *37*, 797-808.

Bliss, T.V., and Lomo, T. (1973). Long-lasting potentiation of synaptic transmission in the dentate area of the anaesthetized rabbit following stimulation of the perforant path. J Physiol *232*, 331-356.

Bourne, J.N., Sorra, K.E., Hurlburt, J., and Harris, K.M. (2007). Polyribosomes are increased in spines of CA1 dendrites 2 h after the induction of LTP in mature rat hippocampal slices. Hippocampus *17*, 1-4.

Brown, E.J., Albers, M.W., Shin, T.B., Ichikawa, K., Keith, C.T., Lane, W.S., and Schreiber, S.L. (1994). A mammalian protein targeted by G1-arresting rapamycin-receptor complex. Nature *369*, 756-758.

Brown, N.F., Stefanovic-Racic, M., Sipula, I.J., and Perdomo, G. (2007). The mammalian target of rapamycin regulates lipid metabolism in primary cultures of rat hepatocytes. Metabolism *56*, 1500-1507.

Brown, R.E. (2006). The life and work of Donald Olding Hebb. Acta Neurol Taiwan *15*, 127-142.

Brugarolas, J., Lei, K., Hurley, R.L., Manning, B.D., Reiling, J.H., Hafen, E., Witters, L.A., Ellisen, L.W., and Kaelin, W.G., Jr. (2004). Regulation of mTOR function in response to hypoxia by REDD1 and the TSC1/TSC2 tumor suppressor complex. Genes Dev *18*, 2893-2904.

Cammalleri, M., Lutjens, R., Berton, F., King, A.R., Simpson, C., Francesconi, W., and Sanna, P.P. (2003). Time-restricted role for dendritic activation of the mTOR-p70S6K pathway in the induction of late-phase long-term potentiation in the CA1. Proc Natl Acad Sci U S A *100*, 14368-14373.

Campbell, D.S., and Holt, C.E. (2001). Chemotropic responses of retinal growth cones mediated by rapid local protein synthesis and degradation. Neuron *32*, 1013-1026.

Chen, X.G., Liu, F., Song, X.F., Wang, Z.H., Dong, Z.Q., Hu, Z.Q., Lan, R.Z., Guan, W., Zhou, T.G., Xu, X.M*., et al.* (2010). Rapamycin regulates Akt and ERK phosphorylation through mTORC1 and mTORC2 signaling pathways. Mol Carcinog *49*, 603-610.

Chong, Z.Z., Shang, Y.C., Zhang, L., Wang, S., and Maiese, K. (2010). Mammalian target of rapamycin: hitting the bull's-eye for neurological disorders. Oxid Med Cell Longev *3*, 374-391.

Corradetti, M.N., Inoki, K., and Guan, K.L. (2005). The stress-inducted proteins RTP801 and RTP801L are negative regulators of the mammalian target of rapamycin pathway. J Biol Chem *280*, 9769-9772.

Crespo, J.L., and Hall, M.N. (2002). Elucidating TOR signaling and rapamycin action: lessons from Saccharomyces cerevisiae. Microbiol Mol Biol Rev *66*, 579-591, table of contents.

Cunningham, J.T., Rodgers, J.T., Arlow, D.H., Vazquez, F., Mootha, V.K., and Puigserver, P. (2007). mTOR controls mitochondrial oxidative function through a YY1-PGC-1alpha transcriptional complex. Nature *450*, 736-740.

Cybulski, N., and Hall, M.N. (2009). TOR complex 2: a signaling pathway of its own. Trends Biochem Sci *34*, 620-627.

Davis, M. (2011). NMDA receptors and fear extinction: implications for cognitive behavioral therapy. Dialogues Clin Neurosci *13*, 463-474.

Davis, S., Bozon, B., and Laroche, S. (2003). How necessary is the activation of the immediate early gene zif268 in synaptic plasticity and learning? Behav Brain Res *142*, 17-30.

Di Nardo, A.A., Nedelec, S., Trembleau, A., Volovitch, M., Prochiantz, A., and Montesinos, M.L. (2007). Dendritic localization and activity-dependent translation of Engrailed1 transcription factor. Mol Cell Neurosci *35*, 230-236.

Duvel, K., Yecies, J.L., Menon, S., Raman, P., Lipovsky, A.I., Souza, A.L., Triantafellow, E., Ma, Q., Gorski, R., Cleaver, S.*, et al.* (2010). Activation of a metabolic gene regulatory network downstream of mTOR complex 1. Mol Cell *39*, 171-183.

Ehninger, D., Li, W., Fox, K., Stryker, M.P., and Silva, A.J. (2008). Reversing neurodevelopmental disorders in adults. Neuron *60*, 950-960.

El-Chaar, D., Gagnon, A., and Sorisky, A. (2004). Inhibition of insulin signaling and adipogenesis by rapamycin: effect on phosphorylation of p70 S6 kinase vs eIF4E-BP1. Int J Obes Relat Metab Disord *28*, 191-198.

Facchinetti, V., Ouyang, W., Wei, H., Soto, N., Lazorchak, A., Gould, C., Lowry, C., Newton, A.C., Mao, Y., Miao, R.Q.*, et al.* (2008). The mammalian target of rapamycin complex 2 controls folding and stability of Akt and protein kinase C. Embo J *27*, 1932-1943.

Feil, R., Wagner, J., Metzger, D., and Chambon, P. (1997). Regulation of Cre recombinase activity by mutated estrogen receptor ligand-binding domains. Biochem Biophys Res Commun *237*, 752-757.

Feng, Z., Zhang, H., Levine, A.J., and Jin, S. (2005). The coordinate regulation of the p53 and mTOR pathways in cells. Proc Natl Acad Sci U S A *102*, 8204-8209.

Fingar, D.C., and Blenis, J. (2004). Target of rapamycin (TOR): an integrator of nutrient and growth factor signals and coordinator of cell growth and cell cycle progression. Oncogene *23*, 3151-3171.

Fitzjohn, S.M., Irving, A.J., Palmer, M.J., Harvey, J., Lodge, D., and Collingridge, G.L. (1996). Activation of group I mGluRs potentiates NMDA responses in rat hippocampal slices. Neurosci Lett *203*, 211-213.

Foretz, M., Guichard, C., Ferre, P., and Foufelle, F. (1999). Sterol regulatory element binding protein-1c is a major mediator of insulin action on the hepatic expression of glucokinase and lipogenesis-related genes. Proc Natl Acad Sci U S A *96*, 12737-12742.

Frey, U., Krug, M., Reymann, K.G., and Matthies, H. (1988). Anisomycin, an inhibitor of protein synthesis, blocks late phases of LTP phenomena in the hippocampal CA1 region in vitro. Brain Res *452*, 57-65.

Frey, U., and Morris, R.G. (1997). Synaptic tagging and long-term potentiation. Nature *385*, 533-536.

Fukunaga, K., Stoppini, L., Miyamoto, E., and Muller, D. (1993). Long-term potentiation is associated with an increased activity of Ca2+/calmodulin-dependent protein kinase II. J Biol Chem *268*, 7863-7867.

Gafford, G.M., Parsons, R.G., and Helmstetter, F.J. (2011). Consolidation and reconsolidation of contextual fear memory requires mammalian target of rapamycin-dependent translation in the dorsal hippocampus. Neuroscience *182*, 98-104.

Gangloff, Y.G., Mueller, M., Dann, S.G., Svoboda, P., Sticker, M., Spetz, J.F., Um, S.H., Brown, E.J., Cereghini, S., Thomas, G.*, et al.* (2004). Disruption of the mouse mTOR gene leads to early postimplantation lethality and prohibits embryonic stem cell development. Mol Cell Biol *24*, 9508-9516.

Ganley, I.G., Lam du, H., Wang, J., Ding, X., Chen, S., and Jiang, X. (2009). ULK1.ATG13.FIP200 complex mediates mTOR signaling and is essential for autophagy. J Biol Chem *284*, 12297-12305.

Garami, A., Zwartkruis, F.J., Nobukuni, T., Joaquin, M., Roccio, M., Stocker, H., Kozma, S.C., Hafen, E., Bos, J.L., and Thomas, G. (2003). Insulin activation of Rheb, a mediator of mTOR/S6K/4E-BP signaling, is inhibited by TSC1 and 2. Mol Cell *11*, 1457-1466.

Garcia-Martinez, J.M., and Alessi, D.R. (2008). mTOR complex 2 (mTORC2) controls hydrophobic motif phosphorylation and activation of serum- and glucocorticoid-induced protein kinase 1 (SGK1). Biochem J *416*, 375-385.

Garelick, M.G., and Kennedy, B.K. (2011). TOR on the brain. Exp Gerontol *46*, 155-163.

Gelinas, J.N., Banko, J.L., Hou, L., Sonenberg, N., Weeber, E.J., Klann, E., and Nguyen, P.V. (2007). ERK and mTOR signaling couple beta-adrenergic receptors to translation initiation machinery to gate induction of protein synthesis-dependent long-term potentiation. J Biol Chem *282*, 27527-27535.

Gingras, A.C., Raught, B., and Sonenberg, N. (1999). eIF4 initiation factors: effectors of mRNA recruitment to ribosomes and regulators of translation. Annu Rev Biochem *68*, 913-963.

Goorden, S.M., van Woerden, G.M., van der Weerd, L., Cheadle, J.P., and Elgersma, Y. (2007). Cognitive deficits in Tsc1+/- mice in the absence of cerebral lesions and seizures. Ann Neurol *62*, 648-655.

Griffin, R.J., Moloney, A., Kelliher, M., Johnston, J.A., Ravid, R., Dockery, P., O'Connor, R., and O'Neill, C. (2005). Activation of Akt/PKB, increased phosphorylation of Akt substrates and loss and altered distribution of Akt and PTEN are features of Alzheimer's disease pathology. J Neurochem *93*, 105-117.

Guertin, D.A., Stevens, D.M., Thoreen, C.C., Burds, A.A., Kalaany, N.Y., Moffat, J., Brown, M., Fitzgerald, K.J., and Sabatini, D.M. (2006). Ablation in mice of the mTORC components raptor, rictor, or mLST8 reveals that mTORC2 is required for signaling to Akt-FOXO and PKCalpha, but not S6K1. Dev Cell *11*, 859-871.

Gwinn, D.M., Shackelford, D.B., Egan, D.F., Mihaylova, M.M., Mery, A., Vasquez, D.S., Turk, B.E., and Shaw, R.J. (2008). AMPK phosphorylation of raptor mediates a metabolic checkpoint. Mol Cell *30*, 214-226.

Han, J., Wang, B., Xiao, Z., Gao, Y., Zhao, Y., Zhang, J., Chen, B., Wang, X., and Dai, J. (2008). Mammalian target of rapamycin (mTOR) is involved in the neuronal differentiation of neural progenitors induced by insulin. Mol Cell Neurosci *39*, 118-124.

Hannan, K.M., Brandenburger, Y., Jenkins, A., Sharkey, K., Cavanaugh, A., Rothblum, L., Moss, T., Poortinga, G., McArthur, G.A., Pearson, R.B.*, et al.* (2003). mTOR-dependent regulation of ribosomal gene transcription requires S6K1 and is mediated by phosphorylation of the carboxy-terminal activation domain of the nucleolar transcription factor UBF. Mol Cell Biol *23*, 8862-8877.

Hara, K., Yonezawa, K., Weng, Q.P., Kozlowski, M.T., Belham, C., and Avruch, J. (1998). Amino acid sufficiency and mTOR regulate p70 S6 kinase and eIF-4E BP1 through a common effector mechanism. J Biol Chem *273*, 14484-14494.

Hardie, D.G., Carling, D., and Carlson, M. (1998). The AMP-activated/SNF1 protein kinase subfamily: metabolic sensors of the eukaryotic cell? Annu Rev Biochem *67*, 821-855.

Harrington, L.S., Findlay, G.M., Gray, A., Tolkacheva, T., Wigfield, S., Rebholz, H., Barnett, J., Leslie, N.R., Cheng, S., Shepherd, P.R.*, et al.* (2004). The TSC1-2 tumor suppressor controls insulin-PI3K signaling via regulation of IRS proteins. J Cell Biol *166*, 213-223.

Hay, N., and Sonenberg, N. (2004). Upstream and downstream of mTOR. Genes Dev *18*, 1926-1945.

Heesom, K.J., and Denton, R.M. (1999). Dissociation of the eukaryotic initiation factor-4E/4E-BP1 complex involves phosphorylation of 4E-BP1 by an mTOR-associated kinase. FEBS Lett *457*, 489-493.

Heitman, J., Movva, N.R., and Hall, M.N. (1991). Targets for cell cycle arrest by the immunosuppressant rapamycin in yeast. Science *253*, 905-909.

Herron, C.E., Lester, R.A., Coan, E.J., and Collingridge, G.L. (1986). Frequency-dependent involvement of NMDA receptors in the hippocampus: a novel synaptic mechanism. Nature *322*, 265-268.

Hershey, J.W. (1991). Translational control in mammalian cells. Annu Rev Biochem *60*, 717-755.

Hoeffer, C.A., Tang, W., Wong, H., Santillan, A., Patterson, R.J., Martinez, L.A., Tejada-Simon, M.V., Paylor, R., Hamilton, S.L., and Klann, E. (2008). Removal of FKBP12 enhances mTOR-Raptor interactions, LTP, memory, and perseverative/repetitive behavior. Neuron *60*, 832-845.

Hosokawa, N., Hara, T., Kaizuka, T., Kishi, C., Takamura, A., Miura, Y., Iemura, S., Natsume, T., Takehana, K., Yamada, N.*, et al.* (2009). Nutrient-dependent mTORC1 association with the ULK1-Atg13-FIP200 complex required for autophagy. Mol Biol Cell *20*, 1981-1991.

Hsu, P.P., Kang, S.A., Rameseder, J., Zhang, Y., Ottina, K.A., Lim, D., Peterson, T.R., Choi, Y., Gray, N.S., Yaffe, M.B.*, et al.* (2011). The mTOR-regulated phosphoproteome reveals a mechanism of mTORC1-mediated inhibition of growth factor signaling. Science *332*, 1317-1322.

Huang, Y.S., Jung, M.Y., Sarkissian, M., and Richter, J.D. (2002). N-methyl-D-aspartate receptor signaling results in Aurora kinase-catalyzed CPEB phosphorylation and alpha CaMKII mRNA polyadenylation at synapses. Embo J *21*, 2139-2148.

Inoki, K., Li, Y., Xu, T., and Guan, K.L. (2003a). Rheb GTPase is a direct target of TSC2 GAP activity and regulates mTOR signaling. Genes Dev *17*, 1829-1834.

Inoki, K., Zhu, T., and Guan, K.L. (2003b). TSC2 mediates cellular energy response to control cell growth and survival. Cell *115*, 577-590.

Jacinto, E., Loewith, R., Schmidt, A., Lin, S., Ruegg, M.A., Hall, A., and Hall, M.N. (2004). Mammalian TOR complex 2 controls the actin cytoskeleton and is rapamycin insensitive. Nat Cell Biol *6*, 1122-1128.

Jaworski, J., Spangler, S., Seeburg, D.P., Hoogenraad, C.C., and Sheng, M. (2005). Control of dendritic arborization by the phosphoinositide-3'-kinase-Akt-mammalian target of rapamycin pathway. J Neurosci *25*, 11300-11312.

Jefferies, H.B., Reinhard, C., Kozma, S.C., and Thomas, G. (1994). Rapamycin selectively represses translation of the "polypyrimidine tract" mRNA family. Proc Natl Acad Sci U S A *91*, 4441-4445.

Jossin, Y., and Goffinet, A.M. (2007). Reelin signals through phosphatidylinositol 3-kinase and Akt to control cortical development and through mTor to regulate dendritic growth. Mol Cell Biol *27*, 7113-7124.

Jurado, S., Benoist, M., Lario, A., Knafo, S., Petrok, C.N., and Esteban, J.A. (2010). PTEN is recruited to the postsynaptic terminal for NMDA receptor-dependent long-term depression. Embo J *29*, 2827-2840.

Kalkman, H.O. (2006). The role of the phosphatidylinositide 3-kinase-protein kinase B pathway in schizophrenia. Pharmacol Ther *110*, 117-134.

Kang, H., and Schuman, E.M. (1996). A requirement for local protein synthesis in neurotrophin-induced hippocampal synaptic plasticity. Science *273*, 1402-1406.

Kelleher, R.J., 3rd, Govindarajan, A., Jung, H.Y., Kang, H., and Tonegawa, S. (2004). Translational control by MAPK signaling in long-term synaptic plasticity and memory. Cell *116*, 467-479.

Kersten, S. (2001). Mechanisms of nutritional and hormonal regulation of lipogenesis. EMBO Rep *2*, 282-286.

Khurana, V., Lu, Y., Steinhilb, M.L., Oldham, S., Shulman, J.M., and Feany, M.B. (2006). TOR-mediated cell-cycle activation causes neurodegeneration in a Drosophila tauopathy model. Curr Biol *16*, 230-241.

Kim, D.H., Sarbassov, D.D., Ali, S.M., King, J.E., Latek, R.R., Erdjument-Bromage, H., Tempst, P., and Sabatini, D.M. (2002). mTOR interacts with raptor to form a nutrient-sensitive complex that signals to the cell growth machinery. Cell *110*, 163-175.

Kim, D.H., Sarbassov, D.D., Ali, S.M., Latek, R.R., Guntur, K.V., Erdjument-Bromage, H., Tempst, P., and Sabatini, D.M. (2003). GbetaL, a positive regulator of the rapamycin-sensitive pathway required for the nutrient-sensitive interaction between raptor and mTOR. Mol Cell *11*, 895-904.

Kim, E., Goraksha-Hicks, P., Li, L., Neufeld, T.P., and Guan, K.L. (2008). Regulation of TORC1 by Rag GTPases in nutrient response. Nat Cell Biol *10*, 935-945.

Kim, J.E., and Chen, J. (2004). regulation of peroxisome proliferator-activated receptor-gamma activity by mammalian target of rapamycin and amino acids in adipogenesis. Diabetes *53*, 2748-2756.

Kimura, N., Tokunaga, C., Dalal, S., Richardson, C., Yoshino, K., Hara, K., Kemp, B.E., Witters, L.A., Mimura, O., and Yonezawa, K. (2003). A possible linkage between AMP-activated protein kinase (AMPK) and mammalian target of rapamycin (mTOR) signalling pathway. Genes Cells *8*, 65-79.

Klann, E., Chen, S.J., and Sweatt, J.D. (1991). Persistent protein kinase activation in the maintenance phase of long-term potentiation. J Biol Chem *266*, 24253-24256.

Klann, E., Chen, S.J., and Sweatt, J.D. (1993). Mechanism of protein kinase C activation during the induction and maintenance of long-term potentiation probed using a selective peptide substrate. Proc Natl Acad Sci U S A *90*, 8337-8341.

Koren, I., Reem, E., and Kimchi, A. (2010). DAP1, a novel substrate of mTOR, negatively regulates autophagy. Curr Biol *20*, 1093-1098.

Kremer, E.J., Pritchard, M., Lynch, M., Yu, S., Holman, K., Baker, E., Warren, S.T., Schlessinger, D., Sutherland, G.R., and Richards, R.I. (1991). Mapping of DNA instability at the fragile X to a trinucleotide repeat sequence p(CCG)n. Science *252*, 1711-1714.

Kumar, V., Zhang, M.X., Swank, M.W., Kunz, J., and Wu, G.Y. (2005). Regulation of dendritic morphogenesis by Ras-PI3K-Akt-mTOR and Ras-MAPK signaling pathways. J Neurosci *25*, 11288-11299.

Lafay-Chebassier, C., Paccalin, M., Page, G., Barc-Pain, S., Perault-Pochat, M.C., Gil, R., Pradier, L., and Hugon, J. (2005). mTOR/p70S6k signalling alteration by Abeta exposure as well as in APP-PS1 transgenic models and in patients with Alzheimer's disease. J Neurochem *94*, 215-225.

Lang, U.E., Heger, J., Willbring, M., Domula, M., Matschke, K., and Tugtekin, S.M. (2009). Immunosuppression using the mammalian target of rapamycin (mTOR) inhibitor everolimus: pilot study shows significant cognitive and affective improvement. Transplant Proc *41*, 4285-4288.

Langstrom, N.S., Anderson, J.P., Lindroos, H.G., Winblad, B., and Wallace, W.C. (1989). Alzheimer's disease-associated reduction of polysomal mRNA translation. Brain Res Mol Brain Res *5*, 259-269.

Laplante, M., and Sabatini, D.M. (2012). mTOR Signaling in Growth Control and Disease. Cell *149*, 274-293.

Lee, D.F., Kuo, H.P., Chen, C.T., Hsu, J.M., Chou, C.K., Wei, Y., Sun, H.L., Li, L.Y., Ping, B., Huang, W.C.*, et al.* (2007). IKK beta suppression of TSC1 links inflammation and tumor angiogenesis via the mTOR pathway. Cell *130*, 440-455.

Ling, D.S., Benardo, L.S., and Sacktor, T.C. (2006). Protein kinase Mzeta enhances excitatory synaptic transmission by increasing the number of active postsynaptic AMPA receptors. Hippocampus *16*, 443-452.

Lisman, J., Schulman, H., and Cline, H. (2002). The molecular basis of CaMKII function in synaptic and behavioural memory. Nat Rev Neurosci *3*, 175-190.

Loewith, R., Jacinto, E., Wullschleger, S., Lorberg, A., Crespo, J.L., Bonenfant, D., Oppliger, W., Jenoe, P., and Hall, M.N. (2002). Two TOR complexes, only one of which is rapamycin sensitive, have distinct roles in cell growth control. Mol Cell *10*, 457-468.

Low, P. (2011). The role of ubiquitin-proteasome system in ageing. Gen Comp Endocrinol *172*, 39-43.

Ma, T., Hoeffer, C.A., Capetillo-Zarate, E., Yu, F., Wong, H., Lin, M.T., Tampellini, D., Klann, E., Blitzer, R.D., and Gouras, G.K. (2010). Dysregulation of the mTOR pathway mediates impairment of synaptic plasticity in a mouse model of Alzheimer's disease. PLoS One *5*.

Ma, X.M., and Blenis, J. (2009). Molecular mechanisms of mTOR-mediated translational control. Nat Rev Mol Cell Biol *10*, 307-318.

Mader, S., Lee, H., Pause, A., and Sonenberg, N. (1995). The translation initiation factor eIF-4E binds to a common motif shared by the translation factor eIF-4 gamma and the translational repressors 4E-binding proteins. Mol Cell Biol *15*, 4990-4997.

Malagelada, C., Jin, Z.H., Jackson-Lewis, V., Przedborski, S., and Greene, L.A. (2010). Rapamycin protects against neuron death in in vitro and in vivo models of Parkinson's disease. J Neurosci *30*, 1166-1175.

Malinow, R., Schulman, H., and Tsien, R.W. (1989). Inhibition of postsynaptic PKC or CaMKII blocks induction but not expression of LTP. Science *245*, 862-866.

Manning, B.D. (2004). Balancing Akt with S6K: implications for both metabolic diseases and tumorigenesis. J Cell Biol *167*, 399-403.

Manning, B.D., and Cantley, L.C. (2003). United at last: the tuberous sclerosis complex gene products connect the phosphoinositide 3-kinase/Akt pathway to mammalian target of rapamycin (mTOR) signalling. Biochem Soc Trans *31*, 573-578.

Mendez, R., Hake, L.E., Andresson, T., Littlepage, L.E., Ruderman, J.V., and Richter, J.D. (2000). Phosphorylation of CPE binding factor by Eg2 regulates translation of c-mos mRNA. Nature *404*, 302-307.

Mendez, R., and Richter, J.D. (2001). Translational control by CPEB: a means to the end. Nat Rev Mol Cell Biol *2*, 521-529.

Mercaldo, V., Descalzi, G., and Zhuo, M. (2009). Fragile X mental retardation protein in learning-related synaptic plasticity. Mol Cells *28*, 501-507.

Morris, R. (1984). Developments of a water-maze procedure for studying spatial learning in the rat. J Neurosci Methods *11*, 47-60.

Noda, T., and Ohsumi, Y. (1998). Tor, a phosphatidylinositol kinase homologue, controls autophagy in yeast. J Biol Chem *273*, 3963-3966.

Panja, D., Dagyte, G., Bidinosti, M., Wibrand, K., Kristiansen, A.M., Sonenberg, N., and Bramham, C.R. (2009). Novel translational control in Arc-dependent long term potentiation consolidation in vivo. J Biol Chem *284*, 31498-31511.

Parkinson, J. (2002). An essay on the shaking palsy. 1817. J Neuropsychiatry Clin Neurosci *14*, 223-236; discussion 222.

Pearce, L.R., Komander, D., and Alessi, D.R. (2010). The nuts and bolts of AGC protein kinases. Nat Rev Mol Cell Biol *11*, 9-22.

Pei, J.J., Bjorkdahl, C., Zhang, H., Zhou, X., and Winblad, B. (2008). p70 S6 kinase and tau in Alzheimer's disease. J Alzheimers Dis *14*, 385-392.

Pei, J.J., and Hugon, J. (2008). mTOR-dependent signalling in Alzheimer's disease. J Cell Mol Med *12*, 2525-2532.

Phillips, R.G., and LeDoux, J.E. (1992). Differential contribution of amygdala and hippocampus to cued and contextual fear conditioning. Behav Neurosci *106*, 274-285.

Piper, M., Anderson, R., Dwivedy, A., Weinl, C., van Horck, F., Leung, K.M., Cogill, E., and Holt, C. (2006). Signaling mechanisms underlying Slit2-induced collapse of Xenopus retinal growth cones. Neuron *49*, 215-228.

Porstmann, T., Santos, C.R., Griffiths, B., Cully, M., Wu, M., Leevers, S., Griffiths, J.R., Chung, Y.L., and Schulze, A. (2008). SREBP activity is regulated by mTORC1 and contributes to Akt-dependent cell growth. Cell Metab *8*, 224-236.

Raught, B., Peiretti, F., Gingras, A.C., Livingstone, M., Shahbazian, D., Mayeur, G.L., Polakiewicz, R.D., Sonenberg, N., and Hershey, J.W. (2004). Phosphorylation of eucaryotic translation initiation factor 4B Ser422 is modulated by S6 kinases. Embo J *23*, 1761-1769.

Raymond, C.R. (2007). LTP forms 1, 2 and 3: different mechanisms for the "long" in long-term potentiation. Trends Neurosci *30*, 167-175.

Reymann, K.G., and Frey, J.U. (2007). The late maintenance of hippocampal LTP: requirements, phases, 'synaptic tagging', 'late-associativity' and implications. Neuropharmacology *52*, 24-40.

Reymann, K.G., Matthies, H.K., Schulzeck, K., and Matthies, H. (1989). N-methyl-D-aspartate receptor activation is required for the induction of both early and late phases of long-term potentiation in rat hippocampal slices. Neurosci Lett *96*, 96-101.

Roberson, E.D., English, J.D., and Sweatt, J.D. (1996). A biochemist's view of long-term potentiation. Learn Mem *3*, 1-24.

Roberson, E.D., and Sweatt, J.D. (1996). Transient activation of cyclic AMP-dependent protein kinase during hippocampal long-term potentiation. J Biol Chem *271*, 30436-30441.

Rosen, E.D., and MacDougald, O.A. (2006). Adipocyte differentiation from the inside out. Nat Rev Mol Cell Biol *7*, 885-896.

Roux, P.P., Ballif, B.A., Anjum, R., Gygi, S.P., and Blenis, J. (2004). Tumor-promoting phorbol esters and activated Ras inactivate the tuberous sclerosis tumor suppressor complex via p90 ribosomal S6 kinase. Proc Natl Acad Sci U S A *101*, 13489-13494.

Rubinsztein, D.C. (2002). Lessons from animal models of Huntington's disease. Trends Genet *18*, 202-209.

Sabatini, D.M., Erdjument-Bromage, H., Lui, M., Tempst, P., and Snyder, S.H. (1994). RAFT1: a mammalian protein that binds to FKBP12 in a rapamycin-dependent fashion and is homologous to yeast TORs. Cell *78*, 35-43.

Sancak, Y., Peterson, T.R., Shaul, Y.D., Lindquist, R.A., Thoreen, C.C., Bar-Peled, L., and Sabatini, D.M. (2008). The Rag GTPases bind raptor and mediate amino acid signaling to mTORC1. Science *320*, 1496-1501.

Santini, E., and Klann, E. (2011). Dysregulated mTORC1-Dependent Translational Control: From Brain Disorders to Psychoactive Drugs. Front Behav Neurosci *5*, 76.

Sarbassov, D.D., Ali, S.M., Kim, D.H., Guertin, D.A., Latek, R.R., Erdjument-Bromage, H., Tempst, P., and Sabatini, D.M. (2004). Rictor, a novel binding partner of mTOR, defines a rapamycin-insensitive and raptor-independent pathway that regulates the cytoskeleton. Curr Biol *14*, 1296-1302.

Sarbassov, D.D., Ali, S.M., Sengupta, S., Sheen, J.H., Hsu, P.P., Bagley, A.F., Markhard, A.L., and Sabatini, D.M. (2006). Prolonged rapamycin treatment inhibits mTORC2 assembly and Akt/PKB. Mol Cell *22*, 159-168.

Sarbassov, D.D., Guertin, D.A., Ali, S.M., and Sabatini, D.M. (2005). Phosphorylation and regulation of Akt/PKB by the rictor-mTOR complex. Science *307*, 1098-1101.

Schieke, S.M., Phillips, D., McCoy, J.P., Jr., Aponte, A.M., Shen, R.F., Balaban, R.S., and Finkel, T. (2006). The mammalian target of rapamycin (mTOR) pathway regulates mitochondrial oxygen consumption and oxidative capacity. J Biol Chem *281*, 27643-27652.

Schmitt, J.M., Guire, E.S., Saneyoshi, T., and Soderling, T.R. (2005). Calmodulin-dependent kinase kinase/calmodulin kinase I activity gates extracellular-regulated kinase-dependent long-term potentiation. J Neurosci *25*, 1281-1290.

Sehgal, S.N., Baker, H., and Vezina, C. (1975). Rapamycin (AY-22,989), a new antifungal antibiotic. II. Fermentation, isolation and characterization. J Antibiot (Tokyo) *28*, 727-732.

Shah, O.J., Wang, Z., and Hunter, T. (2004). Inappropriate activation of the TSC/Rheb/mTOR/S6K cassette induces IRS1/2 depletion, insulin resistance, and cell survival deficiencies. Curr Biol *14*, 1650-1656.

Sharma, A., Hoeffer, C.A., Takayasu, Y., Miyawaki, T., McBride, S.M., Klann, E., and Zukin, R.S. (2010). Dysregulation of mTOR signaling in fragile X syndrome. J Neurosci *30*, 694-702.

Shaw, R.J., Lamia, K.A., Vasquez, D., Koo, S.H., Bardeesy, N., Depinho, R.A., Montminy, M., and Cantley, L.C. (2005). The kinase LKB1 mediates glucose homeostasis in liver and therapeutic effects of metformin. Science *310*, 1642-1646.

Shima, H., Pende, M., Chen, Y., Fumagalli, S., Thomas, G., and Kozma, S.C. (1998). Disruption of the p70(s6k)/p85(s6k) gene reveals a small mouse phenotype and a new functional S6 kinase. Embo J *17*, 6649-6659.

Siuta, M.A., Robertson, S.D., Kocalis, H., Saunders, C., Gresch, P.J., Khatri, V., Shiota, C., Kennedy, J.P., Lindsley, C.W., Daws, L.C*., et al.* (2010). Dysregulation of the norepinephrine transporter sustains cortical hypodopaminergia and schizophrenia-like behaviors in neuronal rictor null mice. PLoS Biol *8*, e1000393.

Soderling, T.R., and Derkach, V.A. (2000). Postsynaptic protein phosphorylation and LTP. Trends Neurosci *23*, 75-80.

Sperow, M., Berry, R.B., Bayazitov, I.T., Zhu, G., Baker, S.J., and Zakharenko, S.S. (2012). Phosphatase and tensin homologue (PTEN) regulates synaptic plasticity independently of its effect on neuronal morphology and migration. J Physiol *590*, 777-792.

Stambolic, V., MacPherson, D., Sas, D., Lin, Y., Snow, B., Jang, Y., Benchimol, S., and Mak, T.W. (2001). Regulation of PTEN transcription by p53. Mol Cell *8*, 317-325.

Steward, O., and Schuman, E.M. (2003). Compartmentalized synthesis and degradation of proteins in neurons. Neuron *40*, 347-359.

Stoica, L., Zhu, P.J., Huang, W., Zhou, H., Kozma, S.C., and Costa-Mattioli, M. (2011). Selective pharmacogenetic inhibition of mammalian target of Rapamycin complex I (mTORC1) blocks long-term synaptic plasticity and memory storage. Proc Natl Acad Sci U S A *108*, 3791-3796.

Stolovich, M., Tang, H., Hornstein, E., Levy, G., Cohen, R., Bae, S.S., Birnbaum, M.J., and Meyuhas, O. (2002). Transduction of growth or mitogenic signals into translational activation of TOP mRNAs is fully reliant on the phosphatidylinositol 3-kinase-mediated pathway but requires neither S6K1 nor rpS6 phosphorylation. Mol Cell Biol *22*, 8101-8113.

Sutton, M.A., and Schuman, E.M. (2005). Local translational control in dendrites and its role in long-term synaptic plasticity. J Neurobiol *64*, 116-131.

Swiech, L., Perycz, M., Malik, A., and Jaworski, J. (2008). Role of mTOR in physiology and pathology of the nervous system. Biochim Biophys Acta *1784*, 116-132.

Tang, S.J., Reis, G., Kang, H., Gingras, A.C., Sonenberg, N., and Schuman, E.M. (2002). A rapamycin-sensitive signaling pathway contributes to long-term synaptic plasticity in the hippocampus. Proc Natl Acad Sci U S A *99*, 467-472.

Tavazoie, S.F., Alvarez, V.A., Ridenour, D.A., Kwiatkowski, D.J., and Sabatini, B.L. (2005). Regulation of neuronal morphology and function by the tumor suppressors Tsc1 and Tsc2. Nat Neurosci *8*, 1727-1734.

Thomas, G. (2002). The S6 kinase signaling pathway in the control of development and growth. Biol Res *35*, 305-313.

Tokuda, S., Mahaffey, C.L., Monks, B., Faulkner, C.R., Birnbaum, M.J., Danzer, S.C., and Frankel, W.N. (2011). A novel Akt3 mutation associated with enhanced kinase activity and seizure susceptibility in mice. Hum Mol Genet *20*, 988-999.

Tomasoni, R., and Mondino, A. (2011). The tuberous sclerosis complex: balancing proliferation and survival. Biochem Soc Trans *39*, 466-471.

Tsien, J.Z., Chen, D.F., Gerber, D., Tom, C., Mercer, E.H., Anderson, D.J., Mayford, M., Kandel, E.R., and Tonegawa, S. (1996). Subregion- and cell type-restricted gene knockout in mouse brain. Cell *87*, 1317-1326.

Tsokas, P., Grace, E.A., Chan, P., Ma, T., Sealfon, S.C., Iyengar, R., Landau, E.M., and Blitzer, R.D. (2005). Local protein synthesis mediates a rapid increase in dendritic elongation factor 1A after induction of late long-term potentiation. J Neurosci *25*, 5833-5843.

Tsokas, P., Ma, T., Iyengar, R., Landau, E.M., and Blitzer, R.D. (2007). Mitogen-activated protein kinase upregulates the dendritic translation machinery in long-term potentiation by controlling the mammalian target of rapamycin pathway. J Neurosci *27*, 5885-5894.

Uhlmann, E.J., Apicelli, A.J., Baldwin, R.L., Burke, S.P., Bajenaru, M.L., Onda, H., Kwiatkowski, D., and Gutmann, D.H. (2002). Heterozygosity for the tuberous sclerosis complex (TSC) gene products results in increased astrocyte numbers and decreased p27-Kip1 expression in TSC2+/- cells. Oncogene *21*, 4050-4059.

Um, S.H., Frigerio, F., Watanabe, M., Picard, F., Joaquin, M., Sticker, M., Fumagalli, S., Allegrini, P.R., Kozma, S.C., Auwerx, J.*, et al.* (2004). Absence of S6K1 protects against age- and diet-induced obesity while enhancing insulin sensitivity. Nature *431*, 200-205.

Vivanco, I., and Sawyers, C.L. (2002). The phosphatidylinositol 3-Kinase AKT pathway in human cancer. Nat Rev Cancer *2*, 489-501.

von der Brelie, C., Waltereit, R., Zhang, L., Beck, H., and Kirschstein, T. (2006). Impaired synaptic plasticity in a rat model of tuberous sclerosis. Eur J Neurosci *23*, 686-692.

Walton, M., Henderson, C., Mason-Parker, S., Lawlor, P., Abraham, W.C., Bilkey, D., and Dragunow, M. (1999). Immediate early gene transcription and synaptic modulation. J Neurosci Res *58*, 96-106.

Wang, X., and Proud, C.G. (2011). mTORC1 signaling: what we still don't know. J Mol Cell Biol *3*, 206-220.

Weiler, I.J., Irwin, S.A., Klintsova, A.Y., Spencer, C.M., Brazelton, A.D., Miyashiro, K., Comery, T.A., Patel, B., Eberwine, J., and Greenough, W.T. (1997). Fragile X mental retardation protein is translated near synapses in response to neurotransmitter activation. Proc Natl Acad Sci U S A *94*, 5395-5400.

Wiegert, J.S., and Bading, H. (2011). Activity-dependent calcium signaling and ERK-MAP kinases in neurons: a link to structural plasticity of the nucleus and gene transcription regulation. Cell Calcium *49*, 296-305.

Woods, A., Johnstone, S.R., Dickerson, K., Leiper, F.C., Fryer, L.G., Neumann, D., Schlattner, U., Wallimann, T., Carlson, M., and Carling, D. (2003). LKB1 is the upstream kinase in the AMP-activated protein kinase cascade. Curr Biol *13*, 2004-2008.

Wu, Z., and Boss, O. (2007). Targeting PGC-1 alpha to control energy homeostasis. Expert Opin Ther Targets *11*, 1329-1338.

Wullschleger, S., Loewith, R., and Hall, M.N. (2006). TOR signaling in growth and metabolism. Cell *124*, 471-484.

Yao, Y., Kelly, M.T., Sajikumar, S., Serrano, P., Tian, D., Bergold, P.J., Frey, J.U., and Sacktor, T.C. (2008). PKM zeta maintains late long-term potentiation by N-ethylmaleimide-sensitive factor/GluR2-dependent trafficking of postsynaptic AMPA receptors. J Neurosci *28*, 7820-7827.

Zearfoss, N.R., Alarcon, J.M., Trifilieff, P., Kandel, E., and Richter, J.D. (2008). A molecular circuit composed of CPEB-1 and c-Jun controls growth hormone-mediated synaptic plasticity in the mouse hippocampus. J Neurosci *28*, 8502-8509.

Zhang, H., Cicchetti, G., Onda, H., Koon, H.B., Asrican, K., Bajraszewski, N., Vazquez, F., Carpenter, C.L., and Kwiatkowski, D.J. (2003). Loss of Tsc1/Tsc2 activates mTOR and disrupts PI3K-Akt signaling through downregulation of PDGFR. J Clin Invest *112*, 1223-1233.

Zhou, X., Babu, J.R., da Silva, S., Shu, Q., Graef, I.A., Oliver, T., Tomoda, T., Tani, T., Wooten, M.W., and Wang, F. (2007). Unc-51-like kinase 1/2-mediated endocytic processes regulate filopodia extension and branching of sensory axons. Proc Natl Acad Sci U S A *104*, 5842-5847.

Zinzalla, V., Stracka, D., Oppliger, W., and Hall, M.N. (2011). Activation of mTORC2 by association with the ribosome. Cell *144*, 757-768.

ACKNOWLEDGMENT

In the first place I would like to express my deepest gratefulness to my parents! Without any reservation they granted relief to me during all the years of my personal and professional development. They thoroughly supported me in all my steps and decisions and always provided a site of recreation in a way only Family can do.

I would like to thank Prof. Markus A. Rüegg for giving me the opportunity to do my PhD in his lab. Thanks to his way of supervision, I acquired not only scientific qualities but also learned many things that go beyond. He placed the responsibility for organizational functions and methodological developments on me and was confident that I would manage. It definitely took a while until the first fruits could be harvested, but thanks to his patience it turned out to be worthwhile.

I could count on a great assistance and unlimited support by Prof. Kaspar E. Vogt. Without his enormous expertise in electrophysiology and his goodwill to help a complete greenhorn such as me, I would never have been able to set up the two Rigs and to learn the technique of patch clamp and field recording, respectively. I highly appreciate Kaspar's scientific and technical support and would like to express my gratitude!

A warm thank goes to all the present and former Rüegg-Lab members! It was a pleasure to work with you – in good times and bad times. Especially the bad times were much more bearable in the presence of good colleagues that knew how to cheer me up.

I would like to thank Prof. David P. Wolfer and his team from the Institute of Anatomy, University of Zurich, for providing the facility and support for the behavioral experiments.

Thanks to *Novartis Stiftung für medizinisch biologische Forschung* and the *SGV* for funding.

I would like to thank Riad Seddik, Mathieu Rajalu, Audrée Pinard, Enrique Perez Garci, Julien Gaudias and Silvia Willadt for assistance in electrophysiological questions.

Several people at the Biozentrum contributed to my work in one or the other way: the staff of the animal facility; the team of the mechanic and electric workshop; the members of the Handschin-Lab, the Barde-Lab, and the Bettler-Lab. Thank you to all of them.

A special thank goes to my sisters, my brother, the "Bios" – especially Anna for proofreading, danke 1000! – and all my other close friends. They had to accept that I usually came "1-2 hours later" and that I often had my mind absorbed with PhD-related issues. Merci for your understanding and mental support! You were a backup of unestimable value to me.

Last but in no case at least, with all my heart I would like to dearly thank Ruedi who went with me through my PhD probably as intensively as I did. To know you being at my side means extremely much to me! SoB!